UNIVERSITAT DE BARCELONA

Surgical Assessment of Insular Gliomas: Operative Technique and Clinical Outcomes

Arnau Benet Cabero

Surgical Assessment Of

THE INSULA

Arnau Benet Cabero, MD

Thesis Directors: Dr. Jose Juan Gonzalez Sánchez
Dr. Andreu Gabarrós i Canals

Surgical Assessment of Insular Gliomas:

Operative Technique and Clinical Outcomes

PhD Candidate (International mention): Arnau Benet Cabero

PhD Institution: University of Barcelona (UB), Faculty of Medicine

Research Institutions:*

2016-2017: Skull Base and Cerebrovascular Laboratory, Department of Neurosurgery, University of California San Francisco, San Francisco, California, USA

2017-2020 Barrow Neurological Institute, Phoenix, Arizona, USA

Director: Dr. Jose Juan Gonzalez Sánchez (UB)
Director & Tutor: Dr. Andreu Gabarrós i Canals (UB)

Research Category:
"Fisiopatologia de les malalties mèdico-quirúrgiques"

**This PhD was designed at the Universitat de Barcelona (Alma Mater). The research was performed at the Universitat de Barcelona, University of California San Francisco (USA) and the Barrow Neurological Institute (USA)*

Nota: Aquesta memòria de projecte de tesis ha estat preparada parcialment en català i anglès per seguir el programa de mención internacional.

None of my achievements are my sole merit. This work belongs to Bus, Christina, Avi, Heura, Jaume, Margarita, Oscar and Rosario. I am because they are.

AGRAÏMENTS

Aquesta tesi doctoral és la culminació de més de vuit anys de dedicació a la recerca en el camp de l'anatomia neuroquirúrgica i al treball de laboratori per a la millora de la tècnica quirúrgica. Aquest treball representa l'assoliment d'un somni d'ïurn, una fita que, en més d'una vegada, semblava inassequible. La reflexió en aquest apunt final de la tesi em porta a definir els factors crítics sobre l'èxit de la mateixa: passió per l'àmbit de treball, empatia i compassió vers els pacients, i support extern. És al support extern a qui dedico aquesta plana.

Al Dr. Josep González, director de tesi i mentor des de l'etapa d'estudiant de medicina. No hi ha paraules per expressar l'impacte personal i professional que el Dr González té en la meva vida. D'ençà que vaig començar el meu camí professional, el Dr Gonzàlez ha estat el meu model professional i personal, a qui admiro pel seu talent, honestedat, integritat professional, altruisme, compassió vers els pacients i capacitat innovadora. Aquesta tesi doctoral és, en gran manera, gracies a tu, Josep.

Al Dr Andreu Gabarrós, director, tutor de tesi i mentor des de l'etapa d'estudiant de medicina. Gràcies al Dr Gabarrós jo aspiro a ser doctorat… sense ell aquesta etapa de la meva vida no existiria. Admiro el Dr Gabarrós per la seva capacitat de liderar un dels serveis de neurocirurgia més punters de l'estat tot mantenint el seu caràcter honest, proper, i afable. Com els grans líders de l'història, l'Andreu utilitza el seu èxit per donar oportunitats a les noves generacions. No oblido que la meva etapa als estats units va començar gràcies a tu, Andreu.

Al Dr Michael T Lawton, chairman and president of the Barrow Neurological Institute. Gràcies al Dr Lawton he desenvolupat una passió profunda i transformadora vers la neurocirurgia cerebrovascular. El Dr Lawton em va donar l'oportunitat de desenvolupar la meva línia de recerca, primer al departament de neurocirurgia a la University of California San Francisco (en la posició de director del *laboratory of neurosurgical anatomy* fins 2017) i darrerament a Barrow Neurological Institute (en funció de *neurosurgical resident* des de 2017). Aquestes institucions, amb màxim prestigi mundial en el camp de la investigació i tècnica quirúrgica, han estat el pilar fonamental pel desenvolupament tècnic de l'objectiu A i B d'aquesta tesi. He trobat la meva passió professional gracies a tú, mestre.

INSTITUCIONS

Aquesta tesi doctoral ha estat dissenyada a la **facultat de medicina de l'Universitat de Barcelona (*Alma mater*)**. L'inscripció de la tesi, seguiment acadèmic, tutories i la redacció de la tesi doctoral han estat desenvolupades a Barcelona. Aquesta es una tesi doctoral amb intenció manifesta de rendir respecte a la institució que m'ha fet metge, i a qui tinc un gran respecte i amor. Tanmateix es una tesi que, des del prinicpi, persegueix la menció internacional i el reconeixemnt en l'àmbit Europeu.

Facultat de Medicina de l'Universitat de Barcelona. Barcelona, Europa

University of California San Francisco -UCSF- (Califòrnia, EUA) és la institució amb més producció acadèmica en neurocirurgia. La meva etapa de recerca a UCSF va ser critica pel desenvolupament dels objectius A i B. El departament de neurocirurgia de UCSF inclou un laboratori equipat específicament pel desenvolupament de tècniques neuroquirúrgiques. Aquest laboratori, que està dissenyat a rèplica d'un quiròfan de neurocirurgia, va permetre el desenvolupament de l'objectiu B amb les màximes garanties de replicabilitat i translació i aplicabilitat clínica. El departament de neurocirurgia de UCSF va assumir els costos derivats del desenvolupament dels objectius A i B.

Fotografia del doctorand durant la simulació quirúrgica en el desenvolupament de l'objectiu B. UCSF, Califòrnia, EUA, 2016

Barrow Neurological Institute -BNI- (Arizona, EUA) és la catedral mundial de la tècnica neuroquirurgica. Al large dels darrers vint anys l'institut BNI ha desenvolupat innovations de tècnica quirúrgica que han transformat el tractament de diverses lesions cerebrals (aneurismes, malformacionns arteriovenoses, glioma cerebral, etc.). L'objetiu C reflecteix la meva etapa a BNI. La meva experiència directa al quiròfan m'ha permès entendre de primera mà l'aplicació directa de la recrea prèvia al laboratori de UCSF. El meu rol de metge resident en neurocirurgia a la sala de cures intensives ha estat crítica per entendre la repercusió clínica de les estratègies quirúrgiques pel tractament de gliomes de la insula. La relació directa amb els i les pacients afectats/des de glioma insular ha esta vital per donar un caire humà i personal a la recerca desenvolupada en aquest treball de tesi doctoral.

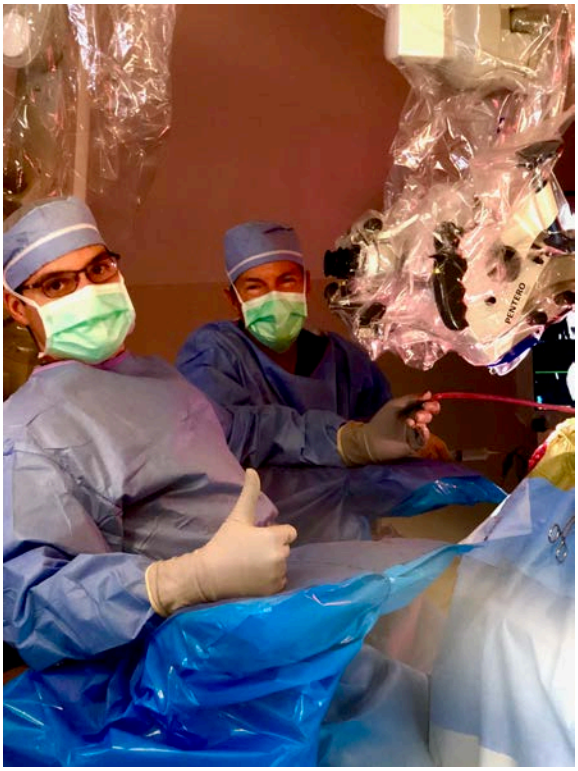

Fotografia durant l'extirpació quirúrgica d'un glioma cerebral. Dr. Kris Smith, i el doctorand. BNI, Arizona, EUA, 2019

RESUM DE LA TESI DOCTORAL EN LA LLENGUA CATALANA

Avaluació de la cirurgia de gliomes de la Insula: tècnica quirúrgica i avaluació dels resultats clínics.

En la present tesis doctoral es presenten els resultats de sis anys d'investigació del doctorand sobre els gliomes que afecten el lòbul de l'Insula. La present tesis doctoral es divideix en tres parts en les que es desenvolupa un programa seqüencial dirigit a la investigació i optimització del tractament quirúrgic de les lesions de la Insula (amb especial atenció als gliomes cerebrals d'alt grau).

En primer lloc es desenvolupa un treball de laboratori per al disseny d'una metodologia òptima per a la simulació quirúrgica d'abordatges Neuroquirúrgics intracerebrals en un model cadavèric. Es descriuen els mètodes i estratègies per al disseny de la composició química del líquid de embalsamament que el cervell humà així com la metodologia per avaluar objectivament l'esmentada fórmula química i el mètode de embalsamament. Es descriu la superioritat del mètode desenvolupat respecte de l'estàndard de preparació de cadàvers però simulació quirúrgica i es discuteixen els avantatges principals del mètode dissenyat respecte la investigació referent a la tècnica neuroquirúrgica. Aquests són, en breu, la millora substancial d'elastança cerebral que permet la retracció del teixit cerebral de forma similar a la cirurgía en ésser humà viu, la disminució de l'exposició del personal de recerca a components carcinogènics com el formaldehid, la superioritat en la preservació del material cadavèric respecte el teixit no embalsamat, etc. L'esmentada metodologia és la base per la segona fase de la present tesi doctoral.

En segon lloc es desenvolupa un projecte d'investigació sobre la tècnica quirúrgica per la ressecció de lesions del lòbul de l'Insula, amb especial atenció als gliomes insulars. Prenent el mètode de simulació neuroquirúrgica desenvolupat a la primera fase d'aquesta tesi, es comparen les dues tècniques principals per l'accés a la Insula: l'abordatge Transilvià i l'abordatge Transcortical. Es descriuen els perfils quirúrgics d'ambdues tècniques quirúrgiques respecte a l'accés a cada una de les parts de la Insula (anterior superior, posterior superior, posterior inferior, i anterior inferior). Es descriu, per primera vegada, la tècnica quirúrgica més favorable per cada part de la Insula i s'introdueixen conceptes claus per la decisió preoperatòria. En termes generals l'abordatge transilvià demostra superioritat en tumors que afecten la part anterior de la Insula, mentre que l'abordatge transcortical és superior en tumors de la part posterior.

En tercer lloc s'estudien els resultats clínics de les tècniques quirúrgiques estudiades en un model de simulació descrit a la fase anterior, per mitjà de la revisió retrospectiva de casos clínics en els quals es varen realitzar cirurgies de glioma insular. L'esmentada investigació retrospectiva es va desenvolupar a University of California San Francisco, Califòrnia, USA (Centre de notable prestigi vers la cirurgia de gliomes insulars), així com a Barrow Neurological Institute, Arizona, USA (centre de prestigi mundial en microneurocirurgia). En aquesta última fase es resumeixen els resultats de laboratori així com l'experiència clínica desenvolupats en aquest treball de tesis doctoral per proveir les bases sòlides per la decisió clínica i tècnica vers el tractament de pacients que pateixen de glioma insular. Específicament, s'estableix que el grau de resecció quirúrgica determina la supervivència del pacient amb glioma insular. Així doncs és important identificar l'abordatge quirúrgic (transsilvià o transcortical) que permet arribar als nivells de resecció quirúrgica superior al 80% del volum del tumor, per optimitzar el resultats clínics tot mantenint la funció cerebral.

Table of Contents

SUMMARY

Background:

Surgical treatment of Insular gliomas is technically challenging and may lead to high postoperative morbidity. However, previous research has proven that maximal safe resection is critical for maintaining quality of life as well as enhancing overall and progression-free survival. Insular gliomas are currently resected through either a transsylvian or transcortical approach. However, there is no objective evidence to aid surgical management to maximize safe resection rates.

Objectives:

To define an optimal treatment strategy for the neurosurgical management of insular gliomas using a sequential research protocol. Phase A1- Design a custom embalming formula for preserving native brain features in cadavers to optimize the validity and clinical applicability of laboratory-based operative research. A2- Design a laboratory method to obtain objective data to assess -and compare- neurosurgical techniques in cadavers. Phase B- Define an optimal surgical technique for the management of each insular glioma of the Berger-Sanai classification system using our surgical simulation method in cadavers. Phase C- Validate the existing anatomical classification of insular gliomas to predict extent of resection (extent of resection) and anticipate neurological morbidity.

Methods:

We aimed to provide sound objective evidence to the surgical management of insular gliomas through a multidisciplinary, sequential method including basic laboratory research, neurosurgical simulation using cadavers and a prospective clinical study. We first developed a customized embalming formula to create a neurosurgical simulation method that best resembles life surgery (a). We then used this optimized surgical simulation method to objectively determine and quantify the best surgical approach (transsylvian vs transcortical) for each type of insular tumor according to the Berger-Sanai insular glioma classification (b). Finally, we carried out a prospective clinical study to assess the predictability of the Berger-Sanai insular glioma classification regarding extent of resection and patient outcomes (c).

Results:

We designed an embalming solution that dramatically improved validity and applicability of research using neurosurgical simulation in cadavers. Our formula optimizes resemblance to life surgery (lower retraction pressure and greater retraction area) compared to the gold standard (formaldehyde). Our embalming method preserved specimens for significantly longer use than un-embalmed cadavers, which allows for complex research designs (such as Phase B of this work). We described cutting-edge surgical simulation techniques to objectivize surgical techniques in the laboratory. Our surgical simulation experiments show that the transcortical approach performs better than the transsylvian approach on all parameters for zones I and IV. On Zones II and III, cortical mapping and specific anatomical features may make the transsylvian approach more favorable. Our prospective clinical study showed that the Berger-Sanai insular glioma classification is a reliable tool to predict extent of resection (highest on zone I, IV) and postoperative complications (lowest on zone II and IV) following surgical treatment.

Clinical and scientific impact:

Overall, this work improved the field of neurosurgical simulation research by providing a detailed description of cadaver preparation (including public disclosure of the embalming chemical formula) and methodology to carry objective measurements to compare surgical techniques. For the first time, we provided objective data to aid the neurosurgeon in choosing the best surgical approach to maximize resection rates of insular gliomas tailored to the Berger-Sanai insular glioma classification. Finally, we validated the Berger-Sanai insular glioma classification as a tool to anticipate resection rates and postoperative neurological complications. As a whole, this work will substantially impact management of insular gliomas and patient informed decisions.

INTRODUCTION

Historical remarks

The insular lobe of the brain, also known as the ***Island of Reil***, is an extraordinary anatomical structure. It is named after Johann Christian Reil, who described this anatomical region as separate from the superficial cortex and introduced it to the anatomic community as "*the insula*" in a series of reports in 1809[1]. Several devoted anatomists dedicated their body of work to the morphological description of the cerebral cortex -and particularly the insula- during the 19th century[2-4]. Oscar Eberstaller, who was an exquisite anatomist, provided the first most accurate and complete morphological description of the Insula in 1887[5], and his detailed anatomical work is still valid today.

Johann Christian Reil

The 20th century brought with it groundbreaking technological advances that allowed studying the insula like never before; in the living, and beyond the surface. It all started with Dr Harvey Cushing (USA 1869-1939), who is regarded as the "*father* of neurosurgery". Dr Cushing was an American surgeon with a devoted commitment to the study and treatment of brain lesions. Influenced by great mentors including Dr Halsted, Dr Cushing developed many surgical techniques to treat brain lesions and developed instruments that made brain access survivable (e.g electrocautery).[6] However, Dr Cushing is most laureated for his work and influence on the creation of neurological surgery as a specialty.[7] On March 1905, Dr Harvey Cushing published an article entitled "The special field of neurological surgery" in a special edition of the ***Johns Hopkins Hospital bulletin***.[8] That article was the first of many that lead to the establishment of neurosurgery as a standalone surgical specialty in 1920.[9,10]

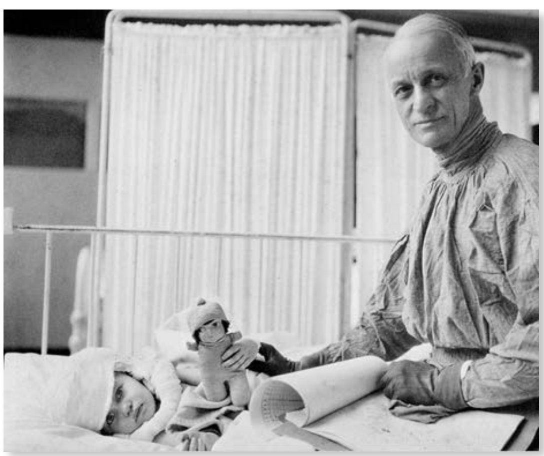

Harvey Cushing, the "father" of neurosurgery

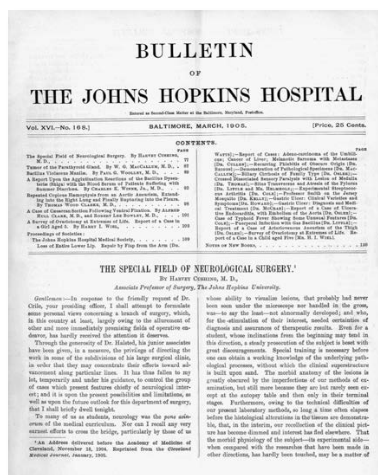

BULLETIN

OF

THE JOHNS HOPKINS HOSPITAL

Vol. XVI.—No. 168.] BALTIMORE, MARCH, 1905. [Price, 25 Cents.

CONTENTS.

The Special Field of Neurological Surgery. By Harvey Cushing, M. D., ... 77

Tumor of the Parathyroid Gland. By W. G. MacCallum, M. D., ...

Bacillus Violaceus Manila. By Paul G. Woolley, M. D., ...

A Report Upon the Agglutination Reactions of the Bacillus Dysenteriae (Shiga) with the Blood Serum of Patients Suffering with Summer Diarrhea. By Charles K. Winne, Jr., M. D., ...

Repeated Copious Haemoptysis from an Aortic Aneurism, Extending into the Right Lung and Finally Rupturing into the Pleura. By Thomas Wood Clarke, M. D., ...

A Case of Caesarean Section Following Ventral Fixation. By Alfred Hull Clark, M. D., and Robert Lee Bowley, M. D., ... 101

A Survey of Ovariotomy at Extremes of Life. Report of a Case in a Girl Aged 5. By Harry I. Wiel, ...

Proceedings of Societies:

The Johns Hopkins Hospital Medical Society, ...

Notes on New Books, ...

THE SPECIAL FIELD OF NEUROLOGICAL SURGERY.[1]

By Harvey Cushing, M. D.,

Associate Professor of Surgery, The Johns Hopkins University.

Gentlemen:—In response to the friendly request of Dr. Crile, your presiding officer, I shall attempt to formulate some personal views concerning a branch of surgery, which, in this country at least, largely owing to the allurement of other and more immediately promising fields of operative endeavor, has hardly received the attention it deserves.

Through the generosity of Dr. Halsted, his junior associates have been given, in a measure, the privilege of directing the work in some of the subdivisions of his large surgical clinic, in order that they may concentrate their efforts toward advancement along particular lines. It has thus fallen to my lot, temporarily and under his guidance, to control the group of cases which present features chiefly of neurological interest; and it is upon the present possibilities and limitations, as well as upon the future outlook for this department of surgery, that I shall briefly dwell tonight.

To many of us as students, neurology was the *pons asinorum* of the medical curriculum. Nor can I recall any very earnest efforts to cross the bridge, particularly by those of us whose ability to visualize lesions, that probably had never been seen under the microscope nor handled in the gross, was—to say the least—not abnormally developed; and who, for the stimulation of their interest, needed certainties of diagnosis and assurances of therapeutic results. Even for a student, whose inclinations from the beginning may tend in this direction, a steady prosecution of the subject is beset with great discouragements. Special training is necessary before one can obtain a working knowledge of the underlying pathological processes, without which the clinical superstructure is built upon sand. The morbid anatomy of the lesions is greatly obscured by the imperfections of our methods of examination, but still more because they are but rarely seen except at the autopsy table and then only in their terminal stages. Furthermore, owing to the technical difficulties of our present laboratory methods, so long a time often elapses before the histological alterations in the tissues are demonstrable, that, in the interim, our recollection of the clinical picture has become dimmed and interest has fled elsewhere. That the morbid physiology of the subject—its experimental side—when compared with the researches that have been made in other directions, has hardly been touched, may be a matter of

[1] An Address delivered before the Academy of Medicine of Cleveland, November 18, 1904. Reprinted from the Cleveland *Medical Journal*, January, 1905.

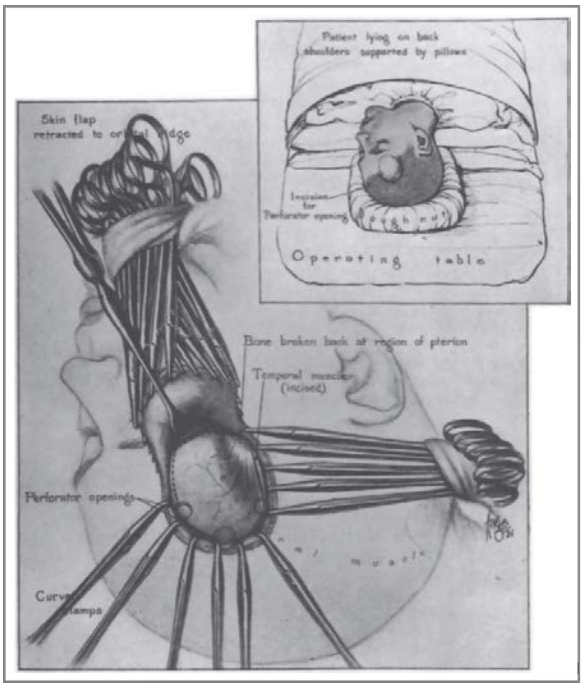

Dr Heuer's original drawing of the Pterional approach in 1920

George Heuer (1882–1950), who trained under Dr Cushing, developed the Pterional craniotomy and reported his surgical experience treating intracranial lesions.[11] This was the first step towards mankind's surgical expedition to the Insula.

On July 27th, 1927 Dr Moniz introduced the cerebral angiography to the world at the Congress of Neurological Society in Paris. In subsequent studies, the cerebral angiogram allowed exquisite anatomical descriptions of the middle cerebral artery and its perforating branches (lateral lenticulostriate and insular perforating arteries) running on and through the Insula.[12-15] The assessment of the patient's perforating arteries in relation to their insular lesions would later be key to the success of surgical treatment of insular gliomas.

In 1980's, Paul Christian Lauterbur and Sir Peter Mansfield invented the magnetic resonance imaging (MRI), for which they received the novel prize. The MRI allowed to see the deep nuclei of the living brain, and study intracranial lesions with an accuracy and detail never seen before.[16] The MRI was later optimized to capture localized function (fMRI) and connectivity (diffusion weighted imaging), which are at the core of brain function research at present time.[17,18] The cerebral angiogram as well as the advanced MRI studies provided unprecedented images of the brain and were at the cornerstone of neurosurgical assessment of insular lesions.

Sir Peter Mansfield, adjusting the prototype of a magnetic resonance imaging machine in 1978

Until the last two decades of the 20th century, neurosurgery was considered a heroic surgical discipline, which required the courage to tackle debilitating disease affecting a very delicate organ -***i.e. the brain***-. The neurosurgeon would often have to navigate through long exposures with poor illumination and minimal visualization of anatomical structures critical to cognitive function. It was a dark, risky and uncharted surgical field were poor outcomes were expected. One man would profoundly change the once primitive neurosurgery into the refined microneurosurgery we know today; Dr Mahmut Gazi Yasargil.[19] Dr Yasargil (b. 1925 Turkey), was a passionate neurosurgeon that combined the intense bearing of Cushing, the surgical skill of Heuer and Dandy, the interest for cerebral angiography from Moniz and the daring verve of Dr Krause. Although use of the microscope in neurosurgery had been introduced previously by Dr Theodore Kurze in the 1950's, it wasn't until Dr Yasargil's work that the operative microscope became essential for intracranial surgery.[20,21] In his masterpiece "Microneurosurgery",[22] Dr Yasargil described a neurosurgery roadmap to safely navigate the intracranial space through the magnified views of the brain using the microscope. Neurosurgical operations became bright, safe and predictable, which made the insula -and other deep brain structures- an achievable surgical target. He first described the pterional transsylvian approach (which will be core to the scientific development of this thesis), and reported his successful experience in resection of tumors of the limbic system, including the insula.[23] His report included 240 patients operated on through this approach with 95% of patients experiencing ***minimal neurological deficits*** *(*with the ability to return to

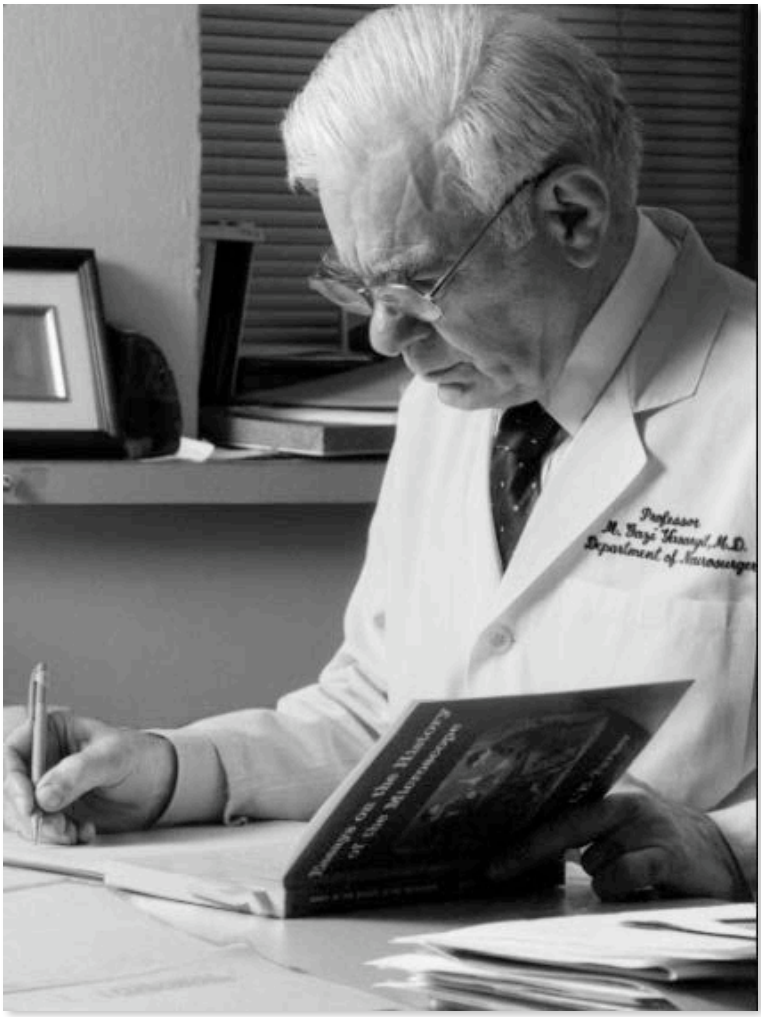

Dr Mahmut Gazi Yasargil is considered the best neurosurgeon of the XXI century

normal life). These results proved that surgical resection of insular tumors was safe and possible. Dr Yasargil used his body of work, which encompassed the initial anatomical descriptions of Reil and Eberstaller, the images using angiography and MRI and his surgical observations to formulate the first surgical classification of the insula.[23,24] Although this classification became obsolete, it attracted international neurosurgical attention to the treatment of insular and paralimbic lesions, which has steadily improved ever since.

During the first two decades of the 21st century, neurosurgery has evolved by the hand of imaging technology, improvements in anesthesia and intraoperative cortical and subcortical mapping. The development of advanced MRI technology (e.g. diffuse weighted imaging) and complex algorithmic post-processing have enabled cerebral tractography. Cerebral tractography uses MRI to capture vectors of water movement in the axons (anisotropy) to display the white matter fascicles (bundles of axons connecting distant functional areas).[17] This allows studying the connectivity of the insula in the living brain in real time, which when paired to a functional MRI (fMRI), may provide a map of cortical and subcortical functions in and around the insula.[18] The development of these advanced imaging techniques allowed for a substantial improvement in the understanding of both the anatomy and function of the insula in the research setting.[25-28] In the clinical setting, preoperative tractography and fMRI enabled the surgeon to understand the relationship between the tumor and the eloquent cortex and white matter tracts within the insula. This data allowed neurosurgeons to design surgical strategies based on the patient's specific features and better anticipate intraoperative findings.[29] Thereafter, preoperative planning for the treatment of insular tumors (e.g. design of trajectory, custom craniotomy size, etc.) became extremely refined and tailored to each particular patient.

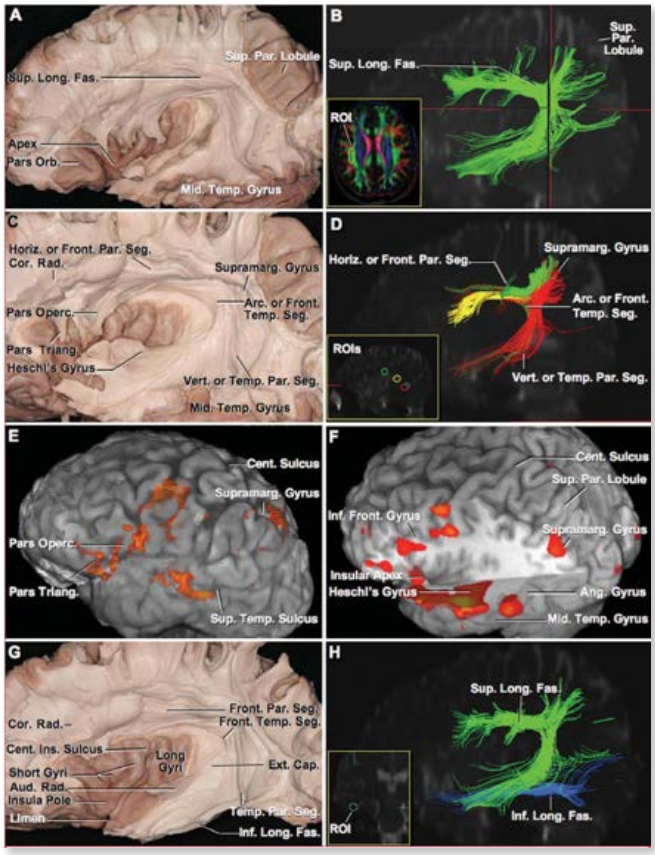

Where the old meets the new. White matter dissection using the Klinger technique in cadavers (left column). Tractography using Diffusion tensor MRI (right column). From Dr Rhoton's "three-dimensional anatomy of the human brain", 2008

Contemporary to the preoperative imaging revolution was the development of intraoperative awake mapping in neurosurgery. The use of electrical stimulation for mapping cerebral function was pioneered by Drs. Foerster and Penfield in 1931.[30-33] Although their studies provided a sound basis for our current understanding of function localization, their techniques were abandoned because they were extremely risky and lead to devastating consequences for their patients.

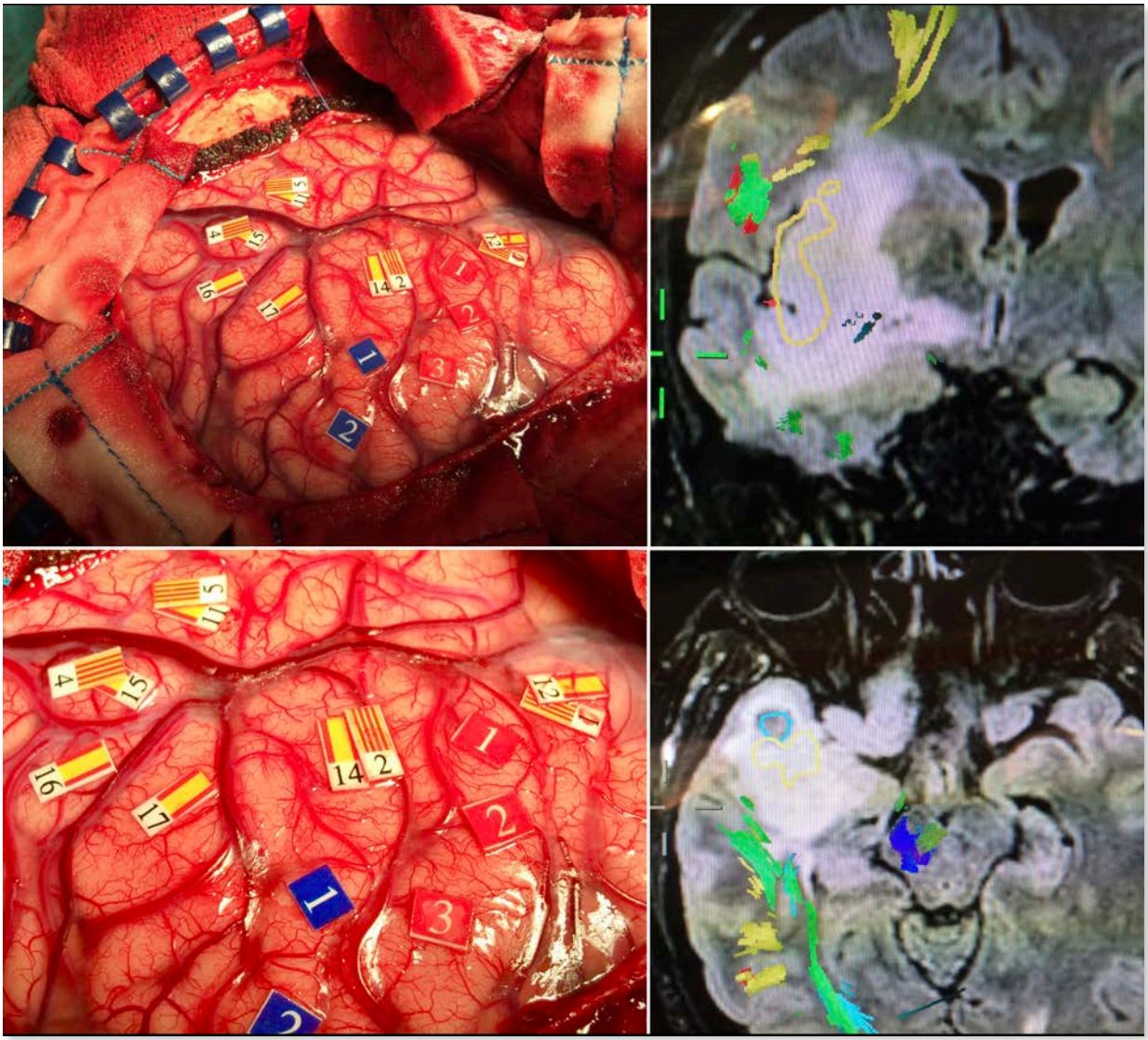

Surgical photographs of an awake intraoperative cortical and subcortical stimulation during resection of an insular glioma. Left pterional craniotomy with language mapping (left column). Screenshots of the navigation system with white matter tractography (right column) Courtesy of Dr Andreu Gabarrós, 2019

The development of neurosurgical anesthesia protocols allowed for prolonged awake craniotomies with acceptable risks of intraoperative seizures and/or cardiovascular compromise.[34,35] This enabled master neurosurgeons like Hugues Duffau, Mitchel Berger and Nader Sanai, with specific interest in the treatment of insular gliomas, to embark into a fascinating intraoperative challenge: to identify and preserve eloquence using awake

mapping. Awake mapping techniques use electrical stimulation (range of 0.5-2 mA) directly to the cerebral cortex with an awake patient under sedation and local anesthetic. Cerebral electrical stimulation depolarizes a focal area of cortex which, in turn, evokes certain responses. The effects of stimulation in the motor cortex translate into movement. However, access to tumors affecting the insula may also require localization of language function, especially when operating on the left hemisphere. Mapping -and protecting- the language function is complex given that speech production and comprehension uses several brain areas connected by a deep fascicle (i.e. arcuate fasciculus). The mechanism of stimulation effects on language are not clearly understood. The principle is based upon the depolarization of local neurons and also white matter fascicles, inducing local excitation or inhibition, as well as the diffusion to more distant areas by way of orthodromic or antidromic propagation. [36] However, the development of the bipolar probe allowed stimulation precision to fall under 5mm with minimal local diffusion.[37] When used with tenacity and determination, the bipolar stimulator would allow detection of language sites in 95-100% of operative cases.[38]

An example of positive stimulation during awake mapping of the insula would be transitory symptoms observed in conduction aphasia, that is, phonemic paraphasia and repetition disturbances.[39] To maximize extent of tumor resection while preserving function, the neurosurgeon could now design the best surgical approach based on preoperative imaging (e.g. MRI-tractography) and implement direct brain mapping during surgery with high confidence that important brain function would be preserved.[34,40,41] Therefore, if the insular tumor is found most reachable at a location where preoperative tractography and intraoperative mapping tested negative for eloquent function, a transcortical approach ***-transgressing the cerebral cortex to reach a tumor underneath-*** would be safe. This led to the widespread popularization of the transcortical approaches to the insula, and a wave of clinical studies describing surgical techniques, complication avoidance and case series with impressive outcomes.[34,35,38,40,42-49] This brings the history of neurosurgical discovery of the insula to present time.

The insula is a magnificent cerebral lobe confined in the depths of the sylvian fissure. To reveal the insula in the living brain, the neurosurgeon has to first "split" the sylvian fissure, which in itself requires skill and anatomical mastery. Many features make the insula a striking anatomical structure of unique beauty and unparalleled mystery. Its topography may appear of simple design to the novice eye (three short and two long gyri), but its true architecture hides within itself rich detail in a complex geometric form (e.g. accessory, transverse gyri and the polar sulcus of eberstaller[5]). The subtleties of the insular cortex may be used to the advantage of the neurosurgeon in many ways. For example, the ***limen recess*** may be used to anticipate the nearest lenticulostriate artery at danger when navigating the deep sylvian cistern. The insula forms the surface from which the middle cerebral arteries will arise to the cerebral cortex, shaping their course into the characteristic angiographic "chandelier" course when the arteries bounce up at the insula's superior and inferior limiting sulcus. The large amount of minuscule perforating arteries (more than 100) piercing the surface of the insula may be discouraging to the novice's attempt to learn them. However, the devastating consequences of severing the wrong perforating branch (e.g. paralysis) should persuade the reader to look for the queues that the topography of the insula provides to identify and protect them. Although the insula has been, in itself, worth the life's body of work of previous anatomists, the nuclei it confines underneath (basal ganglia and longitudinal fascicles) are of similar complexity and neurosurgical relevance; and their relation to the insula will be briefly described in this section. Perhaps the aspect of the insula that passionates and intrigues most academicians is our primitive understanding of its function, which remains a scientific mystery. Thus, this author's attempt to word the anatomy of the insula should be understood within the limits of contemporary

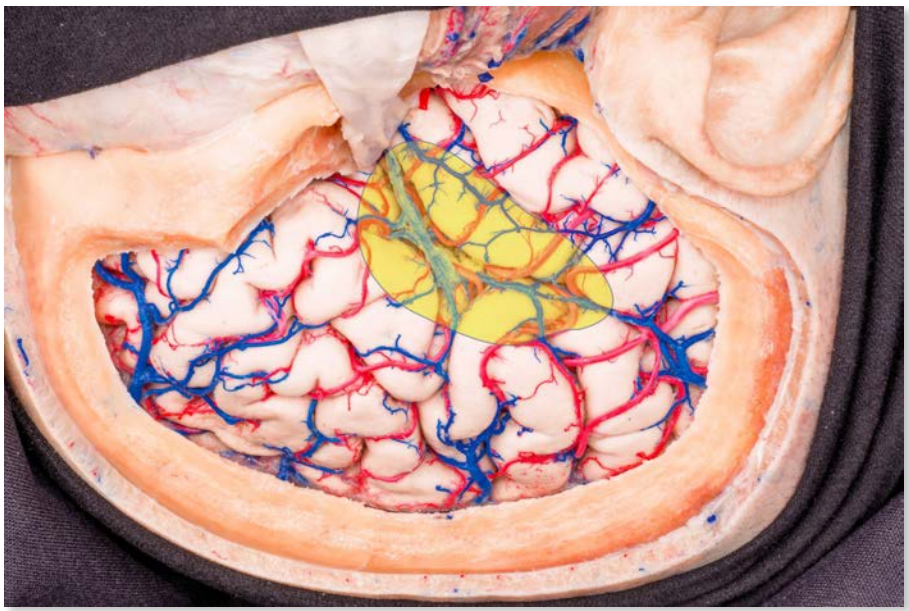

Cadaveric dissection of a right pterional approach with exposure of the lateral convexity. The insula (yellow) is located within the depths of the sylvian fissure beyond the opercula.

knowledge and as prologue of future discovery. Hereby, the anatomy of the insula will be divided into: 1- cortical anatomy; 2- arterial anatomy 3- venous anatomy; 4- anatomy beyond the insula; and 5- function of the insula. The anatomical description is presented from the neurosurgical perspective, as it relates to features relevant to the matter studied in this thesis.

1 Cortical Anatomy of the sylvian fissure and the Insula

On the Sylvian Fissure

The sylvian fissure is a deep canyon that spreads from the sphenoid rim -anteriorly- to the supramarginal gyrus -posteriorly- in the lateral convexity of the brain. It divides the lateral cerebral surface horizontally into the frontal and parietal lobes superiorly, and the temporal lobe inferiorly. The rims of the sylvian fissure are called opercula (i.e. frontal, parietal, and temporal opercula). The sylvian fissure is divided into the "stem" anteriorly (39mm in length), and the posterior ramus posteriorly (75mm in length). The stem begins at the anterior clinoid process, extends laterally and posteriorly along the sphenoid ridge (sphenoidal section) and ends in the cerebral convexity at the level of the pars opercularis of the frontal lobe (operculoinsular section). The most relevant features of the stem are relative to the frontal operculum (at the tail of the stem), where it gives both the anterior horizontal, and anterior ascending rami.[50] The anterior horizontal ramus carves the frontal operculum anteriorly into the pars orbitalis and pars triangularis (the later resembles a triangle). The anterior ascending ramus starts at the tail of its twin -anterior horizontal ramus- and carves a small vertical sulcus into the frontal operculum that divides the pars triangularis (anteriorly) from the pars opercularis (posteriorly). The confluence of the stem, anterior horizontal and ascending rami, and the beginning of the posterior ramus is called "sylvian point". The sylvian point is where the

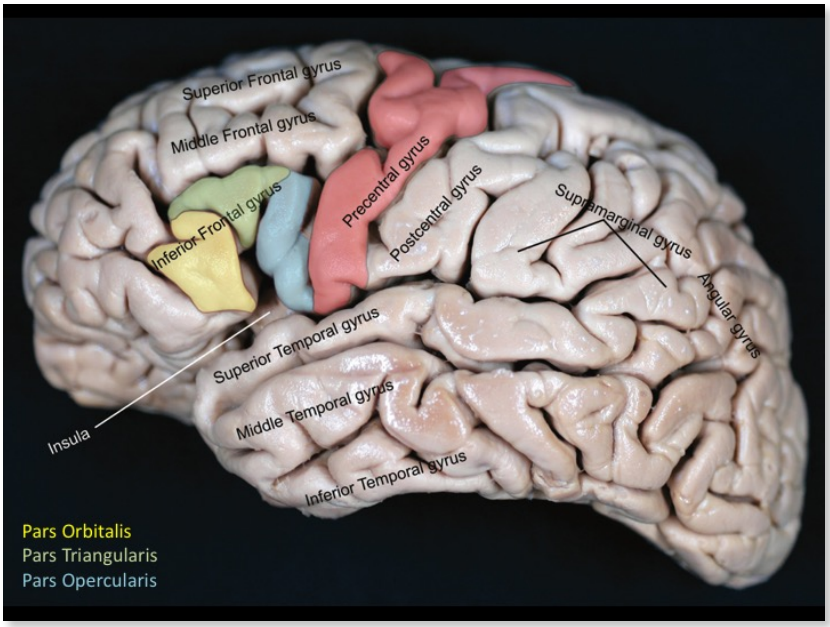

Left convexity of the human cerebrum in a cadaver

sylvian fissure is widest therefore facilitating initial dissection into the subarachnoid space. The sylvian point can be used to infer the location of the insular apex, 12.6mm below it.[51] The posterior ramus of the sylvian fissure extends from the sylvian point posteriorly into the parietal lobe, carving the supramarginal gyrus around its tail. The sylvian fissure becomes deeper as it transitions posteriorly, with a depth of 25mm from the supramarginal gyrus. Important eloquent function resides at the edges of the posterior ramus, including Broca's area, and the premotor and facial motor areas at the frontal operculum; the primary sensory area of the face at the parietal operculum; and the heshl's gyrus (Auditory function) and the Wernicke's area at the temporal operculum.

Cadaveric dissection exposing the insula cortex through a pterional, transsylvian approach.

The sylvian fissure forms a large subarachnoid space -called sylvian cistern- that spans from the carotid cistern at its medial and deepest point, to the lateral sylvian membrane at its most posterior, lateral edge.[52] The deepest wall of the sylvian cistern is found at the sphenoidal section of the sylvian fissure, near the anterior clinoid. There, the sylvian and carotid cisterns meet and form the proximal sylvian membrane, which divides them. The M1 segment of the middle cerebral artery pierces through a ring of arachnoid formed by the proximal sylvian membrane. Above the insula surface, the sylvian cistern contains three membranes

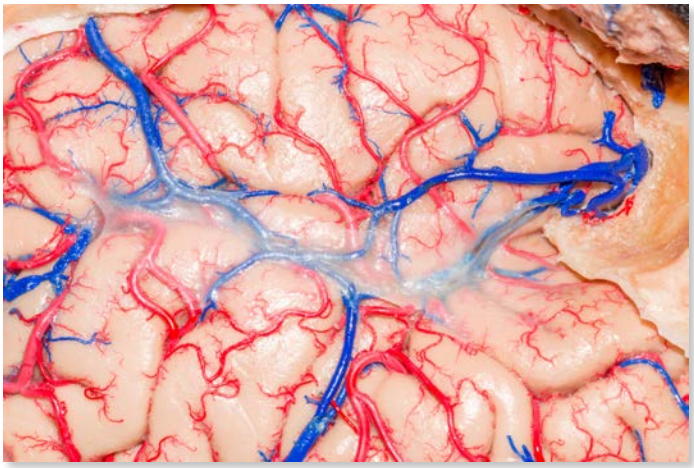

Cadaveric surgical simulation of a left pterional approach with preservation of the external sylvian and outer arachnoid membranes

that divide the subarachnoid space into 4 levels.[52] The deepest level contains the ***medial sylvian membrane***, which attaches to the deepest part of the frontoparietal operculum and the surface of the insula; it contains the M2 branches of the middle cerebral artery. The M2 branches turn into M3 branches by piercing the medial sylvian membrane. The M3 branches, with a lateral trajectory towards the surface of the sylvian fissure, encounter another membrane; the ***intermediate sylvian membrane***. Superficial to the intermediate sylvian membrane is the ***lateral sylvian membrane***, which serves as the floor of the superficial sylvian veins. The M3 branches pierce the lateral sylvian membrane to turn into M4 (cortical branches). The superficial veins and branches of the middle cerebral artery (M4) will run over the lateral sylvian membrane, which is the most superficial sylvian membrane. A global arachnoid membrane covers the whole cerebral convexity: the ***outer arachnoid membrane***. The outer arachnoid membrane encases all cortical vessels, and it is of stronger and thicker consistency. The sylvian fissure contains the middle cerebral artery with its perforators and distal branches, the superficial sylvian vein and the deep middle cerebral vein.

On the Insula

In the adult, the insula sits at the bottom of the sylvian fissure, covered by the opercula. This anatomical disposition has its mysterious origin in the development of the brain. In the third month of life, the fetus develops a slight triangular depression at the anterosuperior aspect of the temporal pole that is noticeable on the cerebral hemisphere. This triangular area will develop into the insula later on, but for reasons yet to discover, this process will take place at a slower pace than the rest of the cortex at the cerebral convexity. The opercula are part of the neocortex that grows at a faster rate than the insula, which is part of the mesocortex. As the opercula overgrows the insula, the insula gets progressively covered in a process similar to how the tectonic plates shape the Earth. The opercula slowly overlap and enclose the insula, resulting in the creation of the sylvian fissure later after birth.

When fully developed, the insula has a triangular pyramidal shape and is separated from the surrounding opercula by the superior, inferior and anterior peri-insular sulci. The anterior peri-insular sulcus (28mm in length) separates the anterior aspect of the insula from the frontal-orbital part of the operculum.[53] The anterior peri-insular sulcus corresponds to the anterior ascending ramus of the sylvian fissure at the convexity. The superior peri-insular sulcus (58mm in length) **[53]** has a horizontal trajectory parallel to the posterior ramus of the sylvian fissure and separates the superior surface of the insula from the frontal-parietal operculum. The superior peri-insular sulcus can be best exposed deep to the sylvian point. The inferior peri-insular sulcus divides the inferior surface of the insula from the temporal operculum and temporal stem. The intersection

between the anterior and superior peri-insular sulci is called anterior insular point. The anterior insular point can be used as a landmark to guide the trajectory towards the anterior limb of the internal capsule, which is located perpendicular and deep to it. The intersection between the superior and posterior peri-insular sulci is called posterior insular point. The posterior insular point indicates the shortest trajectory to the posterior limb of the internal capsule as well as the atrial portion of the lateral ventricle.[53]

The insular stem is divided into anterior and posterior zones by the central insular sulcus. The central insular sulcus is the primary and deepest sulcus of the insula and its course parallels that of the central sulcus of Rolando in the convexity. Identification of the central sulcus of the insula during surgery is key because it reminds of the position of the motor strip in the convexity as well as it contains the central artery (branch of the medial cerebral artery feeding motor and sensory functions). The anterior zone contains 3 short insular gyri (posterior, middle, and anterior), as well as the transverse and accessory insular gyri. The posterior short insular gyrus is defined by the central insular sulcus posteriorly, and the precentral insular sulcus anteriorly. The middle insular gyrus is defined posteriorly by the precentral insular sulcus and anteriorly by the short insular sulcus. The anterior short insular gyrus is defined posteriorly by the short insular sulcus, superiorly by the superior peri-insular sulcus and anteriorly by the anterior peri-insular sulcus and limen insulae. The anterior short insular gyrus projects superiorly into the sylvian point towards the pars triangularis of the frontal operculum, at the anterior insular point. The area where the 3 short gyrus of the insula meet –the vertex of the pyramid- is known as the "insular apex". The insular apex is the area where the insula is nearest to the surface. [53] The transverse insular gyrus is located inferior to the anterior peri-insular sulcus and serves as a junction between the inferior portion of the anterior insula and the posterior frontal orbital region. The accessory insular gyrus extends from the anterior portion of the insular apex to the frontal orbital operculum at its base. The area where the transverse and accessory insular

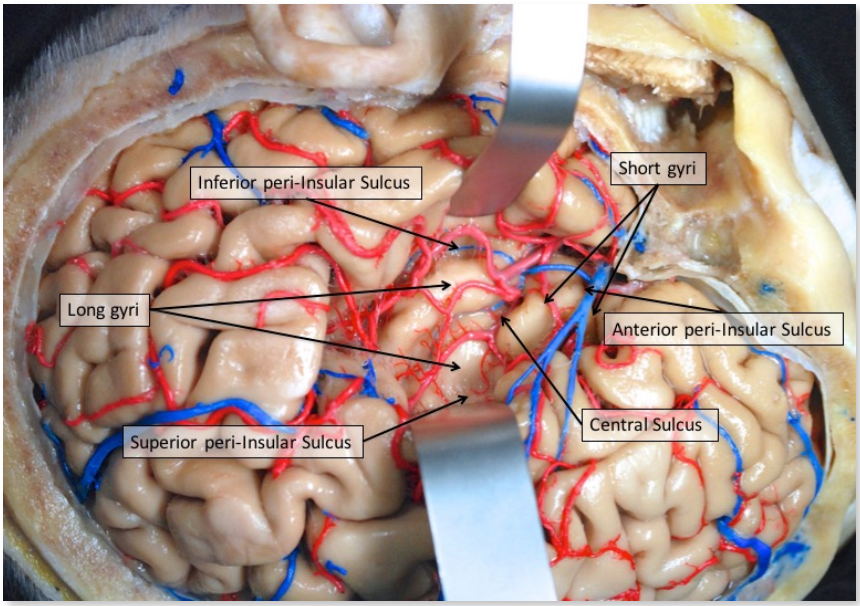

Surgical simulation photograph of a left pterional approach with exposure of the insular cortex

gyri meet is called insular pole.[53] Sometimes there is a small sulcus traversing the insular pole, called the sulcus of Eberstaller, forming a gyrus of Eberstaller under it. Near the insular pole is the limen insulae. The limen insulae consists of a slightly elevated ridge that marks the transition between the sphenoidal and opercular-insular divisions of the sylvian fissure stem. On the surface, the limen insulae is a narrow strip of olfactory cortex that overlies the uncinate fasciculus. During the surgical approach to the insula, the limen insulae is the edge of a cliff from which dissection on the insular stem falls into the depths of the sphenoidal compartment of the sylvian fissure. A key concept of any neurosurgical approach around the limen insulae is the protection of the lateral lenticulostriate perforating arteries. The lateral lenticulostriate arteries enter the anterior perforating substance, which lies just medial to the limen insulae. Fortunately, there is a shallow recess referred to as the "limen recess" between the limen insulae and the most lateral –i.e closest to the insula- perforating artery. At the limen recess, the distance between the nearest lateral lenticulostriate artery and the limen insulae is 15 mm (range 9.7-22 mm).[51]

The posterior insular zone contains the insular cortex posterior to the central sulcus of the insula. The postcentral insular sulcus divides the posterior insular zone into anterior and posterior long insular gyri. Both long insular gyri have a horizontal trajectory that originates from below the insular apex near the limen insulae and ends posteriorly and superiorly towards the frontal and parietal opercula. The inferior long insular gyrus is parallel to the inferior peri-insular sulcus and runs tangential to the transverse gyri of Heshl in the temporal operculum.

Any surgical approach to the insula requires understanding of several key relationships between the cortex around the sylvian fissure (i.e. the opercula) and the surface of the insula itself. The cerebral cortex that constitutes the upper rim of the sylvian fissure is divided into the frontoorbital operculum and the frontoparietal operculum. The lower rim of the sylvian fissure is formed by the temporal operculum.

The frontoorbital operculum is formed by the posterior orbital gyrus, the posterior portion of the lateral orbital gyrus, and the pars orbitalis of the inferior frontal gyrus. The frontoorbital operculum relates to the anterior aspect of the superior peri-insular sulcus and the anterior peri-insular sulcus (i.e. anterior insular point). The posteromedial orbital lobule is found at the medial part of the transverse orbital sulcus and is formed by the the medial portion of the posterior orbital gyrus and the posterior portion of the medial orbital gyrus. These cortex become continuous with the transverse insular gyrus. The posterolateral orbital lobule is found at the lateral and of the transverse orbital sulcus and is formed by the lateral portion of the posterior orbital gyrus and the posterior portion of the lateral orbital gyrus. This cortex is found to merge with pars orbitalis and cover the

anterior surface of the insula. The suborbital gyri is continuous with the accessory insular gyrus and the anterior surface of the anterior short gyrus.[53] [51]

The frontoparietal operculum is formed by the pars triangularis as well as the pars opercularis of the inferior frontal gyrus; the inferior portions of the precentral and postcentral gyri; and the superior portion of the supramarginal gyrus. The superior peri-insular sulcus the findings the limits between the frontoparietal operculum and the insula.

Cadaveric dissection photograph of the left sylvian fissure. A retractor is gently pulling pars triangularis of the frontal operculum to expose the insula

The ***Subtriangular*** gyrus is formed by the cortex medial to the pars triangularis, which covers and becomes continuous with the anterior short insular gyrus. The pars triangularis is found on average 1.8 cm above the superior peri-insular sulcus.[51] The ***subopercular*** gyrus is the cortex medial to the pars opercularis, which covers the short insular sulcus and the middle short insular gyrus. From the tip of the pars opercula R is to the superior peri-insular sulcus measures 2.1 cm. [51] The sub-central gyrus is the cortex medial to both the inferior precentral and postcentral gyri, which covers the central insular sulcus. The inferior postcentral gyrus and the anterior, middle and posterior transverse parietal gyri form the rest of the frontoparietal operculum. The anterior transverse parietal gyrus covers the superior portion of the anterior and posterior long insular gyri, and together with the anterior Heschl's gyrus forms the posterior insular point. The middle and posterior transverse parietal gyri cover the transverse temporal sulcus and the temporal planum in the posterior aspect of insula. At the end of the posterior ramus, the depth of the sylvian fissure is 2.5 cm. The posterior aspect of the

frontoparietal operculum limits with the temporal operculum. These two opercula are divided by the post insular sulcus, which is located at the deep portion of the posterior ramus of the sylvian fissure.

The temporal operculum is formed by the superior temporal gyrus, the temporal pole and the inferior portion of the supramarginal gyrus. The temporal pole and polar planum cover the limen insulae and the inferior surface of the insula, which are near the inferior peri-insular sulcus. The convolutions of the polar planum are called gyri of Schwalbe. These convolutions limited with the anterior part of the inferior peri-insular sulcus. In the lateral surface of the brain, the superior temporal sulcus corresponds to the inferior peri-insular sulcus. The posterior part of the inferior peri-insular sulcus limits with the anterior Heschl's gyrus, which is 3 cm in length.

The peri-insular sulci are related to the lateral ventricle. The superior peri-insular sulcus. course parallel to the frontal horn, atrium and body of the lateral ventricle. The internal capsule separates the peri-insular sulci from the lateral ventricle. The anterior insular point is found approximately 1 cm from the frontal horn of the lateral ventricle. The central insular sulcus is found 2 cm lateral to the body of the lateral ventricle. The posterior insular point is found 1 cm lateral to the atrial portion of the lateral ventricle. The deep of the temporal horn is found approximately 9 mm from the limen insulae at the temporal stem.[53]

2 Vascular anatomy – Arteries

The insula has a surgical, clinical and anatomical relationship with the middle cerebral artery. The insula is supplied entirely by an average of 100 small middle cerebral artery perforators. At the surface of the insula, about 10% of the perforators of the middle cerebral artery will dive deep and supply important structures including the corona radiata and parts of the corticospinal tract. Also, recognizing the pattern of the middle cerebral artery branches in relation to the insular anatomy may allow to protect eloquent cortex of the distal territories (e.g. M2 of the central insular sulcus becomes the central artery at the convexity). As stated above,

Cadaveric photograph of the left insula and the middle cerebral artery branches

understanding the ***limen recess*** may be of advantage protecting the lateral lenticulostriate arteries during surgery. Therefore mastery of the anatomical features of the middle cerebral artery is critical to any surgical approach to the insula. The middle cerebral artery is divided into 4 segments: M1 or sphenoidal, M2 or insular, and 3 or opercular, and M4 or cortical.[51] At the cerebral surface, the middle cerebral artery forms 12 named arteries: Temporal polar, anterior temporal, middle temporal, posterior temporal, temporooccipital, angular, posterior parietal, anterior parietal, central, precentral, prefrontal and orbitofrontal.

Sphenoidal (M1) segment of the MCA

The M1segment begins at the origin of the MCA, at the bifurcation of the internal carotid artery, and extends laterally within the depths of the sylvian fissure along the sphenoid ridge. The M1 segment ends and the M2 segment begins at the site of a 90˚ turn, the genu, near the limen insulae. The average angle of the genu measures 97˚ (range 90–130˚). The average distance of the genu from the limen insulae is 4.8 mm (range 2–9 mm). The average diameter of M1 segment is 3.21 mm (range 2.6–4 mm) and the average length 23.4 mm (range 15–38 mm).54 distal The M1 bifurcates into superior and inferior trunks. However, it can also trifurcate and, in rare occasions, it may divide into four or even five stems. The postbifurcation trunks of the M1 segment run nearly parallel to each other, diverging only minimally prior to reaching the genu. The genu can be easily identified in cerebral angiograms and during surgery, that is why it is conventionally accepted that the genu is the transition from M1 to M2. The M1 is perhaps the most dangerous segment of the MCA because it provides the lateral lenticulostriate arteries. The lateral lenticulostriate arteries arise from the medial aspect of the M1, between the proximal sylvian and the medial sylvian membranes of the subarachnoid space. These arteries pierced the central and lateral portions of the anterior perforated substance. They are critical to the blood supply of the substantia innominata, putamen, globus pallidus, head and body of the caudate nucleus, internal capsule and adjacent corona radiata, and the lateral portion of the anterior commissure. There are an average of 8 lateral lenticulostriate arteries (range from 1-15) and their diameter ranges from 0.1 to 1.5mm (average of 0.5mm). Of note, these arteries do not anastomose between themselves within the subarachnoid space.

Insular (M2) segment of the MCA

After the genu, the MCA turns into M2 and runs first over the limen insulae and then over the cortex of the insula until the peri-insular sulci, where it becomes M3 (opercular). The beginning of M2 is typically formed by the superior and inferior trunks. The average diameter of the superior trunk is 2.5 mm (range 1.6–3 mm) and the average diameter of the inferior trunk is 2.3 mm (range 1.3–3 mm). [54] The branches arising from the postbifurcation trunks that give rise to two or more cortical arteries are called "stem arteries" and do not have specific names. Most of the stem arteries divide into their individual cortical branches (final arteries) at or before reaching the peri-insular sulci. The M2 branches supplying the insula arose from the superior and inferior trunks, the stem arteries and -when present- the middle trunk and/or an accessory MCA.

Superior Trunk. The stem arteries and cortical branches arising from the superior trunk provide the sole supply to the accessory, transverse, and three short gyri. It also supplies the insular apex. The superior trunk together with the inferior trunk supply the anterior long gyrus and central insular sulcus.

Inferior Trunk. The inferior trunk and its branches feed the posterior long gyrus, the inferior limiting sulcus, and the limen area. The inferior trunk branches supply the inferior limiting sulcus in approximately 90% of the hemispheres. The inferior trunk supplies the limen insulae, with minimal contributions from the superior trunk or the early branches.

Early branches and accessory MCA. The early branches supply any part of the insula, except the central insular sulcus. The early branches most commonly supply the inferior limiting sulcus, limen area, and anterior limiting sulcus. The accessory MCA originates far away, from the A1 segment of the anterior cerebral artery. When present, it supplies the accessory, transverse and anterior insular gyri.

Arterial supply to the Insular cortex

An average of 96 insular arteries (range 77– 112 insular arteries) are found supplying the insula. The average diameter of these arteries was 0.23 mm (range 0.1–0.8 mm). [54] The ***insuloopercular artery*** is a larger caliber insular artery that runs along the surface of the insula and provides branches to the medial surface of the operculum. Approximately 90% of insular arteries are short and supply the insular cortex and extreme capsule. The remaining 10% are larger and longer and supply the claustrum and external capsule and as far as the corona radiata. These long insular arteries are mostly located in the posterior

region of the insula along the long posterior insular gyri. There is no known gross anastomosis between the insular and lateral lenticulostriate arteries. Of note, the temporopolar artery is the only cortical branch that does not send perforating branches to the insula.

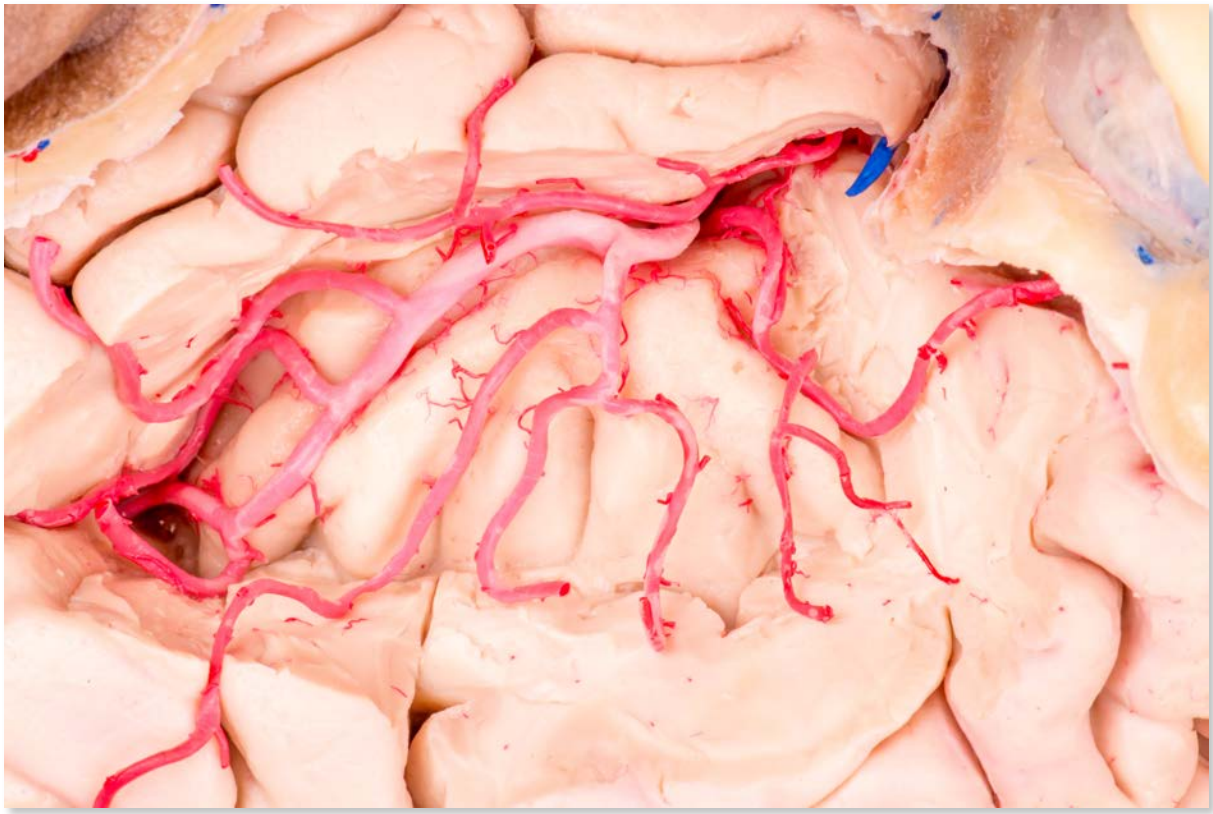

Arterial distribution of the left insula. The M2 segment of the middle cerebral artery originates at the limen

Although the specific arterial supply of the insular cortex is subject to interpersonal variability, there is a pattern that may aid surgical navigation at the insula. The accessory and transverse gyri are most commonly supplied by the stem arteries and the cortical branches arising solely from the superior trunk. The cortical arteries arising from the early branches may also contribute. When the orbitofrontal artery gives a perforator to the insula, it only reaches these two gyri. The anterior short gyrus is supplied by branches arising from the superior trunk. Also, the most common early branch feeding this gyrus is the prefrontal artery. The middle short gyrus is supplied by the branches arising from the superior trunk. When present, the early branches supplying the middle short gyrus are the precentral artery (most often) and the prefrontal artery. The insular apex is mainly supplied by stem arteries arising from the superior trunk. The prefrontal and precentral arteries (in similar contribution) are the early branches responsible for direct supply to the apex as well. The posterior short gyrus is most commonly supplied by branches of the superior trunk. The central artery, followed by the precentral and anterior parietal arteries are the early branches that contribute directly to the posterior short gyrus.

The central insular sulcus and anterior long gyrus are the only insular areas that receive branches from both the superior or inferior trunks in similar percentages and are sometimes referred to as the "alternated zone" or the "mixed zone" in the literature. The central insular sulcus is the most vascularized region in the insula. The central artery supplies the central insular sulcus in all cases. Given the critical distal territory of the central artery (primary motor and sensory cortex), this anatomical relationship is key to the neurosurgeon dissecting on the insular cortex at high magnification. The anterior and posterior parietal arteries supply the anterior long gyrus in most cases. The posterior long gyrus is supplied by branches from the inferior trunk. The angular and temporooccipital arteries exclusively supply the posterior long gyrus. The anterior peri-insular sulcus is supplied by branches arising from the superior trunk. The orbitofrontal and prefrontal arteries exclusively supply this sulcus. The inferior peri-insular sulcus is supplied by branches arising from the inferior trunk and the temporooccipital and posterior temporal arteries as the early branches. The inferior peri-insular sulcus has the most density of perforating arteries after the central insular sulcus. The perforating arteries are found most frequently along the posterior half of the inferior peri-insular sulcus. The limen insulae is supplied by the initial portion of the inferior trunk. Several early branches may contribute to the limen insulae, but the middle temporal artery is the most reliable source, sending more perforators than any other early branch.

Opercular (M3) segment of the MCA

When the M2 branches reach the peri-insula sulci they turn sharply at the edge of the insula with the opercula. This turn, which is best appreciated on a cerebral angiogram, is the transition of the M2 to M3 segments. The trajectory of the middle cerebral artery at this point is called "arterial candelabra" due to its resemblance on cerebral angiogram. The M3 have a straight lateral trajectory and cross the medial, intermediate and lateral sylvian membranes within the sylvian cistern. The M3 arteries supply the cortex of the medial surface of the opercula. Of note, when the temporal polar and orbital frontal arteries arise from the M1 segment (infrequent), they may skip an M2 segment and become M3 directly.

Cortical (M4) segment of the MCA

After traversing the lateral sylvian membrane, the M3 branches turn around the margin of the opercula and run on the cortical surface to their distal -and final- supply areas. That turn, which is also best seen on cerebral angiogram, is the origin of the M4 segment. Although there may be some variability on the branching points (origins) of the final distal M4 branches, the literature is consistent in that there are 12 M4 arteries

(named above). The arteries with special neurosurgical relevance are the central artery, because it supplies the primary motor and sensory cortex, the precentral and prefrontal arteries in the dominant hemisphere, due to its supply to the Broca's and premotor areas, the posterior temporal artery due to its supply to Heschl's gyrus (auditory center), the angular and temporooccipital arteries for their contribution to wernicke's area and the anterior temporal artery,[50,55] given its potential for intracranial bypass.

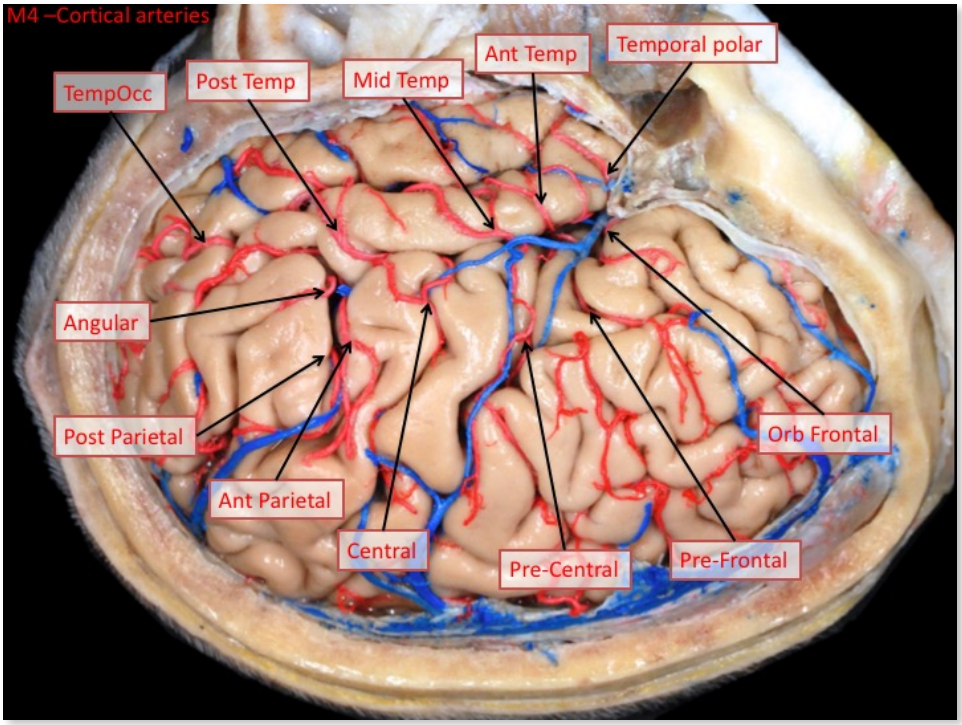

Surgical simulation of a left pterional approach with exposure of the M4 segment -cortical- arteries

3 Vascular anatomy – Veins

The venous outflow of the insula uses the main sylvian fissure vessels: the superficial sylvian vein and the middle cerebral vein.[15] The superficial sylvian vein drains primarily into the sphenoparietal sinus, but it can alternatively drain into the cavernous or sphenopetrosal sinuses. The middle cerebral vein is the largest outflow channel of the insula and it drains primarily into the basal vein of rossenthal although less often it may drain into the sphenoparietal sinus. The sylvian fissure may find collateral flow through a)

the vein of Trollard, along the central sulcus of the convexity, to reach the superior sagittal sinus; or b)the vein of Labbé, along the posterior edge of the temporal operculum, to reach into the sigmoid sinus.

Superficial sylvian vein

The superficial sylvian vein is the largest vein draining the sylvian fissure. It often originates as a single trunk at the posterior edge of the sylvian fissure. The superficial sylvian vein runs fairly straight along the posterior ramus of the sylvian fissure, in the space between the outer arachnoid membrane and the lateral sylvian membrane in the subarachnoid space. In its trajectory along the sylvian fissure, it collects tributaries from the opercula: the frontosylvian, perietosylvian and temporosylvian veins.

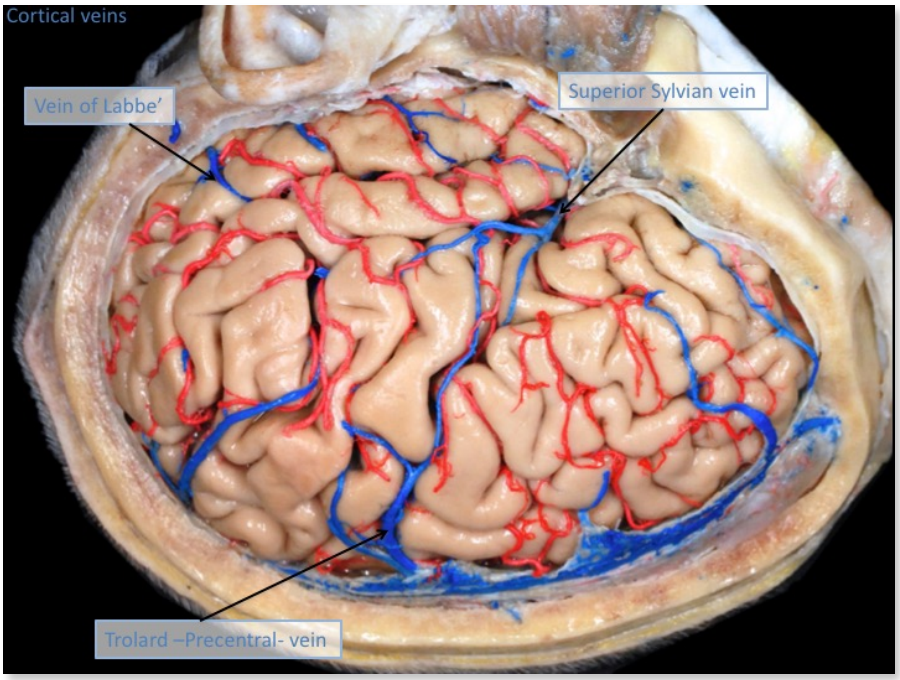

Surgical simulation of a left hemicraniectomy with exposure of the cortical veins

At the most anterior aspect, the superficial sylvian vein curves towards the temporal opercula and empties into the sphenoparietal sinus, after a short run under the edge of the sphenoid ridge. Alternatively, the superficial sylvian vein may dive into the deep proximal sylvian fissure and connect directly to the cavernous sinus or the sphenopetrosal complex.

Middle cerebral vein

The middle cerebral vein is the largest drainage system of the insula. It is formed by the confluence of many insular veins near the limen insulae. The middle cerebral vein is joined by the frontoorbital vein just before reaching the anterior perforated substance, where it receives the olfactory and inferior striate veins.

After passing the anterior perforated substance, the middle cerebral vein receives the anterior cerebral vein: that is the origin of the basal vein of rosenthal. The basal vein of Rosenthal develops from sequential changes involving anastomosis, the lesions, and re-anastomosis of primitive pial venous plexuses.[15] For this reason, the initial portion of the basal vein of Rosenthal is subject to anatomical variability. In less common cases, the middle cerebral vein will receive some deep tributaries of the initial segment of the basal vein of Rosenthal, form a common stem, and then run forward to empty into the sphenoparietal sinus. Of note, obliteration of the middle cerebral vein or superficial sylvian vein along the sphenoid ridge may prove dangerous, potentially causing seizures, facial palsy and aphasia.

Insular venous drainage pattern

The insular drainage consists of 3 groups: Superficial through the superficial sylvian vein, deep through the middle cerebral vein, and transitional, where a complex network of connecting veins bridges superficial and deep drainage. Briefly, the superficial drainage primarily includes the middle short gyrus and the insular apex, the deep venous drainage includes the limen insula, the central sulcus, the long gyri and the inferior peri-insular sulcus, and the transitional area includes the remaining cortex of the insula. The insular veins draining these insular regions are named according to their relationship with the insular sulci and gyri. Of note, the central insular vein exclusively drains the central insular sulcus and anterior long gyrus, and travels for a short distance along with the central insular artery.

4 Anatomy beyond the insula

Beyond the pia-matter of the insula starts a microscopic transition of tissues and cellular layers that carry core brain functions (e.g. putamen, thalamus, internal capsule) as well as function is yet to discover (e.g. claustrum). As part of the paralimbic system, the insula has a very interesting microscopic appearance, similar to other mesocortical structures. The insula has a progressive reduction of granular layer 4 which turns into 3 cytoarchitectural insular areas: Granular, dysgranular, and agranular sections. The granular layer is formed by a typical 6 layered structure found in other cortex regions. Layer 4 becomes thinner in the dysgranular insula, and finally disappears in the agranular insula. Interestingly, cortical layer 5 is mainly composed of large bipolar neurons with an unknown function, as described historically by Santiago Ramon y Cajal and later by Constantin von Economo.[56]

Beyond the cortex of the insula is the extreme capsule. The extreme capsule is defined in the classic literature as the group of fibers located between the insular cortex and the claustrum.[57]At the dorsal (posterosuperior) part of the extreme capsule, a thin layer of short fibers connect the insular gyri and the frontal, parietal, and temporal opercula. The ventral (or anteroinferior) part of the extreme contains a superficial layer of short fibers interconnecting the insular gyri as well as connecting the insula to the frontal and temporal opercula. It also contains a deeper layer formed by fibers of the uncinate and inferior occipitofrontal fasciculi, which cross the amygdalar, ventral, or fragmented claustrum.[25,58]

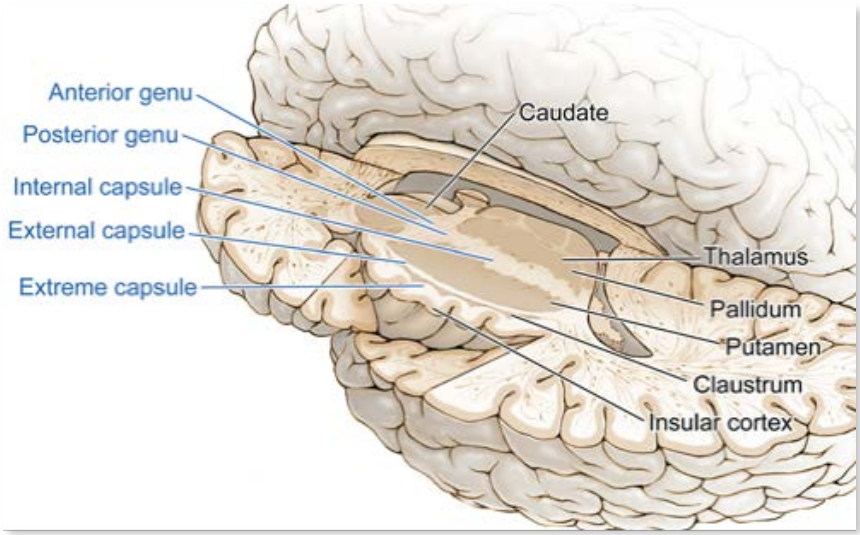

Artistic representation of the anatomy beyond the insula. Courtesy of the University of California San Francisco

Deeper to the extreme capsule is the claustrum. Although it is easily identifiable on computed tomography and MR imaging studies, the functional significance of the claustrum in the human brain is unknown. In humans the dorsal claustrum is posterosuperior, and the ventral claustrum is anteroinferior. The dorsal (or posterosuperior) claustrum is a lamina of gray matter sitting between the putamen (from which it is separated by the external capsule) and the insular cortex (from which it is separated by the extreme capsule). It has a plate sape, which narrows in the upward direction and widens in the downward direction, which forms a triangular shape in coronal crosssections of the brain. The ventral (or anteroinferior) claustrum consists of a group of diffuse gray masses fragmented by both the uncinated and the inferior occipitofrontal fascicle. Some studies further divide the ventral claustrum into two parts: superior and inferior.[25,58] The superior part of the ventral claustrum is continuous with the anteroinferior pole of the dorsal claustrum and extends inferiorly towards the base of the frontal lobe, below the putamen, connecting to the prepiriform cortex. The inferior part of the ventral claustrum is continuous with the posteroinferior pole of the dorsal claustrum, and is directed towards the amygdala. In this area, the ventral claustrum and the amygdala are almost fused one to another.

Beyond the claustrum is the external capsule. The external capsule is classically described as a layer of fibers located between the claustrum and the putamen.[26] The

external capsule contains fibers from the precentral and postcentral gyrus to the dorsal claustrum. As well as fibers running at the from the superior parietal lobule to the dorsal claustrum (at the dorsal aspect of the external capsule). The external capsule shows a clear attachment to the putamen only in the deepest layer. The putamen, internal capsule, globus pallidus (interna and externa) and thalamus nuclei are deeper to the external capsule. These structures are beyond the supply territory of the insular perforators, and its lesions may be accessed through surgical approaches unrelated to the scope of this work.

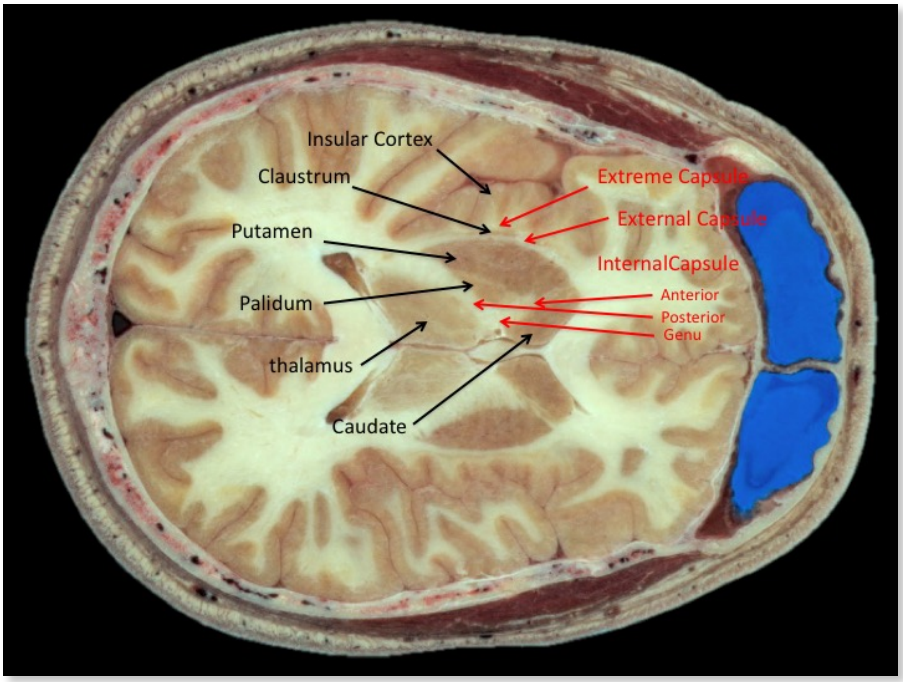

Axial section of the human head at the insula.

Beyond the cortical surface of the limen insulae is the uncinate fasciculus. The uncinate fasciculus supplies the major source of connectivity between the limbic and paralimbic systems. It forms the anterior part of the frontotemporal connection (a.k.a. the temporal stem) between the fronto-orbital region and the temporal pole. Deep into the medial and anterior aspect of the uncinate fasciculus are the fibers connecting the frontomesial (gyrus rectus, subcallosal area) and the temporomesial regions. These include the gray matter of the ventral claustrum as it blends into the amygdaloid nucleus, which is inferomedial to the uncinate fasciculus. [25,26] The uncinated fasciculus together with the anterior commissure, the inferior thalamic peduncle and the basal portion of the occipitofrontal fasciculus for the temporal stem.

Dorsal to the uncinate fasciculus and deep to the anterior insular zone is the inferior frontoccipital fasciculus. The inferior frontoccipital fasciculus is a longitudinal tract that connect the frontal, insular, temporal and occipital lobes. Its direct stimulation during surgery produces semantic paraphasias.[38,40] The inferior frontoccipital fasciculus is the main substance of the ventral portion of the extreme and external capsule. Along its most inferior trajectory, the inferior frontoccipital fasciculus becomes one with the inferior longitudinal fasciculus, adding to the high density of interconnections of this region.

Beyond the confines of the insula, lateral to the superior and inferior peri-insular sulci, is the arcuate fasciculus (also referred as superior longitudinal fasciculus). The arcuate fasciculus connects the areas of Broca, Wernicke and other parts of the convexity, and is responsible for speech and communication. This fasciculus is described as a reversed C-shaped structure that surrounds the insula and connects the frontal, parietal and temporal lobes. Exposure of the arcuate fasciculus requires excision of the cortical gray matter and adjacent superficial short U-fibers of the frontal, temporal, and parietal opercula; the middle frontal, superior, and middle temporal gyri; and the inferior parietal lobule. [25] Many of the frontal fibers of the ruperior part of the arcuate fasciculus end at the region of the inferior parietal lobule to form the frontoparietal or horizontal segment of the superior longitudinal fasciculus. At a deeper level in the temporoparietal area is the frontotemporal or arcuate segment of the superior longitudinal fasciculus. This is a group of fibers that arch around the posterosuperior insular border and run between the posterior temporal region and the prefrontal area. The temporoparietal segment of the arcuate fasciculus runs from the anterior temporal lobe in a posterior direction, lateral to the inferior peri-sylvian sulcus. This group of fibers forms the inferior longitudinal fasciculus or temporo-occipital fasciculus, which is lateral to the optic radiations.[18,25,26]

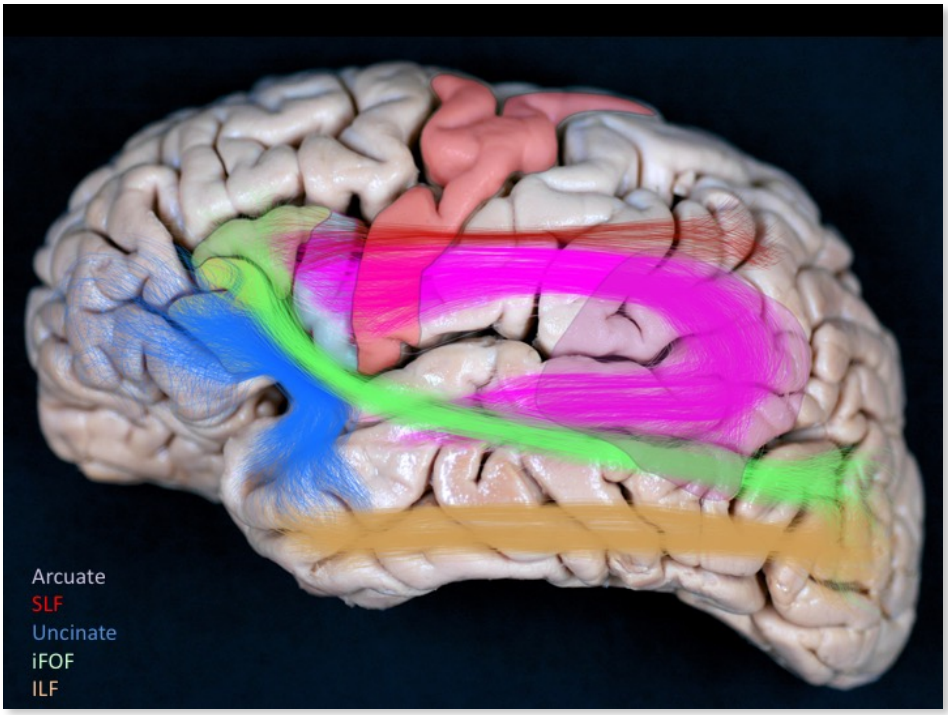

Left cerebral hemisphere with representation of the major white matter fascicles. Red= motor cortex; blue=pars opercularis; green= pars triangularis; purple= Wernicke's area;SLF= superior longitudinal fasciculus; iFOF= inferior fronto-occipital fasciculus; ILF= inferior longitudinal fasciculus

5 Function of the insula

The insula is strategically located at a dense interconnection region, where many longitudinal and association fibers connect. As described above, the insula is densely connected to the eloquent cortex in the convexity through association fibers, to complex cognitive function through longitudinal and association fascicles, to deep emotional processes through the limbic association fibers, and to sensory, visceral and motor function via thalamic and basal ganglia connectivity. A large portion of the insula receives dense sensory input from both thalamic and cortical efforts which carry auditory, olfactory, gustatory, visual and somatosensory information.[56] Therefore the insula is understood as a multimodal integration site, with potential for modulation, relay and processing of sensory function.

Studies using intraoperative direct stimulation found the somesthetic responses predominantly at the posterior insular zone.[59] when direct stimulation is applied to the posterior zone of the insula intermediate somesthetic responses consisted on warmth sensations in the contralateral arm or leg, nonpainful tingling in the contralateral arm, nasal tingling, and dysesthesias in both hands. Gustatory sensations included acid paste

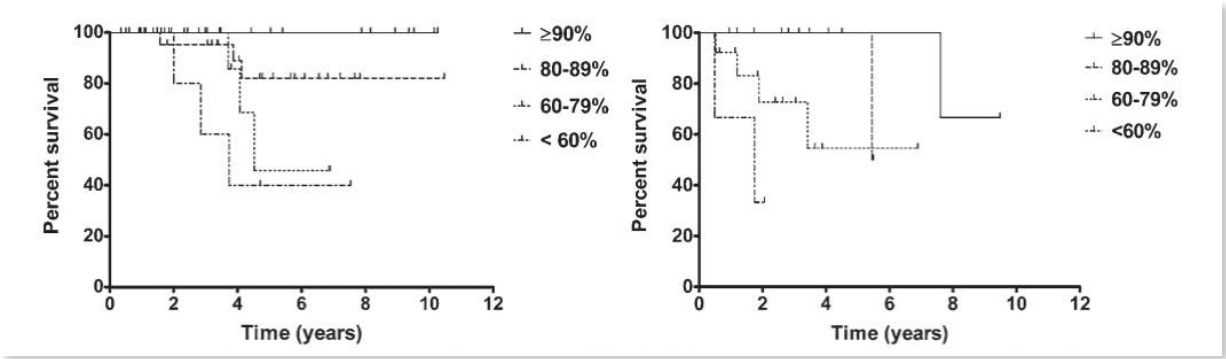

Kaplan-Meier curves revealing the overall survival of patients with Grade II (left) and III (right) insular gliomas, stratified by extent of resection. From Sanai et al Recent surgical management of gliomas, ref 35

or "bad" taste or inhability to recognize flavor.[40,56] Auditory illusions are commonly referred to as hypoacusia of the contralateral ear, visual sensations are described as appearance of a "film before the eyes" as well as a pleasant experience phenomenon reported as "flying away". [59] The posterior insula and adjacent medial operculum are activated by noxious stimuli. Interestingly, the posterior insula tends to respond only when stimulus intensity has almost reached subjective pain levels and does not show saturation for intensities above pain threshold. Conversely, the operculum responds to thermal pulses at perceptive threshold, but do not reflect intensity scale.[60] Clinical observations in both direct intraoperative cortical stimulation as well as stroke suggest that the "experience" of pain can be triggered in the posterior insular cortex. [60] Direct

electrical stimulation to the anterior insular zone activates his visceromotor and viscerosensitive reactions.[59] This stimulation is believed to disturb the neuronal network implicated in the oroalimentary behavior, with immediate viscerosensitive responses such as nausea, epigastric pressure, throat stiffness, or a very unpleasant strangling sensation, and visceromotor responses like chewing movements or lip-smacking. Specific afferents from the thalamus input signaling from many bodily sensations, such as blood oxygenation, carotid baroreceptors and pressure, under and thirst. Core vital modulations, such as heart rate, cardiovascular responses and cerebral blood flow have been linked to electrical changes in the insula.

Connections with the limbic system, in particular with dorsomedial thalamus, stria terminalis, hypothalamus, central amygdala, and parahippocampal gyrus suggest a role in emotional behavior such as fear and anxiety. An example of the limbic function associated to the insula is that of pain dissociation, where patients recognize pain but do not respond negatively to the stimulus.[56] As revealed in functional MRI studies, the insular cortex is also found to contribute to the processing of empathy.

Perhaps the most striking function association of the insula is with the articulation of speech [34,38,40,43-45,47,51,53,56,59,61-63]. Speech is a complex communication ability that characterizes and defines the human being. It is considered a cognitive function critical to interpersonal and social development, and its dysfunction is extremely debilitating. Certain types of brain injury have been associated to speech impairment (known as apraxia of speech, or motor aphasia). There is scientific evidence suggesting a strong association between the insula and the articulation of speech. [61] In a landmark article published in nature, a robust double dissociation was found suggesting that the posterior short insular gyrus is responsible for speech articulation. [61] Several authors reported their clinical experience and outcomes relative to speech and insular tumors, which resonates the evidence supported by basic research.[38,40,42,43,45,47,59,63] This body of work is of key neurosurgical importance, as it translates into the surgical exposure of the insula, specifically in mapping safe entry zones for corticectomy (cortical transgression to access deep lesions); reinforcing the importance of preserving the central artery of the insula; and the importance of subcortical mapping, to name a few.

Surgical Assessment of Insular Gliomas

Many lesions can compromise the insula, including tumors, vascular malformations and aneurysms. The most aggressive (and most devastating) tumor affecting the insula is the glioma, for its aggressive growth and spread to the deep nuclei, high functional eloquence at risk and challenging surgical reach.

Gliomas account for 27% of all brain and 15% of all primary central nervous system (CNS) tumors, according to the American Brain Tumor Association.[64] Gliomas are the most common intrinsic tumors found in the insular region. The insular lobe and paralimbic region are affected by up to 25% of low-grade and 10% of all high-grade gliomas.[35,65] Insular tumors typically present with debilitating symptoms, such as intractable epilepsy or motor dysphasia. [65] For decades, insular tumors were considered inoperable due to lack of understanding of the precise functions of the insular and para-limbic region, in addition to its proximity to eloquent cortices and white matter tracts.[40,66] Over the years, the anatomy and functional aspects of the insula and para-limbic region have been described, allowing for refinement of surgical strategies and better understanding of this anatomical region.[66]

Although lacking class I evidence, there is overwhelming literature documenting the independent role of the extent of gross total resection of low grade insular gliomas on overall survival, progression free survival as well as improved seizure control.[34,35,44,65-70] The extent of resection is significantly related to clinical outcomes as demonstrated by the Kaplan-Meier survival curves.[35] In a retrospective series we published before, we analyzed perioperative outcomes after 115 consecutive surgical resection of insular gliomas focusing on the effect of extent of resection on patient outcomes and morbidity. We then proposed an anatomical classification system for insular gliomas to improve prediction of the likelihood of extent of tumor resection in the preoperative setting.[34]

The insula was divided into four zones using two axis – one in a sagittal plane along the sylvian fissure horizontally and another in a perpendicular plane at the level of the Foramen of Monro-, these included: anterior-superior (Zone I), posteriorsuperior (Zone II), posterior-inferior (Zone III), and anterior-inferior quadrants (Zone IV).[34] This development was considered a cornerstone in the understanding of surgical management of these lesions as insular gliomas could be now classified according to their location and outcomes.[66] In the last stage of this thesis work, we aimed to validate our previous extent of resection predictions to complement the laboratory work and provide clinical perspective on our surgical technique considerations. We applied our previously described insula classification system to a new cohort of insular gliomas to determine the inter-observer reliability among physicians at various levels of clinical expertise and experience.

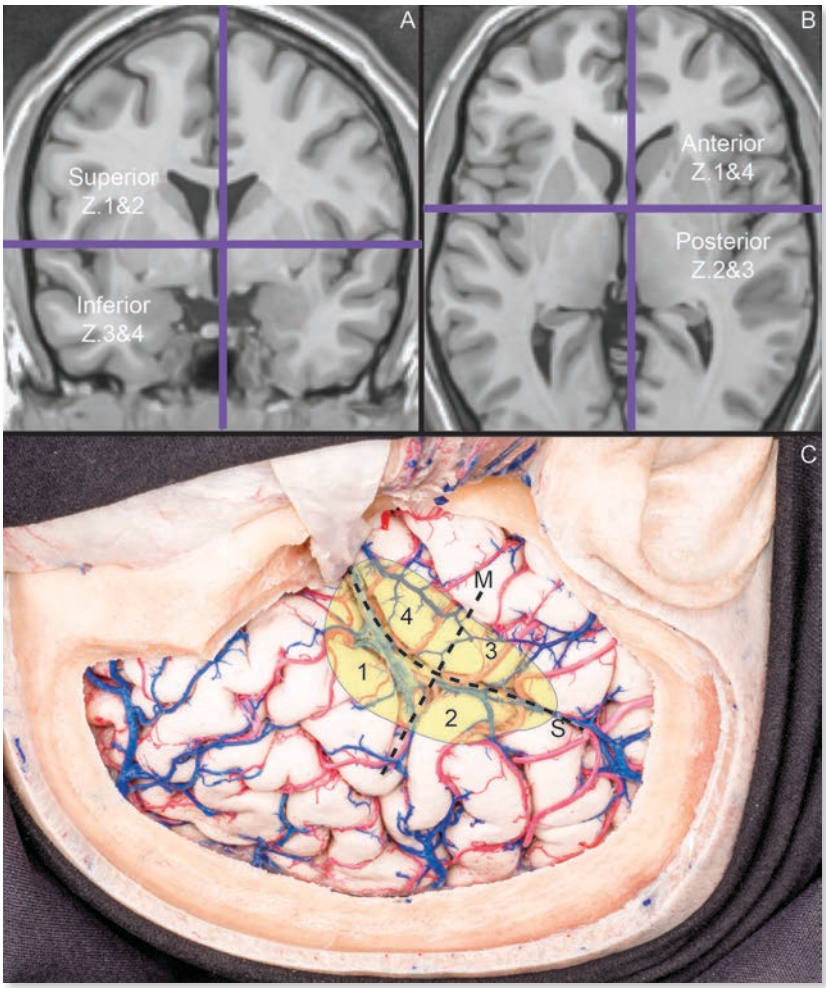

Representation of the four major divisions of the insula. Coronal (a) and axial (b) sections of a T1-weighted MRI with the cross-axis at the foramen of Monro. SC- surgical simulation of a right pterional approach with the zones 1-4 of the insula.

Although lifesaving, operative management of insular gliomas is challenging. In contrast to other regions of the cerebral cortex, surgical access to the insula specifically difficult because its cortex is deep to the cerebral convexity, at the floor of the sylvian fissure and covered by the overhang of the opercula and many critical vascular structures. Additionally, several cortical areas covering the insula are very relevant to the core aspects of human existence. Also, the venous system within the sylvian fissure is often very important for the drainage of the lateral surface of the brain and must be preserved.[71] The presence of a relevant venous system further narrows surgical options for tumor removal. For these reasons, these tumors were often deemed inoperable. The advent of intraoperative electrophysiological monitoring, awake brain mapping, advances in anesthesia and the use of intraoperative magnetic resonance imaging (iMRI) has played a significant role to enabling maximal resection of these tumors while maintaining a reasonable safety margin.[35,66] Prior reports suggest that aggressive resection of both low- and high-grade insular gliomas may carry acceptable morbidity. [29,34,35,38,40,44-47,65,66,68,69] Surgery in the insular region is associated with a 14-59% rate of transient neurologic deficits and upto 20% rate of permanent deficits.[43,69] Complications associated with insular glioma resection include damage to the descending motor fibers, injury to the long M2 perforators or excessive retraction on the opercular regions leading to a deficit involving the Broca's area, horizontal fibers of arcuate fasciculus or uncinate fasciculus fibers and accidental damage to the lenticulostriate arteries (LSA) which can manifest as hemiplegia.[29,54,65]

Surgical access to insular gliomas may be accomplished through two main approaches -the transsylvian (TS) approach and the transcortical (TC) approach-, or a combination of both. In 1992, Yasargil et al. first described a safe transsylvian route for the tumor resection and proposed a classification system based on the tumor growth patterns.[23] However, the transsylvian approach requires wide splitting of the superficial and deep sylvian cisterns and precise dissection around the opercular arteries and their perforators, as well as preservation of the superficial sylvian veins when they are large. It also requires opercular retraction, which is often limited by the superficial sylvian veins bridging the sylvian fissure. Thereby the trans-sylvian approach may often not offer optimal surgical access to achieve the desired surgical results for large insular lesions. On the other hand, the transcortical approach, which uses a trajectory directly traversing the cortex, carries risk to the motor functions and potential language deficits. The lateral surface of the opercula may be mapped during an awake procedure with the use of cortical and subcortical intraoperative stimulation, allowing identification and preservation of functional areas.[29,38,41] Removing "*silent*" cortical areas such as the superior temporal gyrus is an emerging strategy to maximize the extent of tumor resection while preserving the superficial vascular structures.[38,68] We have previously reported our transcortical "window" technique, aiming to get transcortical access through the smallest trajectory while preserving the cortical vessels.[34] In the current clinical practice, it is often the experience of the surgeon, rather than a scientifically-based rationale, that determines which approach (i.e., transsylvian or transcortical) is used. At the time of this work, there is no supportive data based on objective cadaveric surgical simulation to determine the differences in surgical access to the insula between the transsylvian (TS) and transcortical (TC) approaches.

There is a lack of evidence as to which technique (i.e transcranial or transsylvian) or a combination of the two would yield the optimal maneuverability (i.e.surgical freedom, blue), space to access (i.e. surgical window, green) or insular cortex at reach (i.e. surgical exposure, red dotted line) to maximize safe extent of resection for each type of insular glioma. Using a sequential experimental design, we investigated whether there is a significant difference in insular exposure, surgical window, and surgical freedom between the following approaches: the TS approach, the TS after cutting the superficial sylvian veins bridging over the sylvian fissure (TSVC), and the TC approach. Also, we sought to evaluate the venous drainage of the perisylvian region to provide evidence on the likelihood of venous dominancy as a limitation for venous sacrifice during a TS approach. Additionally, the surgical anatomy related to each procedure along with the final surface exposure of the insula was studied.

Performing this research in patients is not feasible and may be unethical. It is not feasible because it requires prolonged and meticulous protocols incompatible with

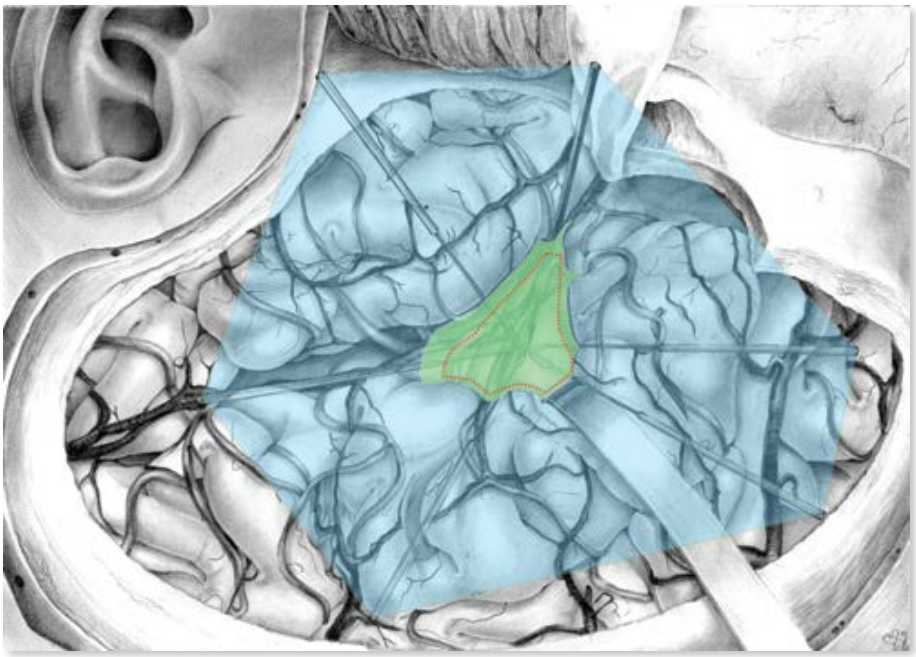

Illustration of the concept of insular exposure, and surgical window and freedom. The left transsylvian approach to insular zone one was conceptualized by the medical illustrator. The insular exposure (dotted shape) is the area over the insular cortex available through a surgical approach. The insular exposure is the amount of access to the insular cortex provided by each approach. The surgical window (dark shade or green), is the area existing between the neurovascular structures limiting the space to access the insula, i.e. the corridor. The surgical window provides information on the space available to pass instruments to a particular insular zone by each approach. The surgical freedom (outer shape or blue) is the area formed by the top of a dissector that, while pivoting on a surgical landmark, it contacts the perimeter of the surgical opening. The surgical freedom allows measuring the degree of maneuverability or ease to manipulate instruments to a particular point in the insula.

anesthesia times. It isn't ethical because it would imply performing human experimentation and procedures not directly related to the benefit of the patient. Therefore we designed a surgical simulation protocol using cadavers to carry this stage of the research. In order to have a valid clinical translation and optimal applicability of the evidence obtained in the laboratory, we sought to improve the current cadaver-based neurosurgical simulation research methodology before conducting this stage of the research.

The most widely accepted method to research in neurosurgical technique is surgical simulation using human cadavers, because it provides the closest approximation to a live surgical procedure with true human anatomy. The main goal of anatomical cadaveric processing is to achieve the most realistic model possible. Several models for neurosurgical training and technical development have been described in the literature.[72-77] There have been several major advances in this field.[72,73,76] However, none of these reports provides advances in cadaveric embalming methods to maintain the physical properties of a living brain while preserving the brain specimen from decay. These properties are key to allowing for complex surgical technique development and testing.

The major physical properties to be considered when addressing embalming research are brain stiffness, preservation time, and biohazard safety. Brain stiffness is at the core of simulating live surgical interaction with brain tissue, and is essential to allow valid measurement of surgical corridors. Preservation time allows for continued use of a dissected specimen for a tedious, sequential acquisition of data during lengthy surgical techniques, as well as allowing comparison of different approaches through the same anatomy. Performing surgical technique research requires long exposure time to the source of data -the cadaver-, which may become unsafe if embalming formulas emanate toxic or biohazardous airborne particles (e.g. formaldehyde).

Two common processing techniques used in cadaveric neurosurgical simulations are cryopreservation (unembalmed, stored frozen) and formaldehyde-based preservation. Cryopreserved specimens provide optimal brain stiffness but have a short preservation time and are considered biohazardous. Formaldehyde-based embalming formulas are the standard for long preservation of specimens. However, formaldehyde substantially increases brain stiffness, making retraction and surgical simulation very difficult and unrealistic.

Additionally, many studies have reported that long-term exposure to high airborne formaldehyde concentrations in the laboratory is hazardous.[78-82] In 2006, the International Agency for Research on Cancer (IARC)[83] and the US Environmental Protection Agency[84,85] classified formaldehyde as a probable human carcinogen. Therefore, there is a need for a customized embalming formula for neurosurgical simulation that enhances brain compressibility (a surrogate for surgical retraction) and enables retraction while preventing microorganism growth and brain decomposition. This becomes extremely important when performing research on the surgical access to the insula -given its deep anatomical location- which requires advanced neurosurgical techniques.

After several years of trial and error, and chemical modifications to conventional embalming formulas, we have designed an embalming formula specific for neurosurgical simulation that enhances brain compressibility and enables retraction while preventing microorganism growth and brain decomposition. This cadaveric embalming formula also decreases potential chemical biohazards to meet the IARC recommendations for laboratory safety. In this first stage of the thesis, we assessed the properties of our proposed formula and compared its application to surgical simulation against standard postmortem processing techniques—cryopreservation and formaldehyde embalming—in a sample of cadaveric specimens. We also analyzed the applications of each technique to neurosurgical training and research and provide recommendations on specimen preparation for neurosurgical simulation research. This provided the foundation upon we

developed stage two, where our surgical simulation method (including the embalming formula) was used to study the surgical profile of the approaches to the insula.

In summary, the current surgical management of insular gliomas is based on surgeon's preference and experience, without an evidence-based guide for surgical planning and no clear objective data to support choosing one surgical technique over another (transsylvian versus transcortical). Also, the gold standard cadaver preparations for neurosurgical technique research is suboptimal, therefore limiting valid and applicable conclusions from laboratory investigation.

This thesis was designed to provide sound evidence on the surgical management of insular gliomas using sequential research that is cumulative and uses basic, applied and clinical research methods. First, I aimed to develop a customized embalming protocol (embalming formula and procedures) to optimize neurosurgical simulation and increase applicability and validity of laboratory research. Second, using the embalming procedure previously defined, I aimed to determine the technical advantages and disadvantages of each surgical technique for insular glioma resection using cadaveric simulations. Finally, I aimed to complement the laboratory findings with a retrospective clinical study to determine the correlation between the anatomical location of the insular gliomas (in zone I-IV) and clinical outcomes and tumor resection rates. The grand view of this research was to provide cumulative evidence to define the best surgical technique for each insular zone (zones IIV) and refine the expected outcomes –and patient expectations- related to treatment of gliomas in each anatomical location.

Study Aims

This thesis aims to define the optimal surgical strategy for the management of insular gliomas. The following hypothesis and objectives are sequential and the evidence obtained is cumulative.

Hypothesis:

1. H0 = The proposed neurosurgical simulation method does provide the same brain retraction, environmental safety and lasting time as the formaldehyde and cryopreserved (unembalmed, frozen) methods. H1 = The proposed neurosurgical simulation method provides more brain retraction, is environmentally safer and last as much as the gold standard.

2. H0 = There is no difference on surgical exposure, freedom or window between the studied surgical techniques when applied to each insular region. H1 = There are specific differences (advantages and disadvantages) to the transsylvian vs transsylvian with venous sacrifice vs transcortical approaches relative to each insular tumor depending on the anatomical zone.

3. H0 = There is no difference on clinical outcomes or resection rate between each insular region. H1 = There is/are difference/es in outcomes and extent of resection rate relative to tumors in different regions of the insula.

Objectives:

1. **To design and customize a surgical simulation method** (including our custom embalming chemical formula) **for preservation of native features of the brain during surgery on postmortem human heads.** Specifically, the objective is to obtain a cadaveric brain retraction profile statistically equal to that of live surgery to optimize applicability and validity of laboratory neurosurgical research using human cadavers. This will function as preliminary evidence to strengthen the validity and generalization of aim "B".

2. **To define the optimal surgical technique for gliomas relative to their location in the insula.** Specifically, to identify which surgical technique (transsylvian vs

transsylvian with venous sacrifice vs transcortical) is better for accessing each anatomical division of the insula (zone I-IV) using surgical simulation in cadavers

3. **To define and validate the correlation between anatomical localization of insular gliomas (zone I-IV) and clinical outcomes and resection rates**. Specifically, to define the surgical outcomes for gliomas related to each insular zone using a retrospective clinical review.

METHODS

Objective A – Customization of the Embalming Protocol (chemical formula and proceedings) for Preparation of Cadaveric Heads

Eighteen human specimens (age range at death 50–95 years) were prepared for surgical simulation to study the properties of 3 cadaveric processing techniques (cryopreservation, formaldehyde-based embalming, and customized-formula embalming). Donors with premorbid conditions of the CNS were excluded from our study. Specimens in the embalmed groups (formaldehyde and custom) were kept immersed in their respective embalming fluids for a mean time of 8 months (range 2 weeks–1 year) before the experiment. Six cryopreserved and 6 formaldehyde embalmed specimens were prepared according to conventional processing techniques for neurosurgical research.[86]

Six additional specimens were prepared using our customized embalming solution. A standard pterional approach was performed in all specimens to compare brain compressibility, retraction profile, and preservation time. One MR image of 2 specimens in each group was obtained. One customized specimen was also prepared to test the feasibility of bleeding simulations.

Head Preparation

All heads were prepared for optimal neurosurgical simulation. The neck was sectioned at vertebrae C5–7 to provide good exposure of cervical vessels and preserve the cervical spinal cord. Common carotid and vertebral arteries along with jugular veins were identified and isolated. Minimal sharp dissection was performed around vessels to prevent undesired rupture of deep arteries and veins, which could cause leakage during silicone injection. Cervical arteries and jugular veins in the embalmed groups were cannulated according to previously described methods.77,86 Arterial and venous systems were cleaned using saline solution until contralateral outflow was clear. This procedure was repeated bilaterally on each cannulated vessel, alternating arterial and venous irrigation. Once all blood clots were cleared from external and internal vascular

systems (carotid and vertebral arteries and jugular veins), the specimens were randomly divided into the customized and formaldehyde groups. Because of their fast decay time, cryopreserved specimens were not cannulated or injected to maximize their experiment time.

Embalming Procedures

Customized and standard formaldehyde embalming solutions were used for comparative analysis. One-half liter of fixative was perfused through common carotid and vertebral arteries (200 ml) and jugular veins (300 ml) in each head. The customized mixture was prepared in the laboratory using the following formula: ethanol 62.4%, glycerol 17%, phenol 10.2%, formaldehyde 2.3%, and water 8.1% (Fig. 1). A conventional 10% formaldehyde solution was used for the formaldehyde group. All embalmed heads were immersed in a 1:10 dilution of the respective embalming fluid and stored at 5°C for at least 2 days before silicone injection. Cryopreserved specimens were frozen at postmortem Day 1–5 at -15°C to -20°C and thawed for approximately 12 hours before proceeding with the surgical simulation.

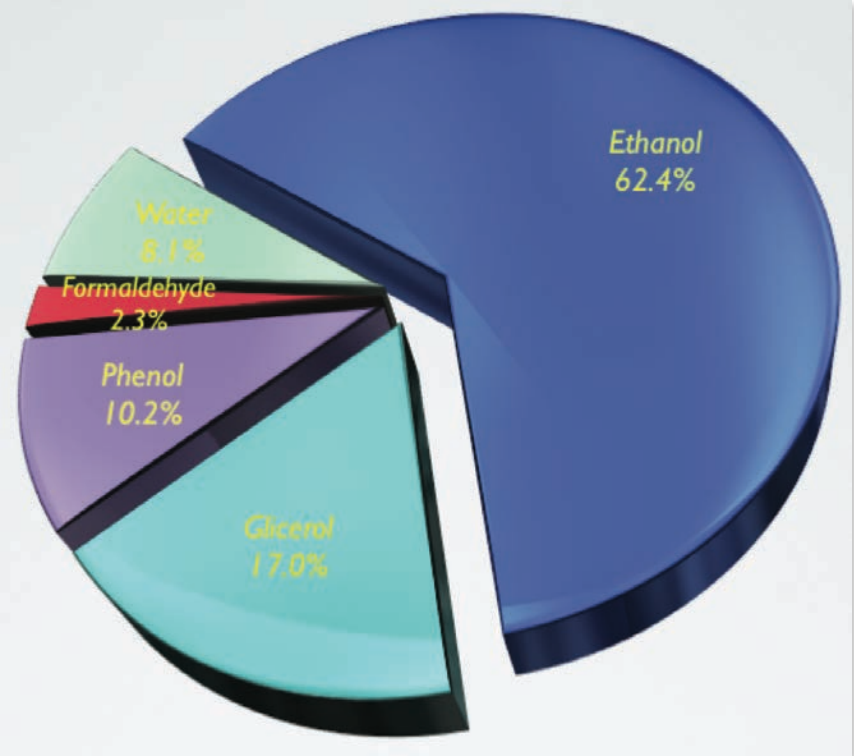

Chemical components of our embalming formula

Vascular Silicone Injection

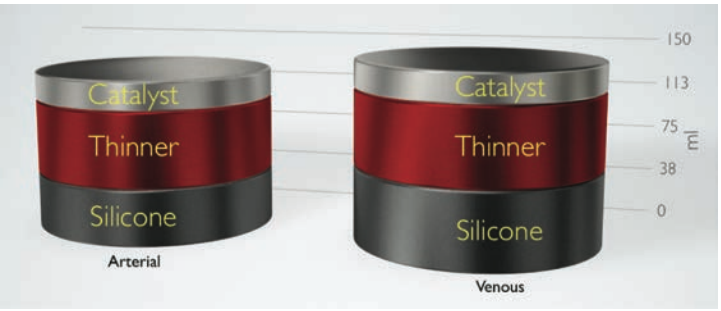

Arterial systems were injected with red silicone, and venous systems with blue silicone. The arterial system—common carotid and vertebral arteries—was processed first to secure filling of the distal and small thalamoperforating arteries. Common carotid arteries were bilaterally injected until vertebral artery colored outflow was observed. Bilateral vertebral artery injection was then performed until the arterial system was fully injected. Finally, the arterial system was clamped except for one carotid artery, which was used to increase arterial pressure to force small-caliber vessels to fill. Upon completion of arterial silicone injection, jugular veins were processed using the same injection principles.

Comparative Analysis

The durability and retraction (stiffness) properties of specimens treated with our customized formula were compared with the properties of specimens treated with cryopreservation and formaldehyde-based preservation. A standard pterional craniotomy was performed on each specimen. The dura mater and arachnoid membranes were carefully removed, and the temporal lobe was gently retracted dorsally to simulate a subtemporal approach. Retraction profiles were measured using an intracranial pressure transducer and monitor (Integra Camino parenchymal intracranial pressure monitoring kit) inserted 8 mm into the inferior temporal gyrus, 4 cm posterior to the temporal pole. Pressure measurements were recorded before temporal lobe retraction and at the tissue retraction limit. This limit was set at the highest, most retractile pressure before tissue damage and was dependent on the retraction profile of each specimen. The optic and oculomotor nerves, supraclinoid internal carotid artery, anterior clinoid process, and tentorium were used as surgical landmarks to compare subtemporal surgical exposures among the processing techniques. The total retraction surface was also measured. Ten pins were inserted along the cortex surface and registered as stereotactic points using a surgical navigation system (Stryker Nav3). The pins remained in the same cortical surface

location throughout the experiment. Stereotactic coordinates were obtained from each pin by touching it with the navigation probe at resting state and at the tissue retraction limit (Fig. 3 right). Surface areas were calculated from the stereotactic coordinates using dedicated software (Surface Area Calculator, BitWise Ideas Inc.) and recorded in a spreadsheet for statistical analysis. Retraction surface was obtained by subtracting the area at retraction limit from the area at resting state.

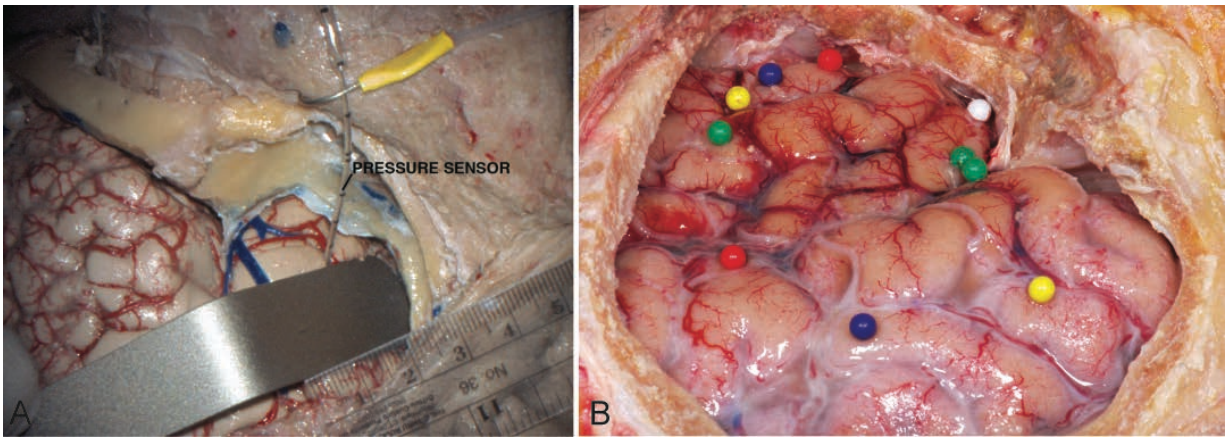

Photographs of the specimen preparation for the morphometric experiments. A; A pterional craniotomy was carried out to expose the lateral surface of the brain. The pressure sensor was introduced into the inferior temporal gyrus near the retractor spatula. B; Ten pins were inserted into the lateral surface of the brain to measure the retraction area in all specimens.

We also sought to study the durability (preservation time) of specimens. Two specimens from each group were prepared and continuously exposed to laboratory working conditions for 2 days. We studied changes in tissue consistency, color, and decay to compare specimen conditions at observational study spreadsheet was completed for the duration of the experiment, and consistency, color, and overall appearance were recorded as dichotomous variables (1 = changes observed, 2 = no changes observed). Subjective appreciations (odor and texture) were also recorded and analyzed after the experiment. To complement the observational study, we administered a blinded survey to a sample of 4 neurosurgery residents and 2 attending neurosurgeons to evaluate the best specimen group after the experiment ended. The volunteers were asked to "please rate hierarchically the images in the attached figure as to their similarity to the real brain in terms of color and texture." Data were collected and descriptive statistics was performed using SPSS Statistics Desktop, version 21.0 (IBMCorp.). The mean retraction pressures, retraction surfaces, and durability lapsing times were compared using independent Student t-test analysis. A $p < 0.05$ was considered statistically significant.

Imaging and Post-processing Techniques

Radiological studies are very important in neurosurgical simulation and research; therefore, 3-T T1-weighted FLAIR MRI was performed on 2 heads from each group on the same day as specimen processing. The radiological images were used to compare the quality and preservation of internal nuclei, cortex, white matter, and the whole encephalon before starting the surgical simulations. In one case, a cryopreserved specimen received on postmortem Day 8 was scanned. Although this specimen provided clear radiological evidence of the decay process in cryopreserved specimens, it was excluded from the morphometric study. The bleeding model for neurosurgical simulation was prepared and tested in 1 customized specimen as described elsewhere.[72,76]

Objective B – To Compare the Transsylvian Approach and the Transcortical Approach for Insular Glioma Resection using Cadaveric Surgical Simulation

We studied and compared the surgical corridors of the TransSylvian (TS), TransSylvian with bridging veins cut (TSVC) and transcortical (TC) approaches (independent variables) to the insula at the UCSF skull base and cerebrovascular laboratory.

Neurosurgical simulation Laboratory, UCSF. California, USA, 2017

An experimental laboratory investigation was designed to measure the insular exposure, surgical window and surgical freedom (dependent variables) resulting from each corridor in 10 specimens (all continuous ratio variables). Additionally, we carried out a descriptive study in 16 specimens to complement the experimental design providing critical information for the surgical planning and approach selection process. The descriptive study included categorical dichotomus variables such as the presence of bridging veins over the Sylvian fissure; dominance of the superficial Sylvian vein complex, presence of vein clustering, continuity from the artery of the central sulcus of the insula to the Rolandic artery, and the relationship between the superior segment of the squamosal suture and the Sylvian fissure. Additionally, the number of M2, M3 and M4, (continuous interval variables), distance from the external acoustic meatus to the foramen of Monro (anterior-posterior and cranial-caudal) and the distance from the temporal pole to the cortical resection margin (continuous ratio variables) were recorded.

Insula surgical classification

To facilitate data interpretation and enhance the surgical relevance of this study, the Berger-Sanai surgical classification scheme of the insula was used to subdivide the insula into 4 zones.[34] Therefore, th e insula was divided into anterior and posterior from the axial projection of the foramen of Monro; and superior to inferior by the Sylvian fissure line projected over the insular cortex. Zone 1 was the anterior-superior quadrant; zone 2 was the posterior-superior quadrant; zone 3 was the posterior-inferior quadrant and zone 4 was the anterior-inferior quadrant.

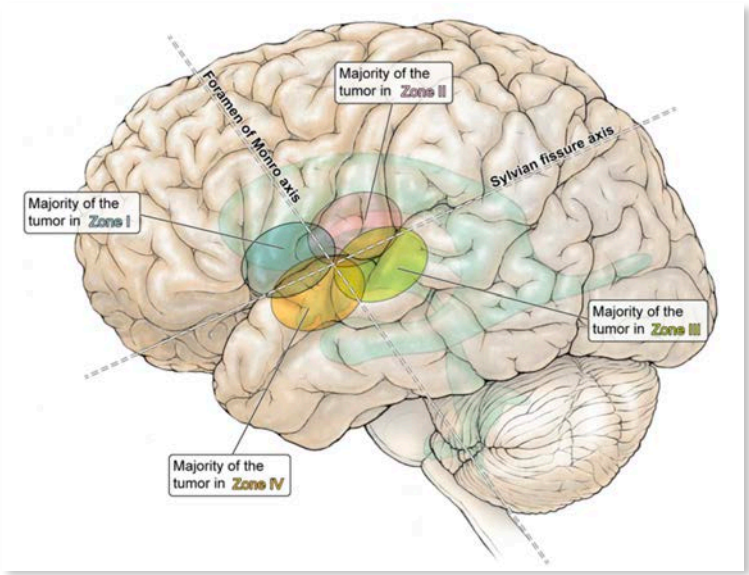

The Berger-Sanai classi cation of insular gliomas separates insular gliomas based on their location above or below the sylvian ssure and anterior or posterior to the foramen of Monro. Artist: Kenneth Probst. Copyright Department of Neurological Surgery, University of California, San Francisco.

Description of the Variables

Independent Variables:

The TS approach utilizes only the Sylvian fissure split and retraction over the opercula or inferior Rolandic cortex to expose the insula. In this approach, the superficial and deep Sylvian cisterns are opened widely throughout the fissure. The TSVC uses the same surgical route created previously by the TS approach with the addition of cutting the bridging veins crossing the Sylvian fissure, therefore allowing additional retraction to the opercula and Rolandic cortex. The TC approach uses different degrees of cortical resection to expose the insula. In the TC, the bridging veins are preserved and the space to access the insula results from multiple windows between the middle cerebral arteries

and the superficial Sylvian veins that will remain intact throughout the procedure. In zones 2 and 3, the TC was further divided into two subcategories. In zone 2, the first set of dependent variables was taken before and after the operculum portion of the precentral gyrus was resected. In zone 3, the first set of dependent variables was taken before and after removing the cortex of Heshl's gyrus. This sub-categorization was set in the experimental design to include the option for a less invasive cortical resection and to investigate the significance of the sacrifice of such cortical areas during a TC approach to the insula.

Dependent Variables:

The insula exposure is the area (cm^2) of insular cortex exposed and surgically reachable for bi-manual dissection. The area was obtained by touching the cortical perimeter with the navigation probe to obtain the stereotactic coordinates as previously described.[87] The surgical window is a polygonal area limited by the structures that, in more superficial planes, confine the surgical route to the insula. The arteries, veins and cerebral cortex were the typical structures limiting the surgical window. The surgical window area was calculated using stereotactic coordinates obtained by touching the limiting structures of the surgical corridor with the navigation probe. Finally, the surgical freedom was also measured. The surgical freedom provides an objective assessment on how freely an instrument can be moved within a surgical corridor and in relation to a particular target. We used a point in the center of each insular zone to determine the surgical freedom (cm^2). A *Rhoton* # 5 dissector was pivoted at the center of each insular zone. Then the handle was moved in the perimeter of the surgical window to capture the contour of the corridor. The navigation probe touched the tip of the dissector handle in each major limiting point (change in trajectory) and recorded a set of stereotactic coordinates.[87] Additionally the extent of cortical resection after a transcortical approach to each insular zone was measured. Three stereotactic points were obtained in each zone by touching the lips

Screenshot of the navigation system after a full experiment on a study cadaver. The coordinates where then processed with dedicated software to obtain the measurements

of the sylvian fissure with the navigation probe. Then the cortex was resected simulating a transcortical approach to the insult at each zone. After the resection was complete, the same points along the Sylvian fissure were touched with the navigation probe now over the resection rim. Three linear measurements were obtained by calculating the distance between each point obtained over the lip of the sylvian fissure (pre-resection) and its equivalent at the resection margin (post-resection).

Specimen preparation

We selected and prepared 16 embalmed human cadaveric specimens (n=16) without previous history of head and neck pathology and with a postmortem window of 72 hours. The specimens were embalmed with our proposed customized formula for neurosurgical simulation. After 5 days immersed in embalming solution, the specimens were prepared for surgical research following our guidelines.[87] A 3-Tesla T-1 weighted magnetic resonance imaging sequence was obtained from all specimens before the study. Radiological data were uploaded to the navigation station. These studies were co-registered to the specimens before each experiment.

Experiment design

The experiments were conducted following a thorough standardized protocol with a detailed stepwise checklist. All significant surgical steps were recorded using stereoscopic (3D) video (Truevision®) and photography (Nikon®). The specimen was rigidly fixed in a three-pin surgical freedom clamp (Mizuho®) attached to a surgical table and then positioned for a pterional approach to the insula. A question mark skin incision was based roughly 1 cm before the tragus, widened 1 cm posterior to the pinna and finished in the midline behind the hairline. The skull was exposed after standard galea dissection and temporalis muscle retraction. At this point, the foramen of Monro was navigated with the stereotactic probe and reference measurements to the external acoustic meatus were obtained. The relationship between the squamosal suture and the Sylvian fissure was obtained with the aid of navigation. The Sylvian fissure was then marked with a skin pen on the skull. A wide pterional craniotomy was designed based on: A) the foramen of Monro, B) the Sylvian fissure (already marked in the skull) and C) the opercula including at least 3 cm of extra cortical surface to allow for retraction. The dura was incised and turned anteriorly over the sphenoid ridge.

The Sylvian fissure was completely split as previously described.[49] All venous channels were carefully dissected and preserved. Self-retaining retractors were applied to the zone 1 operculum and constantly repositioned following the navigation probe as the insular

exposure, surgical window and surgical freedom stereotactic measurements were taken. Dynamic retraction was selected to better reflect a real surgical scenario, where the retraction blades are constantly re-positioned to provide the best space in each surgical maneuver. The amount of retraction, which was measured in length, was the maximum allowed by the bridging veins or before cortical damage. The same procedure was repeated for zones 2, 3 and 4. The arterial and venous cortical systems were manually drawn separately in a printed hemispheric template (one set for each side) map. Number, size and trajectory of the veins were recorded as well.

Next, the veins crossing the Sylvian fissure were marked and cut. All dependent variables were measured again in the zones previously limited by bridging veins (anterior bridging veins = zones 1&4 vs posterior bridging veins = zones 2&3). Following this, the veins previously cut were anastomosed using 6-0 or 8-0 sutures and a ***Lawton bypass set*** (Mizuho America).

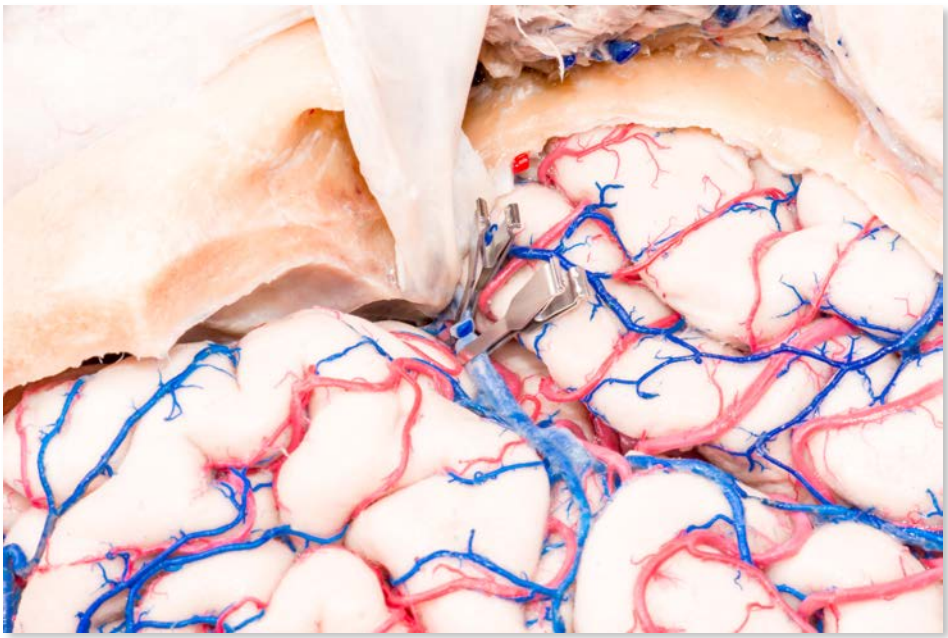

Surgical simulation photograph after a right pterional approach with exposure of the sylvian fissure. The superficial sylvian vein was prepared for reanastomosis.

After restoring the venous system completely, the TC approach was started. The corticotomy was based on the cortical surface identification of the peri-insular sulci with the aid of navigation. The corticotomy was performed using microsurgical instruments and magnified dissection under the surgical microscope (Carl Zeiss Pentero ®), with caution to preserve M3 & M4 arteries transitioning to the cortical surface. Multiple arterial-venous windows were generated after removal of the operculum at the end of each corticotomy. All dependent variables were measured at this point, including the TC subdivision into zone 2 with and without the precentral motor cortex and zone 3 with and without Heshl's gyrus. Reference pins were set along the margins of the corticotomy to reference the previous position of the operculum limits in each case and guide the transition to the next zone. The cortical limits after the corticotomy were drawn in a lateral cortical hemispheric template map to track

the anatomical structures resected. The distances between the cortical resection margin and both the operculum and the temporal pole were also taken at this point. After completion of the TC approach to all zones, all M2 branches were drawn over an insular template map previously printed.

Statistical analysis

All data collected in this study was entered in a spreadsheet that was uploaded into statistical software (JMP® v. 11.0, SAS institute) for statistical processing. Unpaired student t-tests were calculated on the dependent continuous variables to determine significance between the compared variables and groups. A p-value of 0.05 was considered significant. Mean and standard deviation (SD) for continuous variables and percentages for continuous and categorical variables were also calculated from the spreadsheet.

Objective C – Correlation between anatomical classification of insular gliomas and surgical outcomes

Patient Selection

Using a prospectively collected database of insular gliomas assigned to one of the previously described zones, we studied 114 consecutive patients treated in 129 restections within the last decade. Patients were all adults older than 18 years of age who had undergone surgery at the University of California, San Francisco. Perioperative patient parameters including zone classification based on preoperative and FLAIR and T1 post contrast MRI, symptom at presentation, handedness, age at diagnosis, immediate postoperative MRI (within 48 hours of surgery), and histopathology review (in accordance with WHO guidelines) were prospectively collected. Given substantial differences in their natural history patients with WHO I histology, those with multifocal glioma, and gliomatosis cerebri were excluded from analysis. All microsurgical tumor removal was performed as outlined by our prior.[34] The University of California, San Francisco Committee on Human Research approved this study.

Inter-observer reliability of Berger-Sanai Insular Glioma Classification System

According to our prior published protocol the insular was divided into 4 zones. Along the horizontal plane in a sagittal view, the insular was bisected along the Sylvian fissure. This plane was intersected by a perpendicular plane at the level of the foramen of Monro. Tumor location was assigned to 1 or more of these zones. [34] For tumors occupying more than 1 zone, this condition was denoted as such (ex. Zone I + II). For cases in which the tumor occupied all 4 zones, these insular gliomas were defined as "giant". Using this method a total of 9 possible options existed for classification (Zones I, II, III, IV, I-II, I-IV, II-III, III-IV, Giant).

To test agreement of insular zone assignment between clinicians, a subset of 80 cases with a newly diagnosed insular glioma were independently scored by three examiners. With the goal of testing clinicians across a varied distribution of clinical experiences, one junior level neurosurgery resident, one junior level neurosurgery faculty, and one senior neurosurgeon were chosen to participate. Participants were blinded to each other's

score. The kappa coefficient was used to determine the significance of this agreement. Interpretation of the kappa coefficient was performed in accordance to prior published reports in which 0 indicated agreement equivalent to chance; 0.01-0.20 slight agreement; 0.21-0.40 fair agreement; 0.41-0.60 moderate agreement; 0.61-0.80 substantial agreement; 0.81-0.99 almost perfect agreement; and a kappa coefficient of 1 indicated perfect agreement (Griessenauer 2014).

Patient outcome measurements

Patients underwent sequential neurological examinations by four clinicians: the senior attending neurosurgeon, a neurosurgical resident, a speech and language neurophysiologist, and attending neuro-oncologist. Clinical examinations were performed preoperatively, every day during the postoperative period, and at each follow up appointment (4-6 weeks, and 3-6 months following surgery). Short-term neurological morbidity was defined as new onset language, or sensorimotor deficits within the first 3-5 postoperative days. Long-term neurological morbidity was defined as dysfunction 90 days after surgical intervention. Our protocol for language function testing has been described in prior publications. [29] Differences between findings of the 4 examiners were adjudicated by accepting the results showing greater impairment. Magnetic resonance imaging results were studied to confirm that the patient's symptoms were not a result of tumor progression. Malignant progression was defined as a change in histopathology for WHO grade II and III tumors to higher-grade lesions on a subsequent surgery (including biopsy or re-operation).

Volumetric Analyses

Low- and high-grade tumors were analyzed volumetrically by measuring hyperintense regions on axial T2 fluid-attenuated inversion-recovery (FLAIR) (low-grade gliomas) and T1-weighted contrast-enhanced MR images (high-grade gliomas). Each tumor was segmented manually across all slices with region-of-interest analysis to compute pre- and postoperative volumes in cm^3. The extent of resection (ER) was calculated as follows: [100 – (postoperative tumor volume/preoperative tumor volume)*100], with 100% indicating gross total resection (GTR) and <100% representing subtotal resection (STR). We did not consider clinical outcome when determining tumor volume and ER.

Statistical Analyses

Descriptive statistics were calculated for all variables and stated as median unless otherwise specified for continuous variables and frequency of distribution for categorical variables. Cross-contabulations were generated, and Wilcoxon signed rank test (for continuous variables) and chi-square (for categorical variables) tests were used to compare distributions. The Fisher exact test was used if more than 80% of values were less than 5. The Kappa coefficient was used to determine strength of agreement between clinicians. All p values were obtained from 2-sided tests, with statistical significance defined as $p<0.05$. All statistics were analyzed using JMP statistical software version 10.0.2 (SAS Institute, Inc., Cary, NC). The UCSF Institutional Review Board approved the study.

Ethical Review

This study protocol has been reviewed and approved by the University of California, San Francisco committee on human research (official approval number: 14-13002). An informed consent was obtained at the time of admission from all study participants enrolled in the clinical phase of the study.

RESULTS

Objective A: Customized embalming formula versus the Formaldehyde and Cryopreservation subgroups

All formaldehyde and customized specimens were completely embalmed. The cortex surface along the watershed area was uniformly embalmed. Surgical simulation experiments were successfully performed in all specimens included for morphometric

Group	Measure	No. of Specimens	Min	Max	Mean ± SD
formaldehyde	control pressure (mm Hg)	6	0	30	10.00 ± 12.198
	pressure at tissue retraction limit (mm Hg)	6	83	125	103.50 ± 14.419
	retraction area (cm^2)	6	0.32	0.69	0.4633 ± 0.14774
customized	control pressure (mm Hg)	6	1	18	6.50 ± 5.992
	pressure at tissue retraction limit (mm Hg)	6	32	40	35.67 ± 3.011
	retraction area (cm^2)	6	0.89	2.14	1.4350 ± 0.43702
cryopreserved	control pressure (mm Hg)	6	0	8	3.33 ± 3.670
	pressure at tissue retraction limit (mm Hg)	6	18	35	24.17 ± 5.981
	retraction area (cm^2)	6	1.23	3.62	2.1100 ± 0.89376

* Control pressure, pressure tissue break, and retraction area were measured in each specimen.

Table: Descriptive variables

study. One cryopreserved specimen with advanced decay observed during MRI was excluded from the morphometric experiment sample and replaced.

Retraction profiles

The subtemporal approach was completed in all specimens. Retraction profiles (retraction pressure and surface) of customized and cryopreserved specimens were very similar to each other and clearly better than the formaldehyde specimen. The subtemporal approach provided equivalent exposure of the entire incisural space and the cavernous sinus in cryopreserved and customized specimens. However, only the tentorium and the superior cerebellar artery in the middle incisural space were exposed in the formaldehyde group. At maximal retraction, deep plane maneuvering and dissection around the parasellar region were identical in the customized and cryopreserved groups and very difficult in the formaldehyde group.

Retraction Pressure

Retraction pressure studies were performed to assess the brain compliance and retraction capabilities of each group. Overall mean retraction pressures were maximal in the formaldehyde group and lowest in the cryopreserved group. At maximal retraction point, our customized formula provided a retraction pressure almost 3x lower than formaldehyde [36+/-3 (SD) mmHg vs. 103+/-14 mmHg, P<0.01], but slightly higher than cryopreservation [36+/-3 (SD) mmHg vs. 24+/-6 mmHg, P<0.01].

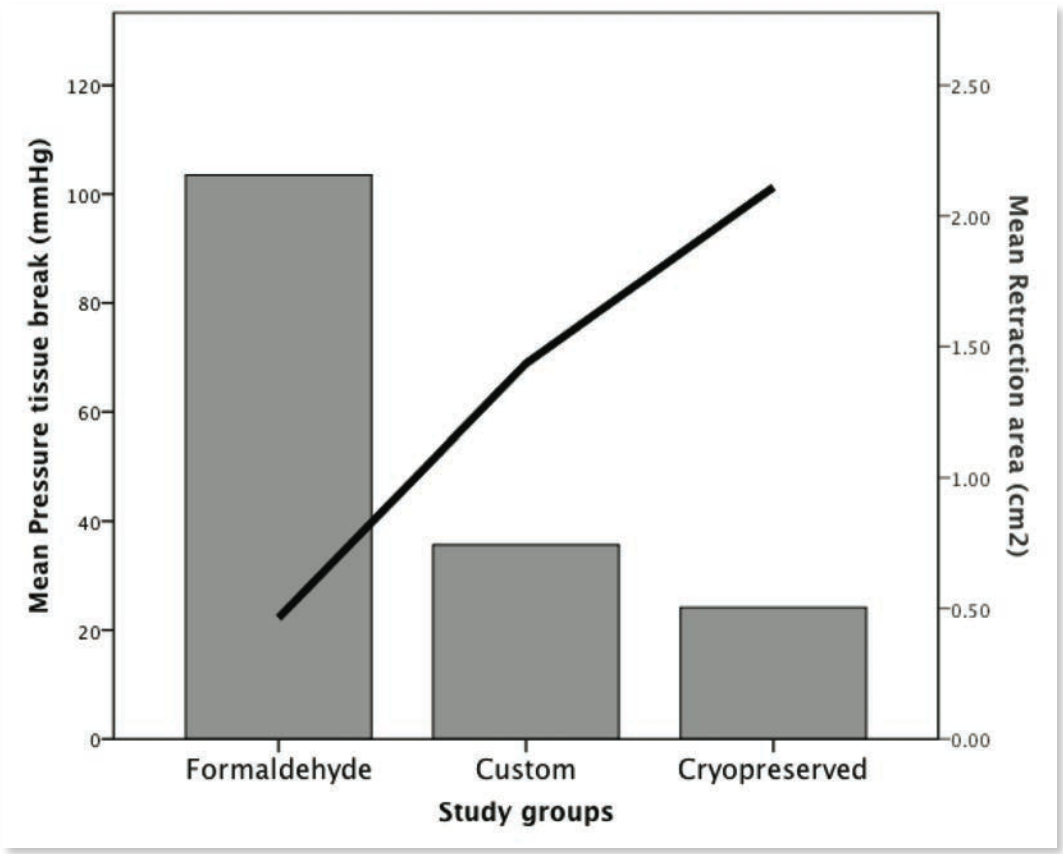

Retraction profile graphic of the study groups. The formaldehyde group had the highest mean pressure at tissue break (over 100 mmHg, Bar) and provided the least retraction area (0.5 cm^2, line). The customized and cryopreserved groups had similar retraction profiles. The customized group offered almost three times less resistance to retraction than the formaldehyde. The cryopreserved group provided the largest retraction surface (2.3 cm^2, line) with lowest retraction pressure (24 mmHg Bar).

Retraction surface

Retraction surface was calculated to assess brain stiffness during a standardized neurosurgical procedure and to compare the surgical area gained during retraction. There was no statistical difference between the customized and cryopreserved groups (P=0.13). The retraction area of the customized group was almost four times larger than that of the formaldehyde group [1.44+/-0.4cm2 (SD) vs 0.46+/-0.1cm2, P<0.01]. These retraction profiles provided different access to the incisural space and posterior fossa structures.

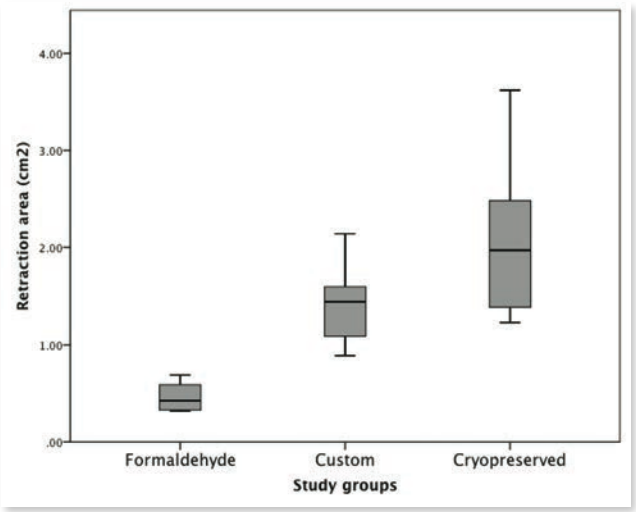

Box plot of the retraction area of each group. The formaldehyde specimens provided less retraction area than the other groups. There was no statistical difference between the custom and the cryopreserved specimens, which had more variability and one outlier

Specimen condition

We have observed that flushing the vascular system with isotonic saline solution instead of tap water both prevents brain and tissue edema and provides optimal cleaning of blood clots. In our experience, the low osmolality of the tap water produced massive edema in all cases. This was prevented by the use of isosmolal saline solution instead of tap water. In addition to the use of saline solutions, manually injecting at low pressure and repeated cleansing of the vessels is also preferable. This procedure increased the illustrative quality in all specimens, but especially in those treated with our customized formula. Complete silicone injection was achieved in all specimens regardless of their embalming method. All thalamoperforator arteries and other distal vessels were fully injected and no subarachnoid silicone leak was observed. The customized specimens exhibited color and texture closer to life-like properties than the formaldehyde-preserved specimens.

Using only a 2.3% of formaldehyde in the customized formula, we reduced formaldehyde content by 78% compared to standard embalming solutions. Texture and color were similar for the cryopreserved and the customized specimens at the time of brain exposure. However, formaldehyde-fixed specimens were stiffer and of slightly darker color. Degradation of tissue consistency and color were observed in the cryopreserved specimens after being continuously exposed to the working environment for 4 hours, whereas customized and formaldehyde-preserved specimens maintained their properties throughout the entire experiment. While evident signs of brain liquefaction were observed in the cryopreserved specimens after working hour 40, consistency and color were preserved in both customized and formaldehyde-fixed specimens. The customized specimens were consistently rated favorably to the formaldehyde and cryopreserved group at the end of the experiment. Changes in consistency were observed in the cryopreserved group from hour 2. All the observational variables –color, consistency and overall appearance- were rated 1 (change observed) from hour 4 consistently throughout the experiment. Sporadic changes in color and overall appearance were noted in both embalmed groups, which resolved with tissue hydration.

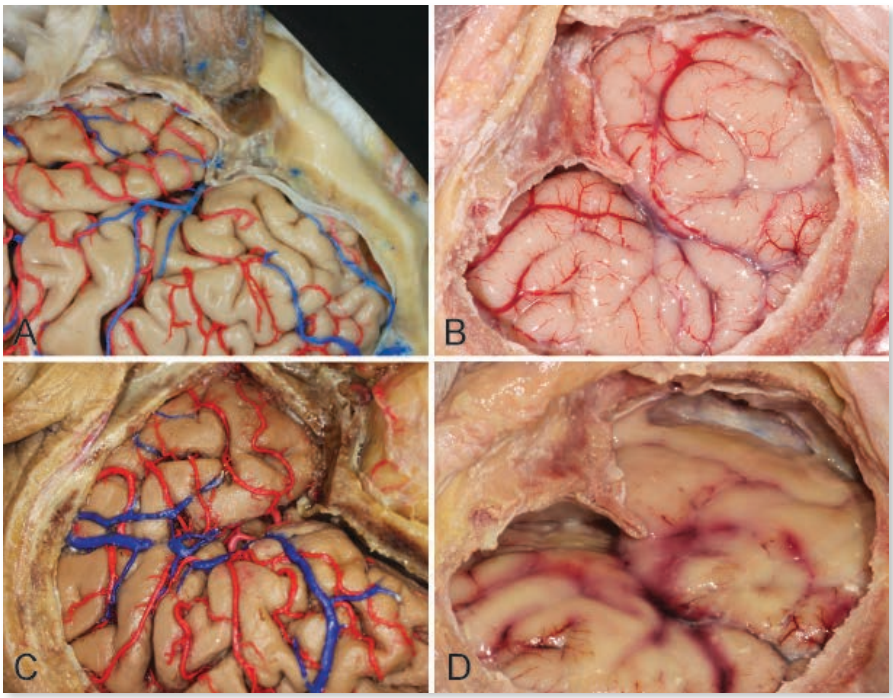

Photographic report of the specimen condition. The customized (a); cryopreserved –non-embalmed- (b and d); and formaldehyde (c) groups were exposed to continuous dissection during 48 hours. The color and texture of the customized and cryopreserved specimens was similar. The formaldehyde group was darker in color and stiffer in texture than the other groups. All specimens were maintained wet during the experiment time. The customized and formaldehyde groups maintained the initial conditions and no changes were noticed. In contrast, the cryopreserved specimen showed advanced signs of decay at hour 40 (d).

Formaldehyde vapors emanated by formaldehyde-fixed specimens were noticeable in the working environment immediately after positioning the head for dissection. Placing the specimens under running water for 15 minutes before dissection diluted the vapors. Unpleasant, aggressive odor from decay and microorganism growth prevented researchers from continuing dissection of cryopreserved specimens at working hour 7. In

contrast, no microorganism growth or brain decay was obvious in the embalmed specimens during the study.

Imaging and post-processing techniques

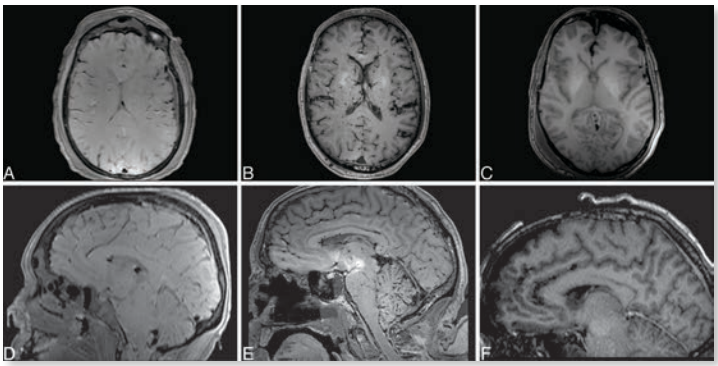

Radiologic study of the sample. An axial (a,b,c) and sagittal (d,e,f) 3D T1-weighted magnetic resonance imaging of the formaldehyde (a,d); customized (b, e) and cryopreserved (c,f) specimens showed better overall results in the customized group. The cortex and subcortical nuclei were best identified in the cryopreserved group and not identified in the formaldehyde group. The cryopreserved specimen showed signs of decay and pneumoencephalus.

Overall, radiologic studies performed on the customized specimens showed equivalence with the cryopreserved group, whereas the formaldehyde group imaging was notably worse. Although T1-weighted MRI of the customized group showed optimal definition of the cortex, sulci, and white matter, some artifacts and hyperintensities were observed randomly aong the internal nuclei. The best images of the internal nuclei were obtained from the cryopreserved group. The embalmed specimens had better tissue preservation than the cryopreserved, which showed signs of brain shrinking and a frontal pneumoencephalus. At postmortem day 8, the cryopreserved specimen showed signs of advanced decay compared to the embalmed groups.

The bleeding model for neurosurgical simulation reported by Aboud et.al[72] was also tested in one customized specimen. Brain movements encompassing arterial beating were observed at a normal arterial pressure resembling live surgery. Hemorrhage from deliberate arterial rupture permitted deep surgical field hemostasis simulation. Gentle retraction of the sylvian fissure together with careful sharp dissection and hemostasis allowed exposition of the middle cerebral artery in a highly simulative surgical scenario.

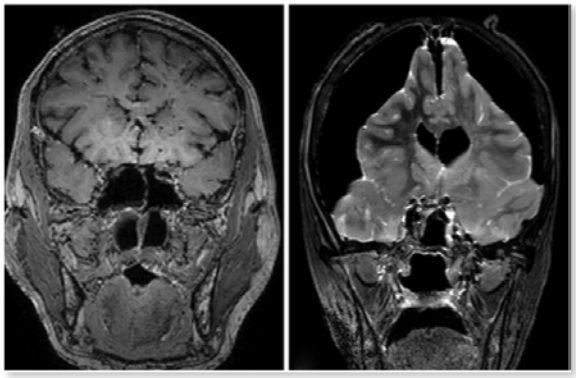

Coronal 3D T-1 magnetic resonance imaging of the customized (a) and cryopreserved (b) specimens at postmortem day 8. The cryopreserved specimen showed evident signs of decay in the form of mount of fuji pneumoencephalus with its superior surface tethered to the superior sagittal sinus.

Objective B: Assessment of the surgical approaches to insular gliomas

Data collected in the present study includes quantitative analysis of surgical variables, - surgical window, insular exposure and surgical freedom-, for each approach. It also includes a descriptive analysis of the surgical anatomy of the trans-Sylvian and transcortical approaches to the insula.

Morphometric assessment

To ease the data interpretation, insular exposure and surgical freedom for each technique, i.e. TS, TSVC and TC, were grouped and provided for each insular zone.

Zone 1

The TC corridor yielded the best exposure of the insula in zone 1 compared to both TS [4.62±0.6 (SD) vs. 7.21±0.8 cm^2, P <0.05] and TSVC [5.21±0.98 (SD) versus 7.21±0.8 cm^2, P <0.05]. Even when the veins were cut, the TC approach offered 140% more insula exposure than the trans-Sylvian approach. In addition, sacrificing the bridging veins in zone 1 did not increase either the final insula exposure or the surgical freedom when the trans-Sylvian corridor was used. The mean surgical window obtained in the TC was larger than the TS [6.18±0.6 (SD) versus 9.65±1.7 cm^2, P <0.05]. The maximal retraction length at zone 1 was 1±3 cm. Cortical resection for total exposure of zone one was 1.5±0.5cm at the inferior frontal gyrus. Although the TC provided significant increase in surgical freedom compared to that of the TS (137%, P<0.05), there was no statistical difference when compared to the TSVC.

Zone 2

Results obtained in zone 2 were proportional to the degree of the corticotomy. During the TC dissection, when the opercular rim of the precentral gyrus was preserved, the surgical window, the insular exposure, and surgical freedom were equivalent to that of the TSVC. The mean insula exposure in the TC group was larger than the TS [2.76±0.8 (SD) versus 3.51±0.8 cm^2, P <0.05] but comparable to that of the TSVC [3.56±0.7 (SD) versus 3.51±0.8 cm^2, P =0.9]. There was no statistical difference in insular exposure

between the TS and the TSVC, therefore cutting the bridging veins was not advantageous in zone 2.

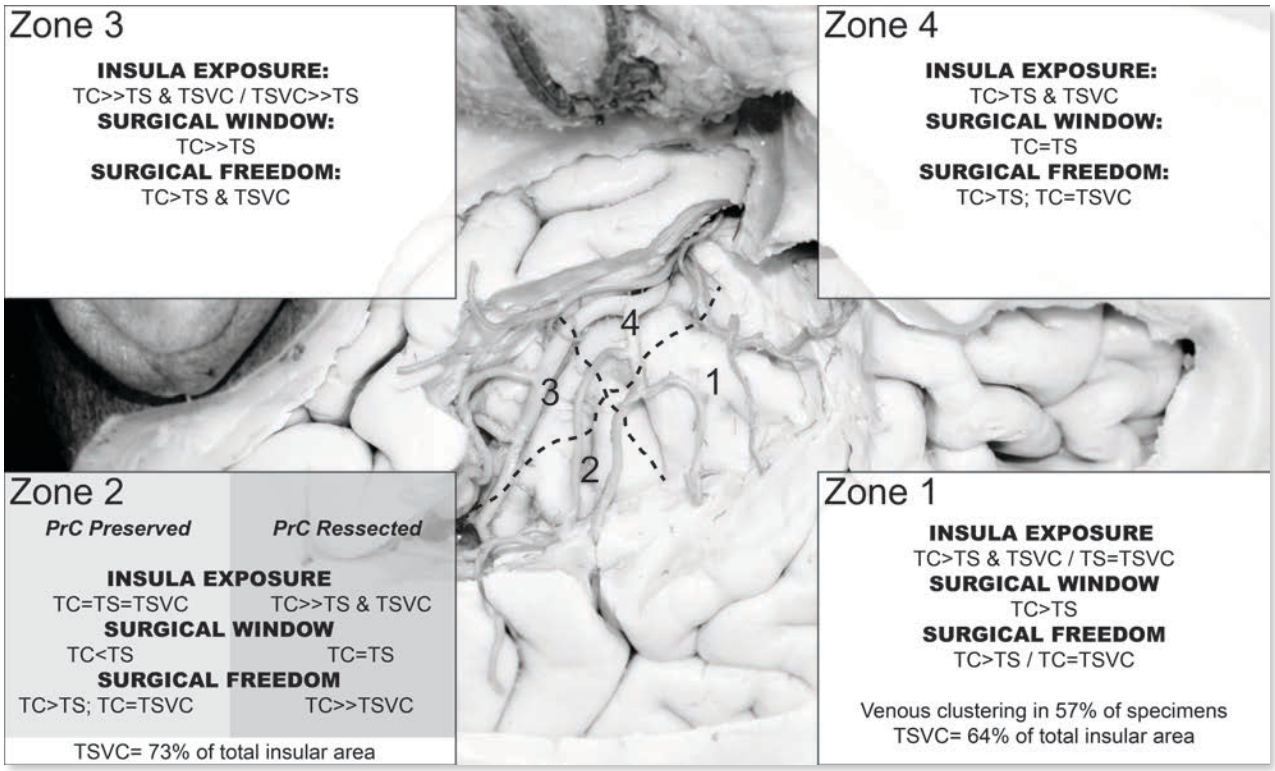

Summary of the comparative analysis between the TS, TSVC, and TC approaches to each zone of the left insula. A photograph of the surgical simulation after a left TC approach was taken and used to illustrate the division of the insular cortex into 4 zones according to the Berger-Sanai classification of the insula. The sylvian line (anterior-posterior dashed line) divides the insula into ventral and dorsal parts. The Monro foramen and its lateral projection (superior-inferior dashed line) divide the insula into rostral and caudal parts. Zone II is further divided into 2 groups depending on the degree of frontoparietal opercula corticotomy during the TC approach. In Zone III, the TC group includes partial resection of Heschl's gyrus. All results included in the vignettes are statistically significant. PrC = precentral gyrus; TC= transcortical; TS= transsylvian; TSVC= transsylvian with veins cut.

The mean surgical window provided by the TS was greater than that of the TC (with precentral gyrus preserved) [4.43±1.1 (SD) versus 3.42±0.7 cm^2, P <0.05]. The maximal retraction length at zone 1 was 1.2±2 cm. The surgical freedom between the TS, TSVC and TC was similar.

On the other hand, resection of the opercular rim of the precentral gyrus during the TC, provided a clear advantage on the TC over all other groups. Specially, the insula exposure obtained in the TC was 146% that of the TSVC (P<0.05). Also, the surgical windows obtained during the TC and TS were similar [5.08±0.8 (SD)versus 4.43±1.1 cm^2, P =0.16]. Moreover, the mean surgical freedom obtained in the TC was 171% that of the TSVC (P< 0.05). Complete TC exposure of the insular cortex at zone 2 required removal of the inferior 1.2±0.2cm of the precentral and postcentral gyri. This allowed complete

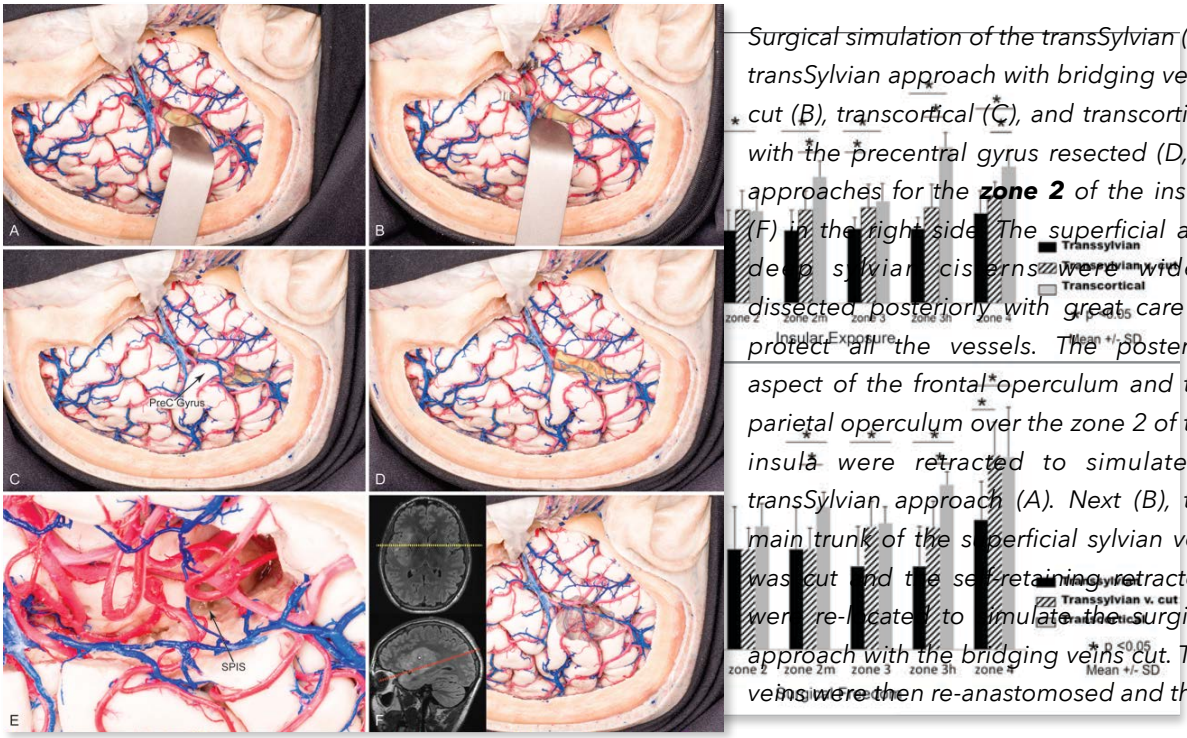

*Surgical simulation of the transSylvian (A), transSylvian approach with bridging veins cut (B), transcortical (C), and transcortical with the precentral gyrus resected (D, E) approaches for the **zone 2** of the insula (F) in the right side. The superficial and deep sylvian cisterns were widely dissected posteriorly with great care to protect all the vessels. The posterior aspect of the frontal operculum and the parietal operculum over the zone 2 of the insula were retracted to simulate a transSylvian approach (A). Next (B), the main trunk of the superficial sylvian vein was cut and the self-retaining retractors were re-located to simulate the surgical approach with the bridging veins cut. The veins were then re-anastomosed and the opercula were allowed to return to its natural position. The transcortical approach was performed respecting both the cortex of the pre-central gyrus and the venous complex and the large veins to the dorsal aspect of the parietal lobe (C). Next (D and E), the opercular rim of the pre-central gyrus was resected to simulate a complete transcortical approach. A close-up picture of the transcortical approach to zone 2 reveals that the insular cortex of such zone was completely exposed and the superior peri-insular sulcus was also accessible (E). Multiple windows were created between the M3 arteries and the superior sylvian veins, forming multiple flexible corridors to the insular surface. A typical zone 2 insular tumor was photographically fused to the surgical simulation to illustrate the relationship to the cortex (F). An axial –superior- and sagittal –inferior- views of a typical zone 2 insular tumor were included in figure F to show the relation of the tumor to the Monro line (yellow) and the Sylvian line (red). Abbreviations: SPIS; superior peri-insular sulcus, PreC; pre-central gyrus, the yellow semi-transparent labels represent the surgical corridor provided by each approach to the insula.*

exposure of the superior peri-insular sulcus, the anterior and posterior long gyri and Heshl's gyrus in the temporal operculum.

Zone 3

The TC approach provided better surgical exposure than the TS [3.89±0.6 (SD) versus 2.85±0.4 cm^2, P <0.05]. If Heshl's gyrus was removed, the insula exposure of the TC was superior to that

Graph of the statistical analysis of the insular exposure (upper) and surgical freedom (lower) obtained during the transsylvian approach (TS), transsylvian approach with bridging veins cut (TSVC) and transcortical approach (TC). The mean, standard deviation (error bars), and statistical significance of the difference in insular exposure (upper) or surgical freedom (lower) for the TS, TSVC, and TC approaches to the insula are shown for each zone. The TC approach provides more insular exposure than the TS and TSVC except in Zone II. Only when the opercular rim of the precentral gyrus was resected did the TC approach provide more exposure than the

of the TSVC. Cutting the bridging veins during the TS at zone 3 increased insular exposure substantially [3.64±0.8 (SD) vs. 2.85±0.4 cm^2, P <0.05].). Resecting Heshl's gyrus provides 156% of the insula exposure obtained during a TC approach. When the TC included resection of Heshl's gyrus, the insular exposure obtained was 164% that of TSVC, which was statistically significant (P<0.05). When Heshl's gyrus was resected during TC, the surgical window was 176% that of the TS (P<0.05). The TC group provided greater surgical freedom than that of the TS group [334.16±43 (SD) vs. 221.14±105 cm^2, P <0.05] but similar to that of the TSVC (P=0.75). However, after Heshl's gyrus resection, the surgical freedom obtained in the TC was the greatest (P<0.05). Cutting the bridging veins during the TS approach did not increase the surgical freedom (P=0.09). The maximal retraction length at zone 3 was 1±2 cm. Cortical resection for complete exposure of zone 3 was 1.3±0.3cm of the superior temporal gyrus

Zone 4

The TC corridor provided greater insular exposure than both TS [5.2±0.6 (SD) versus 3.44±0.8 cm^2, P <0.05] and TSVC [5.2±0.6 (SD) versus 4.11±0.5 cm^2, P <0.05]. Cutting the veins during the TS approach did not increase insula exposure [TSVC 4.11±0.5 (SD) versus TS 3.44±0.8 cm^2, P =0.08]. There was no difference in the surgical window between the TC and the TS [5.96±1.1 (SD) versus 5.38±1.2 cm^2, P =0.28]. The TC provided greater surgical freedom than the TS [508.8±131 (SD) versus 341.7±101 cm^2, P <0.05], but equivalent to that of the TSVC [508.8±131 (SD) versus 513.14±87 cm^2, P <0.05]. TSVC yielded superior surgical freedom than TS [513.14±87 (SD) versus 341.76±101 cm^2, P <0.05]. The maximal retraction length at zone 4 was 1±3 cm. To achieve complete exposure of the inferior peri-insular sulcus we had to resect the entire width of the superior temporal gyrus from the foramen of Monro anteriorly to 1.5±0.6 cm posterior to the temporal pole.

Surgical anatomy

In zone 1, the TS corridor allowed exposure to the insular apex and the cortex just below the Sylvian fissure, however only the TC corridor provided exposure of the superior peri-insular sulci. The TSVC corridor provided exposure to 64% of zone 1, which included the apical portion of the accessory gyrus as well as the proximal portion of the anterior, middle and posterior short gyri. A vein cluster arising from the prefrontal cortex in 57% of cases severely limited exposure to the middle short gyrus and the posterior half of the anterior short gyrus. The middle short gyrus of the insula was better accessed when the TSVC corridor was used, because the main bridging veins cross the Sylvian

fissure at this region. However, the TSVC did not provide a significant increase in surgical

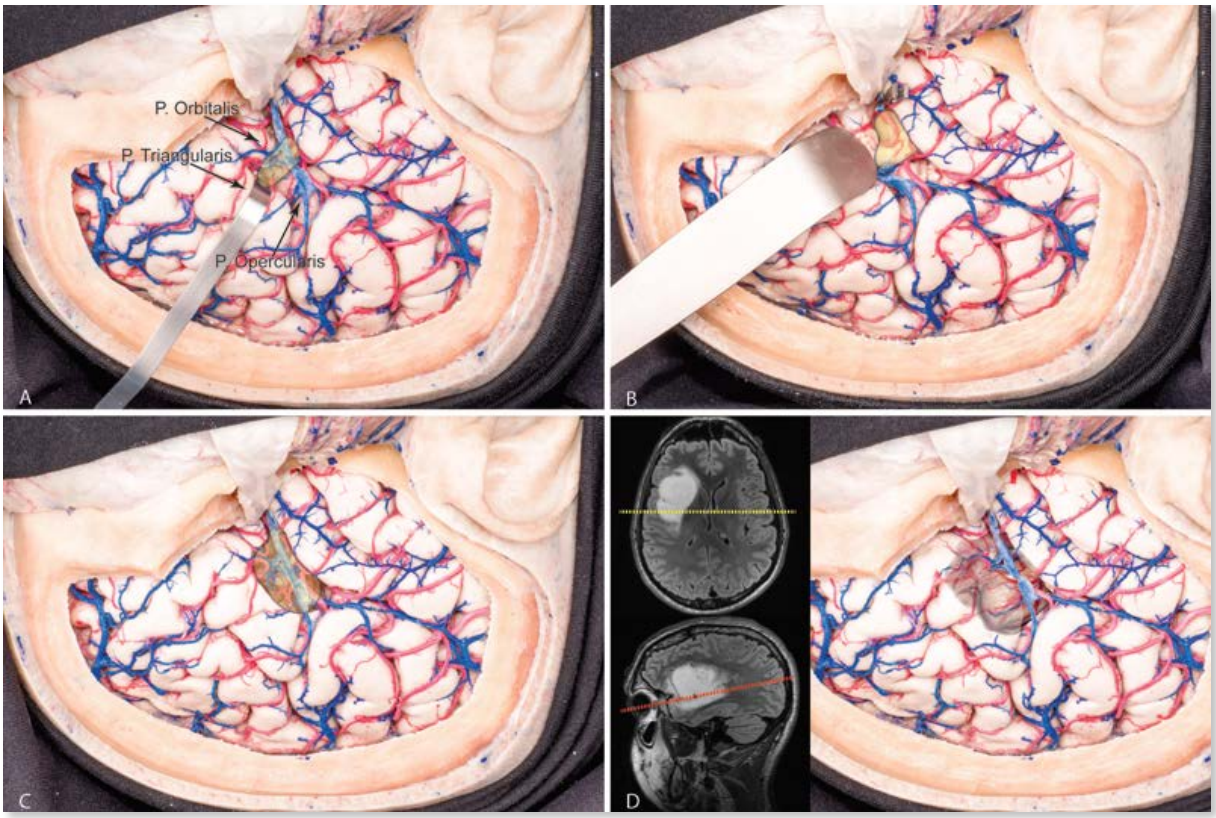

Surgical simulation of the transSylvian (A), transSylvian approach with bridging veins cut (B), and transcortical (C) approaches for the ***zone 1*** *of the right insula (D). A right-side pterional approach was carried out and the dura was incised and reflected towards the sphenoid bone. The superficial and deep sylvian cisterns were dissected completely with great care to protect all the vessels. The frontal operculum over the zone 1 of the insula was retracted to simulate a transSylvian approach (A). Next (B), the superficial sylvian vein was cut and the self-retaining retractors were re-located to simulate the surgical approach with the bridging veins cut. The veins were then re-anastomosed and the frontal operculum was allowed to return to its natural position. The transcortical approach was performed respecting the venous complex and the large veins to the dorsal and orbital aspect of the frontal lobe (C). A typical zone 1 insular tumor was photographically fused to the surgical simulation to illustrate the relationship to the cortex before any surgical maneuver was started (D). An axial –superior- and sagittal –inferior- views of a typical zone 1 insular tumor were included to show the relation of the tumor to the Monro line (yellow) and the Sylvian line (red). Abbreviations: P; pars, yellow semi-transparent labels in each photograph represent the surgical corridor provided by each approach to the insula.*

exposure. Only the TC corridor provided complete exposure of the superior peri-insular sulcus and the entire area of the anterior, middle, posterior and accessory insular gyri in zone 1. In addition, if the head turned down 15 degrees (by either increasing trendelenburg or tilting the back rest down) and the surgical table was tilted to the ipsilateral side, the Eberstaller gyrus and the lateral lenticulostriate arteries were also exposed. The corticotomy necessary to reach zone 1 completely required excision of 60% of the pars orbicularis and opercularis, and 20% of the pars triangularis.

In zone 2, the insular exposure through the TS corridor was limited to the Sylvian line whereas removing the lateral rim of precentral gyrus during the TC corridor allowed greater exposure of the posterior long gyrus and the anterior long gyrus. The narrow shape of the posterior half of the Sylvian fissure limited the TS corridor severely. Even cutting the bridging veins during the TSVC approach and retracting under maximal pressure, only 73% of the total area of the anterior and posterior long gyri was exposed. The TSVC could not expose the superior peri-insular sulcus. When the lateral rim of the precentral gyrus was preserved, the majority of the anterior long gyrus was covered underneath. For this reason, when the TSVC was used and maximal retraction was applied along the entire frontal-parietal opercula, exposure of zone 2 was not significantly different between these two groups.

In zone 3, cutting the bridging veins (TSVC) while using a TS approach allowed for greater exposure of the inferior part of the anterior and posterior long gyri. However the planum temporalis and inferior peri-insular sulcus were only completely exposed through the TC approach. Heshl's gyrus is a large portion of the posterior part of the temporal operculum. It stays on the surgical trajectory to the planum temporalis and inferior and posterior aspect of the posterior long gyrus of the insula. Therefore, if Heshl's gyrus is kept intact during the TC, the final insular exposure is similar to that of a TSVC with maximal retraction applied uniformly to the superior temporal gyrus. However, if Heshl's gyrus is removed as part of the TC approach, zone 3 of the insula may be exposed completely along with the inferior peri-insular sulcus. Ninety percent of Heshl's gyrus was excised to expose zone 3 completely. Also, the long gyri can be further dissected towards zone 2 if the head is tilted down 10-20 degrees (trendelenburg or lowering the back rest of the surgical table).

In zone 4,

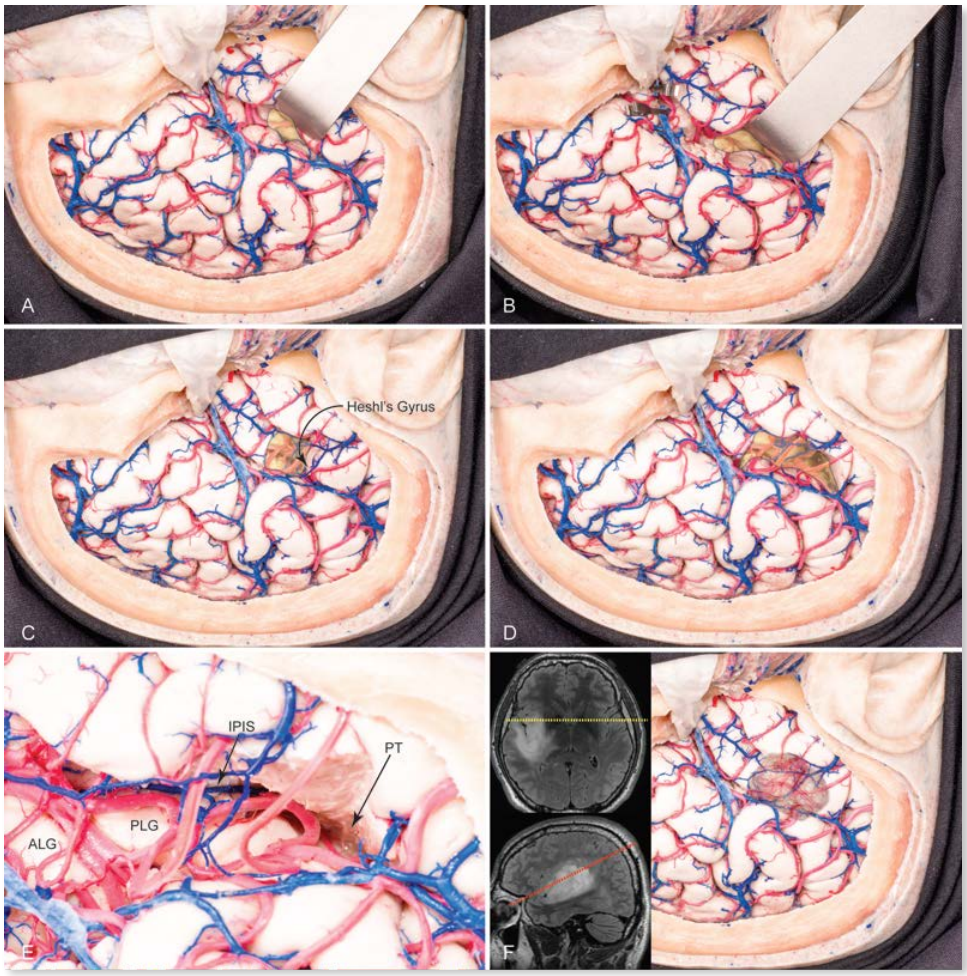

Surgical simulation of the transSylvian (A), transSylvian approach with bridging veins cut (B), transcortical (C) and transcortical with the Heshl's gurys resected (D,E) approaches for the ***zone 3*** *of the right insula (F). The superficial and deep sylvian cisterns were completely exposed with great care to protect all the vessels transitioning to the cortex. The posterior segment of the temporal operculum over the zone 3 of the insula was retracted to simulate a transSylvian approach (A). Following this, the superficial sylvian vein was cut and the self-retaining retractors were re-oriented to simulate the surgical approach with the bridging veins cut (B). Next, the veins were re-anastomosed and the temporal operculum was allowed to return to its original position. The transcortical approach was performed next, preserving both Heshl's gyrus and the Sylvian venous complex (C). Following this, Heshl's gyrus was resected for a complete transcortical approach to the zone 3 of the insula (D and E). A close-up photograph of the transcortical exposure of the insula revealed complete exposure of the zone 3 cortex as well as the planum temporale and inferior peri-insular sulcus (E).The large veins to the dorsal aspect of the temporal and occipital lobes and the Labbé complex as well as the transitioning M4 branches were preserved during all the transcortical dissection. These vessels formed multiple corridors to access the surface of the insula. A typical zone 3 insular tumor was photographically fused to the surgical simulation to illustrate the relationship to the cortex before starting the surgical simulation (F). An axial –superior- and sagittal –inferior- views of a typical zone 3 insular tumor were included to illustrate the relation of the tumor to the Monro line (yellow) and the Sylvian line (red). Abbreviations: ALG; anterior long gyrus, PLG; posterior long gyrus, IPIS; inferior peri-insular sulcus, PT; planum temporale; yellow semi-transparent labels= surgical corridor provided by each approach to the insula.*

exposure of the insula did not significantly increase by cutting the bridging veins (TSVC) during a TS corridor. In the other hand the TC allowed full insula exposure. The TS corridor exposed the anterior portion of the anterior long gyrus and the insular apex. In more than half of our specimens, there was a large bridging vein limiting the inferior exposure of the insula in zone 4 through the TS corridor. When this vein was cut (TSVC) the arachnoid dissection could be further

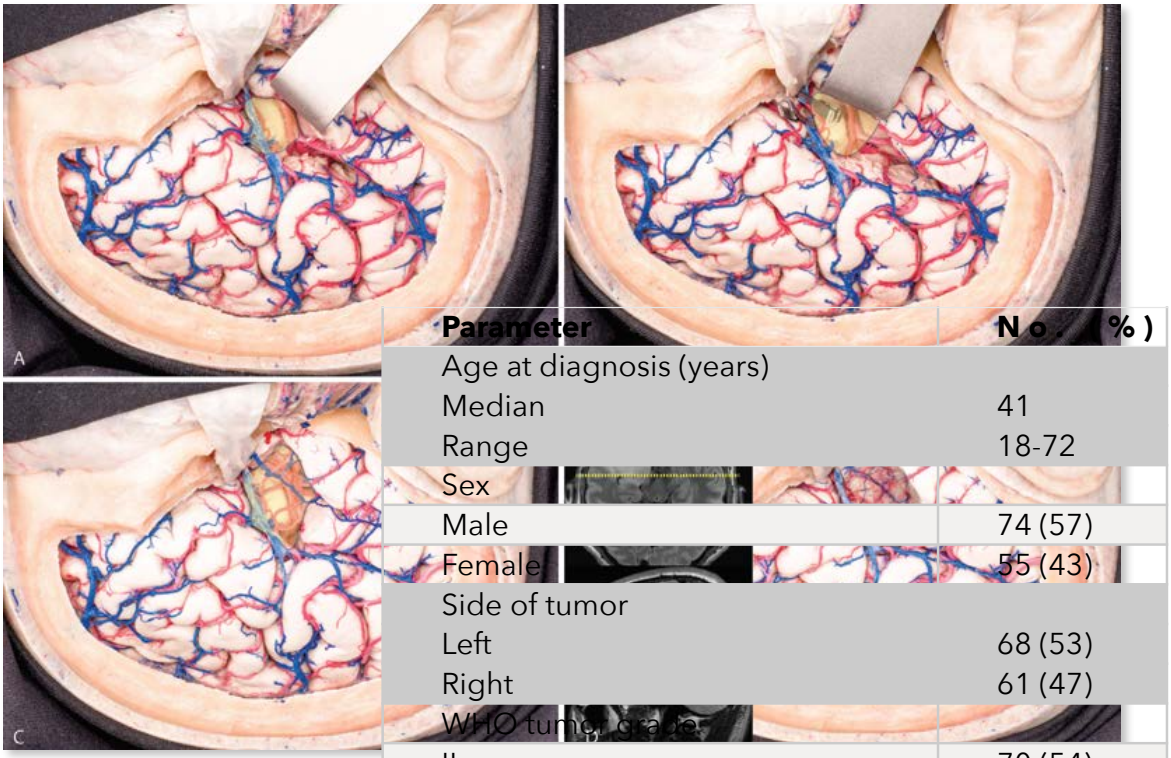

*Surgical simulation of the transSylvian (A), transSylvian approach with bridging veins cut (B), and transcortical (C) approaches for the **zone 4** of the right insula (D). The superficial and deep sylvian cisterns were completely dissected with great care to preserve all the transiting vessels. The temporal operculum over zone 4 of the insula was retracted to simulate a transSylvian approach (A). Following this (B), the superficial sylvian*

Parameter	No. (%)
Age at diagnosis (years)	
Median	41
Range	18-72
Sex	
Male	74 (57)
Female	55 (43)
Side of tumor	
Left	68 (53)
Right	61 (47)
WHO tumor grade	
II	70 (54)
III	44 (34)
IV	15 (12)
Tumor Volume (cm^3)	
Median	48.5
Range	0.11-245.7
Insular glioma location by zone	
I	40 (31)
II	2 (1.6)
III	17 (13.2)
IV	14 (10.9)
I-II	4 (3.1)
I-IV	21 (16.3)
II-III	7 (5.4)
III-IV	12 (9.2)
Giant	12 (9.2)
Handedness	
Right	126 (97.7)
Left	3 (2.3)

Table: Patient demographics

Symptoms at presentation	
Seizure	88 (68)
Cognitive decline	3 (2.3)
Headache	9 (7)
Incidental	2 (1.6)
Language deficit	1 (1)
Motor deficit	3 (2.3)
Asymptomatic recurrence	23 (17.8)
Type of surgery	
Motor mapping	122 (94.6)
Language mapping	58 (45)
Awake surgery	58 (45)
New	80 (62)
Re-operation	49 (38)
Adjuvant oncologic treatment	
Patients with post op chemotherapy	107 (82.9)
Patients with post op radiation	82 (63.6)
Malignant progression	49 (38)
Clinical follow up (years)	
Median	3.5
Range	0.26-25.8
Extent of resection (%)	
0-40%	1 (1)
41-69%	19 (14)
70-89%	58 (45)
>90%	51 (40)
Median	85
Range	40-100

Table: Patient demographics, continued

dissected towards the inferior peri-insular sulcus, which was seen upon maximal retraction of the superior temporal gyrus and by tilting the head upwards 20 degrees. However, there was a statistically significant increase in insula exposure in zone 4 when the TC was used. This exposure included the inferior peri-insular sulcus and the insular portion of the planum polaris.

Venous drainage

The venous drainage patterns of the lateral surface of the brain were carefully studied to determine their dominance in the venous outflow. Specifically the number of bridging veins and their relationship to the different zones, and the clustering patterns were recorded. The data on the venous drainage patterns provided below could provide the neurosurgeon with valuable evidence on the number of cases were

the TSVC option would not be viable.

We found bridging veins crossing the Sylvian fissure in 70% (11/16) of the specimens. A dominant drainage pattern was determined if the number and size of veins draining anteriorly was greater compared to the number and size draining to the Labbé complex and bridging veins to the superior sinus. We found it in 87% (14/16) of our sample. Of the dominant venous patterns, 50% (8/16) had good alternative outflow through either anastomoses to the superior sagittal sinus bridging veins, the Labbé complex or parallel veins that do not cross the Sylvian fissure or a combination. There were dominant bridging veins with poor collateral drainage in 30% of specimens. Venous clustering around the pre-frontal or premotor cortex draining the lower part of the lateral surface of the frontal lobe was found in 56% (9/16) of the specimens.

Surgical landmarks

From the observational and descriptive analysis of the surgical anatomy of the pterional trans-Sylvian approach, three key relationships were consistent throughout the study: the relationship between the middle cerebral artery (M2) at the central sulcus of the insula and the rolandic artery (M4); the relationship between the Sylvian fissure the superior segment of the squamosal suture; and, the craniometric relation between foramen of Monro and the external acoustic meatus at the surface of the skull. Additionally, the corticotomy maps drawn during the TC step of the experiment were consistent throughout the study.

There were 2-4 trunks of the M2 that branched into 12±2 M3 branches on the insular surface. In all our specimens, the M2 branches running through the central sulcus of the insula became the precentral (Rolandic) artery, feeding the precentral and postcentral gyri. In the majority of cases (81%; 13/16) , this artery remained on the surface of the operculum easily identifiable on the lateral surface of the brain. However, in 18% (3/16) of cases, the M3 component of the artery running in the central sulcus of the insula coursed in the depth of the precentral sulcus of the brain and became superficial at 0.8±0.2 cm from the operculum rim.

Since the foramen of Monro plays a critical role in the surgical division of the insula and the design of a tailored minimally invasive craniotomy, superficial references to identify it were seen and recorded in all the specimens. The external acoustic meatus was identified in all surgical simulations. It was used as a key landmark to approaximate the position of foramen of Monro. Therefore it served as a reliable proxy to establish the

division of the insula into anterior (1&4) and posterior (2&3) zones before performing the craniotomy. The foramen of Monro was 1.9±0.26 cm anterior and 4.42±0.6 cm cranial to the external acoustic meatus.

The squamosal suture was a reliable landmark to infer the position of the Sylvian fissure, which defined the surgical division of the insula into superior (1&2) and inferior (3&4) zones. The superior portion of the squamosal suture, from the pterion anteriorly to its major inferior bend posteriorly corresponded to the Sylvian fissure in the majority (14/16) of the sample and was inferior to the Sylvian fissure in only one (8%) specimen.

Objective C: Correlation between anatomical classification of insular gliomas and surgical outcomes.

Patient Demographics

The study population included 74 men and 55 women with a median age of 41 years (range 18-72) (table). Eighty patients (62%) underwent primary craniotomy, whereas 49 (38%) had undergone at least 1 prior procedure. Sixty-eight patients (53%) had left sided tumors and there were 58 (45%) awake craniotomy procedures. Patients most commonly presented with new onset seizures (n=88, 68%), asymptomatic glioma progression (n=23, 17.8%), motor deficits (n=3, 2.3%), cognitive decline (n=3, 2.3%), and language deficits (n=1, 1%). Incidental insular gliomas were rare, representing 1.6% of cases (2 patients). Of the 129 operations, the most common tumor histological grade was WHO II (n=70, 54%), followed by WHO grade III (n=44, 34%), and WHO grade IV (n=15, 12%). Median tumor volume was 48.5 cm3 with a range between 0.11-245.7 cm3. Fifteen percent (n=19) of insular tumors were confined within the insula while the majority (85%) were based in the insula and extended outwards to involve the frontal, temporal, or parietal lobes. One hundred and seven patients (82.9%) were treated with postoperative chemotherapy and 82 (63.6%) underwent postoperative radiation therapy. Median follow up was 3.5 years (range 0.26-25.8 years). Malignant transformation from WHO grade II to WHO grade III or WHO grade III to WHO grade IV happened in 49 (38%) patients. Tumor laterality was evenly distributed (table).

Insular Glioma Location

Based on our prior report (Sanai 2010), insular gliomas were assigned to one of 9 zones. The majority of insular gliomas were located in the anterior part of the insula (anterior to the foramen of Monro) and 31% (40 cases) within the anterior-superior quadrant (Zone I), 10.9% (14 cases) within the anterior inferior quadrant (zone IV), and 16.3% (21 cases) within zone I-IV (total of 58.2% of cases within the anterior insular). Twelve insular gliomas (9.2%) were "giant", involving all 4 zones.

Inter-observer reliability of Berger-Sanai Insular Glioma Classification System

Inter-observer reliability was tested using preoperative FLAIR or T1 gadolinium enhanced MRI in 80 patients with new WHO II, III, and IV insular gliomas. Three neurosurgeons with a range of clinical experience scored the location of each tumor according to our previously published zone classification criteria (Sanai 2010). Inter-observer agreement was 89% (41 of 46 patients) for WHO II gliomas, 84% (21 of 25 patients) for WHO III anaplastic gliomas, and 100% (9 of 9 patients) for WHO IV gliomas. Overall intra-observer agreement was 89%. We found a strong inter-observer reliability tagreement with a kappa coefficient of 0.857 (95% confidence interval; CI 0.77-0.94, $p<0.001$). There was no correlation between observer agreement and WHO Grade ($p=0.42$).

Extent of Resection

Following tumor resection, 1 patient (1%) had an extent of resection less than or equal to 40%. Nineteen patients (14%) had extent of resection between 41-69%, Fifty-eight (45%) had extent of resection between 70-89%, and 51 (40%) had more than 90% extent of resection. The median extent of resection was 85 (range between 40-100%) and mean extent of resection was 83 across all zones. Among WHO grade II gliomas (70 patients), the median extent of resection was 81% and fifty-five patients (79%) had an extent of resection greater than or equal to 70% (this included 32 patients (46%) with a 70-89% resection and 23 (33%) with an >90% resection). A total of 44 patients had anaplastic astrocytoma with a median extent of resection of 88%. Forty-one patients (93%) had

extent of resection greater than or equal to 70% (this included 23 patients (52%) with a 70-89% resection and 18 (41%) with a >90% resection).

Zone	*Volume (cm^3)*	*WHO II no. (%)*	*WHO III no. (%)*	*WHO IV no. (%)*	*Median EOR (%)*	*Prior series (Sanai 2010)*	*P value**
I (n=40)	*49.1*	*24 (60)*	*12 (30)*	*4 (10)*	*90.1*	*93.8*	*0.47*
II (n=2)	*11.4*	*0 (0)*	*1 (50)*	*1 (50)*	*83.5*	*67.4*	*0.41*
III (n=17)	*22*	*9 (53)*	*4 (23.5)*	*4 (23.5)*	*88*	*90*	*0.75*
IV (n=14)	*20.1*	*5 (35.7)*	*7 (50)*	*2 (14.3)*	*89.5*	*88.8*	*0.79*
I-II (n=4)	*72*	*2 (50)*	*1 (25)*	*1 (25)*	*86.5*	*71.3*	*0.35*
I-IV (n=21)	*52.3*	*12 (57.1)*	*8 (38.1)*	*1 (4.8)*	*75*	*81*	*0.06*
II-III (n=7)	*63.8*	*5 (71.4)*	*1 (14.3)*	*1 (14.3)*	*85*	*82.9*	*0.77*
III-IV (n=12)	*41.4*	*6 (50)*	*5 (41.7)*	*1 (8.3)*	*82*	*84*	*0.61*
Giant (n=12)	*91.2*	*7 (58.3)*	*5 (41.7)*	*0 (0)*	*80*	*72.7*	*0.60*

Table: Summary of resected gliomas by zone. Distribution and extent of resection of insular gliomas. Dark column highlights prior study.

Among WHO IV gliomas (15 patients), the median extent of resection was 97% and 13 patients (87%) had an extent of resection greater than or equal to 70% (this included 3 patients (20%) with 70-89% resection and 10 (67%) with >90% resection). Zone II insular gliomas were the smallest with median tumor volume of 11.4 cm3 while "giant" insular gliomas had a median volume of 91.2 cm3 . The greatest extent of resection was accomplished in tumors located in Zone I (median Extent of resection 90.1%) and IV (median extent of resection 89.5%). In our initial series the smallest extent of resection was associated with zone II tumors, however with a greater willingness to maximize resections using a transcortical surgical corridor through face motor cortex, extent of resection increased to 83.5%. Zone continued to be predictive of mean extent of resection with highest mean extent of resection demonstrated in zone I (87.2%) and III (88%) tumors while mean extent of resection was most modest in zone I-IV (75%), Giant (76%), and III-IV (78%) tumors [mean Extent of resection of zone II, IV, I-II, and II-III insular gliomas was 83.5%, 87.4%, 84%, and 84% respectively] (p=0.002). There were no differences in mean extent of resection after comparing mean extent of resection between tumors across all zones in our two insular glioma series.

In addition to the fact that zone remain a good predictor of mean extent of resection, there was also a positive correlation between tumor size and extent of resection. Mean glioma volume was highest in giant (91.6 cm3), followed by zone I-II (72 cm3), and zone II-III (63.8 cm3) tumors. Smallest mean tumor volumes were observed in zone II (11 cm3),

zone III (22 cm3), and zone IV (20.1 cm3) tumors (p=0.002). Patients with extent of resection <40% had a median tumor size of 38 cm3 (mean 38 cm3), those with extent of resection 41-69% had median tumor volume of 46 cm3 (mean 61 cm3), extent of resection 70-89% had median volume of 62 cm3 (mean 62 cm3), while those with an extent of resection >90 had median glioma volume of 25 cm3 (mean 46 cm3) (p=0.0183).

Impact of glioma molecular characterization on Extent of resection

The literature is inconsistent regarding the rate of 1p and 19q chromosomal co-deletions in insular gliomas (Wu 2010, Goze 2009). In our series we found 60 tumors

(47% of tumors), which were WHO grade II oligodendroglioma (n=24), WHO II oligoastrocytoma (n=24), or WHO III anaplastic oligodendroglioma or oligoastrocytoma (n=12). Forty-three percent (n=23) of WHO II and III insular oligodendroglioma and oligoastrocytomas has 1p19q chromosomal co-deletions while fifty-seven percent (n=31) of insular oligodendrogliomas did not have a chromosomal 1p19q co-deletion (p=0.04).

	<40%	*41-69%*	*70-89%*	*>90*	*P value*
PTEN deletion (n=32)	*0 (0%)*	*2 (10%)*	*6 (29%)*	*13 (62%)*	*0.22*
P53+ (n=62)	*0 (0%)*	*6 (13%)*	*19 (44%)*	*22 (47%)*	*0.2816*
EGFR amplification (n=33)	*0 (0%)*	*1 (8%)*	*5 (38.5%)*	*7 (54%)*	*532*
IDH1 (132) mutation (n=71)	*0 (0%)*	*11 (21%)*	*23 (43%)*	*19 (36%)*	*0.09*
1p19q co-deletion (n=69)	*0 (0%)*	*4 (16%)*	*14 (56%)*	*7 (28%)*	*453*

Table: Impact of tumor molecular characteristics on extent of resection

Previously published reports have suggested that IDH status confers a higher degree of resectability on WHO III and IV gliomas. Therefore we analyzed extent of resection focusing on IDH+ insular gliomas. Within WHO II insular glioma population, IDH+ tumors had a mean extent of resection of 81%, while IDH- WHO II insular gliomas had a mean extent of resection of 86% (p=0.62). WHO III IDH+ insular gliomas had a mean extent of resection of 79% while IDH- WHO III insular gliomas had a mean extent of resection of 88% (p=0.06). The mean extent of resection for WHO IV IDH+ insular gliomas was 83%, while IDH- WHO IV insular gliomas had a mean extent of resection of 95% (p=0.31). After controlling for WHO grade, we found no correlation between glioma molecular markers

(PTEN, p53, EGFR amplification, IDH1 mutation, and 1p19q co-deletion) and extent of resection or zone classification.

Morbidity Profile

The overall short-term complication rate was 26.4% (34 complications in 129 procedures). Short-term neurological complications (within 3–5 days after surgery) were most frequently found after procedures involving Zone 1 and Giant insular gliomas. New motor neurological deficits excluding face motor weakness (within 3–5 days after surgery)

	*short-term**	*Long-term***	*Prior series long-term disability*
Language deficit	*21 (16%)*	*0 (0%)*	*0 (0%)*
Motor deficit	*10 (7.7%)*	*2 (1.6%)*	*2 (1.7%)*
Face motor deficit	*12 (9.5%)*	*1 (0.8%)*	*2 (1.7%)*

Table: Postoperative morbidity. Short term= 3-5 days. Long term= >90days

were found in 7.8% of the procedures (10 of 129). New face motor deficits were observed in 9.3% (12 of 129). Early postoperative language deficits occurred in 16.3% (21 of 129). At 3-month follow-up, 99.2% of face motor deficits resolved. The overall long-term (90- day) neurological deficit rate was 3.2%. All but 1 language deficit resolved (0.8%), while the long-term rate of motor disability also remained low at 1.6% (n = 2). These rates compared favorably with outcomes we reported in prior retrospective series.

Zone	*No complications*	*Early complications*
I	*31 (33%)*	*9 (26%)*
II	*2 (2%)*	*0 (0%)*
III	*14 (15%)*	*3 (8.8%)*
IV	*13 (14%)*	*1 (3%)*
I-II	*2 (2%)*	*2 (5.9%)*
I-IV	*17 (18%)*	*4 (12%)*
II-III	*2 (2%)*	*5 (15%)*
III-IV	*8 (8%)*	*4 (12%)*
Giant	*6 (6%)*	*6 (18%)*

Table: Short-term complications based on insular zone classification

DISCUSSION

Objective A: Customized embalming formula versus the Formaldehyde and

Cryopreservation subgroups

This study shows that the customized embalming formula provides optimal brain retraction profile, long use time, and low biohazard risk for neurosurgical simulation in cadavers. Overall, the customized group provided the best feature combination for cadaveric neurosurgical research. We found that the specimens embalmed with the customized formula offered three times less retraction pressure while providing four times more surgical retraction area compared to the formaldehyde group. When surgical simulation was performed, we obtained best access to surgical landmarks and maneuverability in the customized and the cryopreserved groups. Nevertheless, cryopreserved specimens had a very limited working time due to fast decay (4 hours for research purposes). Moreover, our radiological studies showed that the customized and cryopreserved groups provided better anatomical detail than the formaldehyde group, although random hyperintense artifacts were identified in the customized specimens. Also, we have tested that surgical bleeding simulation is feasible in our customized-embalmed specimens.

The key concept when choosing the processing technique is to know exactly the dissection objectives and requirements of the proposed work, together with a thorough understanding of the different properties of the available preservative methods. There are many specimen-processing techniques available for laboratory use, and each has specific advantages and disadvantages.

Solutions containing large formaldehyde concentrations have been used as the standard in specimen preservation because they provide long-term preservation and prevent microorganism growth. Even though these are desired properties, formaldehyde remains a suboptimal fixation method for neurosurgical simulation because the brain stiffness it produces makes retraction very challenging. However, this property has provided researchers with an excellent processing method for gross anatomy teaching

and white matter dissection. Formaldehyde-related brain hardening combined with sequential freezing cause axons to separate from each other, thus facilitating dissection of fine fiber bundles[25,26,90,91]. In contrast, color distortion is a well-known drawback that has an important impact on the illustrative work. White, pallid cortical and subcortical structures are far from natural brain color and sometimes can be difficult to contrast with cranial nerves during surgical simulation.

It has been widely accepted that cryopreservation (not embalmed) is the cadaveric processing technique that less modifies the biological properties of brain tissue. Nonetheless, the natural appearance of the brain only lasts a very limited time. At working hour 4 (around post-mortem day 2-5), specimens are no longer useful for neurosurgical simulation research as liquefaction prevents reliable morphometric analysis and tissue distortion becomes evident. This is a major drawback during hands-on courses or other teaching activities where an extended period of time but reliable anatomy and surgical maneuverability are needed to understand and practice the different surgical approaches. Another significant drawback of cryopreserved specimen is biohazard safety. Because unembalmed specimens lack germicide agents, uncontrolled microorganism growth can occur early in the dissection process. However, unembalmed specimens continue to be used in procedure demonstrations and educational workshops because they used to be the only method to offer features most similar to a living brain in the operating room (i.e., the possibility of brain retraction). In our opinion, our customized embalming technique, opens a new possibility that enables brain retraction and provides brain features similar to those of cryopreserved specimens, while offers a more cost-effective and safer option.

The customized embalming formula takes advantage of the best formaldehyde properties – long preservation time and microorganism growth prevention – combined with a retraction profile and physical properties similar to what can be achieved with cryopreservation. Also, a substantial reduction in formaldehyde concentration makes this option safer for researchers according to IARC recommendations.

Surgical simulation profiles

Despite important advances in surgical simulation[72,74,77,86,92] an embalming formula customized to enable brain retraction while preserving living brain properties still remained necessary to recreate neurosurgical scenarios in cadavers. In 2002, Aboud et.al. introduced a revolutionary laboratory model for neurosurgical training that enabled blood hemorrhage simulation in cadaveric specimen.[72] This advance represented a breakthrough in neurosurgical approach recreation because it allowed training of bleeding avoidance, management and control in a human cadaveric surgical scenario.

However, one of the major limitations reported in their study was not directly related to the model but to brain embalming. Formaldehyde-related brain stiffness was reported to be a major limitation for surgical exposure and cerebral retraction. To overcome this limitation, they used cryopreserved, partially embalmed cadavers. Although brain relaxation allowed retraction and wide surgical exposure in this case, specimen working time was reported to be very limited.[72] In the present study, we observed the same limitations in cryopreserved –unembalmed- and formaldehyde-preserved specimens. However, customized-preserved specimens overcame these limitations. In addition, prolonged and multi-session work is possible because embalming fixatives preserve the brain for at least two days of continued exposure to the working environment. In this study, the customized and formaldehyde specimens were kept immersed into their respective embalming fluid for 8 months (mean 8 months, range 2weeks-1 year), which in our experience represents the approximate embalming-time at the time of use of the specimens in the laboratory. Immersion in embalming fluid during storage and prevention of specimen desiccation during dissection is critical in preserving the original qualities in both the formaldehyde and customized groups and determines its prolonged use. In our experience using this embalming fluid for our studies during the last 5 years, this specimens maintain their properties for months, even years, if maintained in optimal conditions (nonfrozen and submerged in embalming fluid."

Imaging and post-processing techniques

Radiologic studies in cadaveric specimen represent an excellent option to complement training and research in neurosurgical laboratories. Computerized tomography and MRI of the specimens provide useful spatial orientation and become essential in assisting new landmark and approach research during surgical simulation experiments. In our study, radiological imaging obtained from customized specimens provided more detail of the anatomical structures than the formaldehyde group and showed less decay distortion (e.g., pneumoencephalus) than the cryopreserved group. Artifacts detected in T1-weighted MRI of the customized group are likely to be caused by the high glycerol content of the embalming mixture rather than a fixation failure. Post-dissection cross-sectional examination confirmed distal and uniform embalming perfusion.

The customized specimens provided an unparalleled surgical scenario when using the bleeding model. Our formula provided brain retraction capabilities, allowing surgical exposure, vascular dissection, and bleeding control in a very realistic scenario.

Biohazard risk and health standards

Health protection is a primary concern and has to be seriously considered in a surgical-simulation laboratory. Although general protection standards (physical barriers) always have to be used, special measures tailored to embalming chemicals are necessary to provide a safe workplace.

Neurosurgical simulation, especially for research and illustrative purposes, takes time, and a continued dissection process demands a high level of concentration to perform meticulous and precise anatomical exposures. In our study, microorganism growth together with unpleasant aggressive odor and evident signs of tissue decomposition forced researchers using cryopreserved specimens to finish dissection prematurely. This situation can be frustrating because dissection targets and research objectives most often are achieved in the last steps of dissection work. Moreover, intense continued work in a crowded workplace (e.g., hands-on workshops) lowers the ventilation rate and increases room temperature, thus increasing the decay rate in cryopreserved specimen and formaldehyde airborne particles when using formaldehyde specimens. Maintaining these circumstances over prolonged time can potentially result in a harmful biohazard situation. Therefore, the federal government and the State of California have established permissible exposure limits for chemical exposures in the workplace.

Airborne formaldehyde is the most harmful volatile chemical among those included in the present study and has the strictest biohazard security control codes. [93] It has also been considered a carcinogenic agent by many institutions and government regulations. [80-82,93,94] Although formaldehyde is still needed to prevent microorganism growth (specially fungi), Formaldehyde content in the customized embalming fluid described here was almost 80% less than conventional formaldehyde mixture. Furthermore, customized specimens provided a less aggressive and contaminated environment than formaldehyde and cryopreserved specimens. Researchers noticed no airway or mucosal irritations when working with either the customized or cryopreserved group. However, slight to mild oropharynx and eye mucosal irritation was present when using formaldehyde specimens.

Fixative and germicidal properties of the customized embalming formula are provided mainly by phenol and ethanol. Although phenol is considered to be more hazardous than ethanol, its toxic effects are limited to skin contact. Furthermore, IARC evaluation on phenol concludes that it is "not classifiable as to its carcinogenicity to humans".[95] Thus, biohazard airborne particles in the laboratory are drastically reduced when using customized specimen. However, pertinent physical barriers are strongly recommended during specimen or embalming mixture manipulation and high ventilation rate of the workplace as well.

OBJECTIVE B: ASSESSMENT OF THE SURGICAL APPROACHES TO INSULAR GLIOMAS

The laboratory research from ***objective B*** shows that the TC corridor provides the greatest access to lesions, such as gliomas, within the insular region. The evidence is that even when the comparison between TC, TS and TSVC is limited to the confines of the insula, the TC still provides the best overall surgical exposure, window and freedom. In our dissections, the degree of corticotomy in zones 2 and 3 provided significantly different surgical profiles. We found that the value of cutting the bridging veins during a TS approach was maximal in zone 3, where it provided a significant increase in insular exposure. From our observations of the venous drainage of the lateral surface of the brain, we identified a venous pattern that would make the TSVC unsafe in 30% of cases due to the existence of large dominant Sylvian bridging veins with poor alternative outflow to the Labbé or superior sagittal sinus complex. Also, venous clustering at the pars triangularis, opercularis and motor cortex was observed in 56% (9/16) of specimens, further limiting the transSylvian corridor to zones 1 and 2.

The present study suggests that the optimal surgical strategy to obtain maximal exposure for an insular glioma requires careful assessment of each patient's tumor location within the insula. Determining the tumor location in relation to the different zones of the insula allows for pre-operative estimation of the extent of tumor resection[34] and anticipation of the surgical approach that will be required once the cortex is exposed. If the tumor is limited at the Sylvian line in zones 1 and 4 (anterior), our data suggests that the tumor could be sufficiently exposed through a transSylvian approach. However, if the tumor is located in zones 2 and 3 (posterior), using a transSylvian approach may require splitting the Sylvian fissure completely and using both extensive retraction and venous sacrifice. This is especially important if the tumor invades into zone 3. However, if the tumor is located either in the periphery of the Sylvian line or expands to or beyond the peri-insular sulci, only the transcortical approach will provide a sufficient surgical profile to attempt maximal resection, regardless of the zone. In such cases, direct cortical and subcortical mapping will determine the trajectory and degree of resection in each particular patient.

Whereas cutting the Sylvian bridging veins during TS might seem reasonable, our results suggest that such an option could entail serious venous drainage problems in 30% of cases. Also, we identified clustering of veins in the opercula in more than half of our specimens. Regardless of the overall venous pattern, we consider that a cluster of bridging veins draining the majority of blood from the inferior frontal gyrus and inferior

parietal lobule is, in itself, a limitation to the TSVC. In his study on the cerebral veins, Seeger identified that the direction of the venous blood flow at the lateral surface of the brain was towards the Sylvian fissure in 56% of cases, followed by the Labbé complex and the bridging veins to the superior sagittal sinus.[97] This finding confirms the important role that the Sylvian venous system plays in the venous outflow of the lateral surface of the brain. In the subset of patients harvesting critical bridging veins that must be preserved, our findings suggest that the TS approach might be insufficient to expose tumors sitting within the Sylvian line, especially in the posterior zones (2&3).

There are a few reports on the surgical technique and clinical outcomes of the transSylvian approach to insular tumors.[23,43,45,46,63,98] There is common consensus between all groups that large amounts of retraction are required to expose the insula when using the transSylvian corridor, which we have confirmed in our study. However, none of these reports mention the rate in which the Sylvian bridging veins were cut. In their series, Lang et al stated that 2-2.5 cm of retraction was required to expose the insular tumor[43,63]. However the authors did not mention the standard deviation of their measurements, whether they found significant differences in the different parts of the opercula or if the measure referred to the retraction length to one operculum or the distance between opercula after splitting the Sylvian fissure. We addressed this uncertainty in our study by measuring the maximal retraction length that could be applied to each operculum without damaging the venous system. In all our specimens, we could not apply 2cm of retraction length without cutting the bridging veins. Also, when preserving the venous system (TS) the insular exposure was limited and significantly inferior to that of TSVC and TC. From these findings, we suspect that the majority of large insular tumors successfully removed via the TS were, instead, TSVC. Although a TSVC corridor would be an acceptable option for those cases where the venous bridging veins could be spared (70%) and the insular tumor is within the confines of the peri-insular sulci, we find a major limitation of this strategy in the remaining 30% of patients, in which a TC approach would potentially overcome this limitation.

Previous studies have shown that TC approaches to subcortical lesions are safe[34,38,63,98]. Furthermore, our group has reported the first large surgical experience for insular tumors using the transcortical approach[34]. Our data suggests that the TC approach provides a better surgical profile than the other options. In fact, the maximal difference in insular exposure between the TC and the TSVC was observed in the posterior insular zones, where the TS corridor is severely limited by the narrow Sylvian cistern. However, the surgical profile of the TC approach to the posterior zones is highly dependent on brain mapping and therefore impossible to predict before surgery. Although cortical sacrifice is inherent to the TC corridor, direct cortical and subcortical stimulation during awake surgery allows the neurosurgeon to identify function and work around eloquent areas. In contrast, when dissecting the Sylvian cistern, especially the

posterior portion, the neurosurgeon has to perform meticulous dissection of critical neurovascular structures in a very narrow corridor. In a study of surgical approaches to temporal tumors in 235 patients, Schramm et. al. [98,99] reported that the TS approach was associated with the highest combined rate of complications, which could be caused by inadvertent subpial dissection or transection of an insular artery. Using a transSylvian approach to insular tumors, Hentschel et. al. reported a post-operative speech complication rate of 30%, which they attributed to transient ischemia related to both retraction and arterial dissection. These results are congruent with the evidence of our morphometric analysis, where large amounts of retraction over the opercula, including the pars opercularis and the precentral gyrus, are required for maximal insular exposure.

The transcortical approach to the insula uses direct cortical and subcortical stimulation to assess and preserve cortical function. While the anatomical location of cortical function is variable, there are general patterns of functional anatomy that may guide surgical planning. In zone 1, the transcortical approach transgressed 60% of pars orbicularis and opercularis, and 20% of pars triangularis. In the dominant hemisphere, language function is classically described in Brodmann areas 44 and 45 (also known as Broca's area). In our experience, only the posterior aspect of pars opercularis of the dominant hemisphere is highly involved in speech production[100]. However, in patients with tumors affecting pars opercularis, transcortical resection using constant cortical mapping may be safe.[100] In zone II, the opercular segment of the precentral gyrus, which may account for the contralateral motor control of the face, sits above of the anterior long gyrus of the insula. Our data show that removing the opercular portion of the precentral gyrus provides 146% insular exposure and 171% surgical freedom compared to TSVC. There is evidence of recovery after resection of the facial motor cortex in the non-dominant hemisphere,[101] which has been in line with the surgical results published by our group[34] and that of Duffau et. al.[40] If resection of the facial motor cortex in the dominant hemisphere is attempted, it should be limited to pure facial expression, which will cause transient central facial paralysis. After studying a series of 14 patients who underwent an awake transcortical approach for tumors affecting zone 2 of the insula and the inferior parietal lobule, Maldonado et.al. identified speech function in the majority of cases. Interestingly, they found high inter-individual variability in the anatomical location of language. Therefore, awake cortical and subcortical stimulation must be performed in each case to assess the location of functional cortex and white matter tracts for language, which will further characterize the final transcortical corridor in each patient.[102] The posterior margin of the transcortical approach in zone 2 involved 1 cm of the postcentral gyrus, which may account for the somatosensory function of the contralateral half of the face. In zone 3, exposure of the posterior long gyrus and planum temporalis requires excision, to some degree, of Heshl's gyrus. When Heshl's gyrus is resected along with the anterior segment of the superior temporal gyrus, the insular exposure becomes 164% that of the TSVC. The primary auditory cortex, located at the Heshl's gyrus in both

hemispheres, receives bilateral afferent sensory signaling from the cochlear and superior olivary nucleus via the inferior colliculus and medial geniculate body of the thalamus.[103] In a recent study, Javad et.al. provided evidence of a link between the auditory areas through interhemispheric transcallosal pathways using diffusion tensor imaging in humans[104]. Hence, complete resection of Heshl's gyrus in one hemisphere (e.g. TC to zone 3 of the insula) should not cause a perceivable loss in audition. Nonetheless, our experience is congruent with other authors in that resection of the superior temporal gyrus under direct cortical stimulation is safe.3[4,40] Cortical resection to expose zone 3 does not involve the angular gyrus, or regions posterior to Heshl's gyri, which, in the dominant hemisphere, may account for wernicke's area (Brodmann area 22). When resecting tumors in zone 2 and 3 of the insula, constant direct cortical and subcortical stimulation of the superior temporal gyrus and parietal operculum are performed before any corticectomy to assess for language function, especially in the dominant hemisphere.[40] The arcuate and middle longitudinal fascicles, and Wernicke's area, which are in the vicinity of Heshl's gyrus, are presumed to be a core part of the language pathway, therefore potentially limiting the transcortical corridor around the primary auditory cortex in the dominant hemisphere. However, the location and composition of such areas and tracts varies considerably in the population. Therefore intraoperative functional mapping becomes essential to guide the resection in each patient.

Although the use of intraoperative navigation is very important in modern neurosurgery, it should not replace anatomical knowledge. In this study, we identified two anatomical landmarks that may be used to infer the location of the insular zones before opening the skull. We found a strong correlation between the division of the insular lobe into anterior and posterior parts and the external acoustic meatus over the skull surface. Also, we found that the superior segment of the squamosal suture could be used to infer the location of the Sylvian fissure, which divides the insular lobe into dorsal and ventral segments. Knowledge of these anatomical relations may aid in tailoring the craniotomy to the insular lesion.

Thorough knowledge of the arterial blood supply beyond M2 is critical to preserve function while dissecting an insular tumor. When using microsurgical dissection around the insula, the high power magnification reduces peripheral view. It is crucial to recognize the cortical distribution related to each M2 artery transiting within the middle cerebral artery's candelabra, as it is being dissected. We have found that the M2 artery running over the central sulcus of the insula becomes the Rolandic artery in 100% of our specimens, which is in agreement to the findings reported by Ture et. al. in their study on the insular arteries54. Interestingly, we observed that the M3 segment of the Rolandic artery runs in the depth of the operculum in 18% (3/16) of cases, which requires careful dissection when using the TC corridor to approach zones 1 or 2.

Limitations of Objective B

Human postmortem surgical simulation provides the best alternative to surgical experimentation because it is safe, provides a very realistic scenario of the human anatomy, and allows for prolonged research time. On the first stage of this work,[87] we described our customized surgical simulation methodology for neurosurgical research. One of the most relevant findings of the study was that he retraction profile was not statistical different between specimens prepared with our customized embalming formula and un-embalmed (i.e. fresh) cadavers.[87]

This new method overcomes the major limitations for surgical simulation when using classical cadaver processing techniques (brain stiffness and inability to retract), allowing for a very realistic surgical simulation with life-like manipulation of the brain. Therefore, the comparison of surgical access to the insula in this work uses the most advanced cadaveric neurosurgical research methods to determine the surgical profile of the transSylvian and transcortical approaches to the insula.

However several limitations may limit direct application of our findings to clinical practice. These limitations are intrinsic to all postmortem research. These limitations include absence of anatomical distortion due to mass-effect; the lack of effective brain relaxation; and the impossibility to study cortical function. Evacuation of cerebrospinal fluid, thorough dissection of arachnoid adhesions, and opercular retraction allowed splitting the sylvian fissure widely in all our simulations. However, clinical maneuvers such as brain relaxation techniques such hyperventilation and the use of brain osmotic agents could not be applied therefore limiting the surgical results of the study. The mass effect related to insular lesions may cause substantial anatomical distortion and should be considered in the pre-operative planning. However mass effect is highly variable and case-specific. We used specimens without known brain lesions to maximize statistical power and internal validity when comparing surgical approaches.

Direct assessment of cortical function is an inherent limitation of postmortem research and may limit the clinical application of this study. Localization of brain function is specific to each patient and situation (e.g. neural plasticity) and therefore the impact of cortical function location to the transcortical approach is inherently diverse and should be assessed in every case.

Objective C: Correlation between anatomical classification of insular gliomas and surgical outcomes.

Prior studies showed that maximal surgical resection of insular gliomas enhances overall survival, progression free survival, and seizure outcome [42] [34,35,38]. Furthermore surgery can be accomplished with a median EOR of 80-82% and minimal morbidity of long-term language (0%) and motor function (2.6%)[34,38,43,44]. In our previously published retrospective series of patients with insular gliomas we assessed postoperative morbidity and patient survival while describing an anatomical grading system for the classification of intrinsic insular tumors. Using this classification system we now analyze prospectively collected data for a wide distribution of patients with insular gliomas to determine the significance of the "Berger-Sanai" classification system with respect to extent of resection and inter-observer variability between clinicians. We found this system to be highly reliable with minimal variability between clinicians and highly predictive of the expected mean EOR across all zones.

Few insular based gliomas are confined entirely within the insula (15% in this series). Furthermore depending on where within the insula a glioma is based the surgical approach and anatomical considerations vary. For this reason a common terminology is helpful when discussing individual lesions. Yasargil et al proposed a classification system based on whether the lesion is restricted to the insula (type 3), part of the insula (type 3A), or include the adjacent operculum (3B),[23] In this classification system, insular lesions that involve one of the paralimbic orbitofrontal and temporopolar areas are classified as type 5A and if both areas are involved then it is considered type 5B [23]. We found this classification system failed to address several of the anatomical features relevant to surgical treatment of insular gliomas such as proximity to potentially functional areas.

Therefore we proposed an anatomical classification system based on splitting the insula along the sylvian fissure and foramen of Monro, thereby dividing it into 4 parts (Zones I-IV)[34]. This approach has allowed us to think about and describe each insular tumor in relation to (1) the perisylvian language network (above and below the sylvian fissure in the dominant hemisphere), (2) primary sensory and motor areas (commonly for zone I or II gliomas), (3) Heschl's gyrus (zone III gliomas), (4) and middle cerebral artery branches (particularly lateral lenticulostriate branches found within the suprasylvian region of zone I). It is critically important that a classification system have little variability between examiners. We tested this by asking 3 clinicians at varying stages in their careers

to rate a cohort of insular gliomas finding strong correlation between examiners (kappa coefficient 0.857).

Furthermore, we set out to determine if zone classification was predictive of EOR. We found no differences in mean EOR between the 2 published series. In this prospective series we reconfirmed our prior observation that zone classification was predictive of EOR with highest mean EOR seen in Zone I and III tumors. We also showed that zone classification appears to be predictive of short-term postoperative morbidity with a modestly higher early complication rate seen in Giant and zone I tumors and lowest complication rates seen in zone II and IV tumors ($p=0.03$). In this current series we identified a slightly higher rate of short-term face motor deficits, which likely corresponds to the improved EOR seen in zone I and II insular gliomas due to a greater willingness to extent a trans-cortical window of entry through face motor areas for purposes of enhancing EOR. Long-term patient morbidity continued to be minimal at 2.3% and virtually unchanged from our initial series.

Recently published reports suggest that insular oligodendrogliomas have a higher rate of chromosome 1p and 19q deletions and that the presence of an IDH1 mutation in WHO III and IV gliomas might suggest a greater degree of surgical respectability[105,106]. We therefore integrated tumor molecular characterization in our analysis and similar to Wu et al found a high (43%) incidence of 1p19q co-deletion in insular oligodendrogliomas.[106] This might contribute to the prolonged overall and progression free survival common to insular gliomas[34,35]. We however found no differences in surgical resectability of insular gliomas of any grade or zone based on IDH status.

To the authors' knowledge, the combined experience of our published data represents the largest series of patients with insular gliomas at the time this thesis was prepared. Even so, there are study limitations that which must be considered. Though we've previously demonstrated the importance of EOR on survival and malignant transformation, the number of patients between the 2 series remains insufficient to accurately demonstrate an extent of resection threshold for low and high-grade insular gliomas. Furthermore, though there was little inter-observer variability between clinicians with varying degrees of clinical experience and expertise, it remained an internal single institution validation. The adoption of this classification system with external multi-institution validation is a topic of future direction.

Integrated discussion of all objectives

The evidence collected in this sequential research supports that our customized surgical simulation method for neurosurgical technique research is superior to the gold standard.88 Data from our comparative analysis –objective A- showed that our custom embalming method provides durable life-like brain features with lower biohazardous exposure to the researcher. A more realistic simulation model enhances the clinical translation of any findings obtained using neurosurgical simulation in cadavers. There are different embalming options available in the market than those included in the study. [96] Also, there are tissue softeners that presumably reduce brain stiffness by removing formaldehyde (fixative) out of the specimen. Although it is beyond the scope of this study to compare all the available processing techniques, the proposed customized embalming formula is easier to produce and use than other techniques that require special chemicals, successive embalming and softening steps, or complex measurements. We chose to assess our customized formula relative to the gold standards (formaldehyde-based and unembalmed methods) which are widely used internationally. This laboratory research allowed us to launch a complex technical cadaveric assessment of the neurosurgical approaches to the insula, with the reassurance that our methods were the most robust in the literature.

Therefore the research on neurosurgical simulation on cadavers in objective A was foundational to the development of objective B, which follows. The evidence from the objective B of this work showed that the transcranial approach offered the best overall surgical exposure, window and freedom in zones II and III (posterior) of the insula.62 There are 3 surgical strategies and techniques to approach insular gliomas; the transSylvian approach; the transSylvian approach with the bridging veins cut; and the transcortical approach. Overall, the transcortical approach provided improved access to the insula than the transSylvian approach. Although in some circumstances the TC and TSVC provide similar surgical exposure and surgical freedom, cutting bridging veins may be unsafe in 30% of patients. Cortical and subcortical mapping is critical before and during the transcortical approach to the posterior zones (2 and 3). That is because the facial motor and somatosensory functions (zone2) and the language pathways (zone 3) may be involved. The greatest insular exposure in zones 2 and 3 is found after resection of the precentral gyrus and superior temporal gyrus. While the TC and TSVC provide equivalent access to the insula in zones 1 and 2, a TC approach may be superior to access zones 3 and 4 (inferior). Therefore preoperative radiological assessment and our insula classification scheme are the only reliable tools in guiding preoperative surgical planning. This section of the thesis demonstrates that the TC approach may be superior to the TSVC approach in resecting gliomas that, while primarily within the confines of the

insula, extend to and beyond the peri-insular sulcus. With this said, neurosurgeons may consider the TS and TSVC approaches for small to moderate size tumors located within the confines of the insula. Selecting the surgical option providing the greatest insular exposure should also help reduce surgical morbidity.

Finally, in objective C of this work we used the cumulative knowledge in objectives A & B as foundation to transition into clinical research. We found that the insula classification used in objective B was predictive of surgical success (best extent of resection seen in zones I and IV), postoperative morbidity (worst complication rate in Zone I and least in zone II &IV). We also proven that the insula classification used in objective B is robust and has little interobserver reliability.89 Maximal resection of insular gliomas within safe surgical limits continues to be the best strategy to improve patient outcome with acceptable morbidity. Our proposed classification system is highly reliable and provides valuable information to anticipate insular glioma EOR and short-term morbidity. The information provided by this body of work may be of extreme relevance when communicating to our patients because it allows, for the first time, to explain anticipated outcomes and reasonable treatment expectations based on the patient's specific tumor class. The combined experience of our patient group in objective C and our previously published report represents the largest series of insular glioma resections in the world at the time of this thesis.

Scientific and clinical impact of the thesis

The results of this doctoral work have a direct and transformational impact in each of the topics involved. The scientific breakthroughs and most important advances in the field are as follows:

1. The development of a neurosurgical simulation method that is life like an applicable the real surgery. This is a transformational change in methodology in the field of neurosurgical research because it allows a high fidelity simulation and therefore better clinical application of the findings in the surgical laboratory.

2. The objective definition of the benefits and limitations of each surgical approach to the insula. Up to now, there has not been objective data regarding the surgical profile (advantages and disadvantages) of the different surgical corridors to

the insula.

3. Validation of the surgical- anatomical classification of the insula and it's correlation with survival and extent of tumor resection. This validation is critical to decision making and surgical planning and offers a robust scientific background to patient decision making.

4. Improvement on the general knowledge regarding clinical expectations on each of the subtypes of insular gliomas. Clinical expectations and options are key in insular glioma decision making, this research improves our knowledge of the behavior as well as the surgical success custom to each insular glioma region.

5. Advancements regarding the understanding of the clinical behavior on each glioma subgroup in reference to their anatomical localization. This allows for a more tailored advice to a patient with a specific tumor within the insula.

Reflexió Personal de cloenda

El diagnòstic de glioma insular es devastador tant per al pacient com pel seu entorn pròxim. Invariablement, el pacient es troba amb la necessitat existencial d'esbrinar "quant de temps em queda de vida". En la gran majoria de casos les expectatives no superen els 24 mesos d'esperança de vida al diagnòstic, la qual cosa relativitza de manera extraordinària el valor atribuït a cada Mes de vida i, per a molts, "cada dia es inavaluable". És en aquesta circumstància quan l'evidència fruit del treball comprès en l'objectiu C és fonamental per a la formació d'expectatives d'evolució clínica i esperança de vida dels pacients amb glioma insular. El treball investigador en l'objectiu C ha estat motivat específicament per millorar -sinó resoldre- l'asfixiant incertesa temporal i crisi existencial que pateixen la majoria dels pacients diagnosticats de glioma insular. És per a aquests pacients, a qui la vida els afligeix amb un diagnòstic terminal inesperat, que tot esforç científic es imprescindible i necessari.

CONCLUSIONS

The following are the most substantial conclusions of this work:

1. The customized embalming formula for neurosurgical simulation designed in this work provides optimal brain retraction profile, long use time, and low biohazard risk for neurosurgical simulation in cadavers.
2. Specimens embalmed with the customized formula displayed three times less retraction pressure while providing four times more surgical retraction area compared to the formaldehyde group
3. Cryopreserved specimens had a very limited working time due to fast decay (4 hours for research purposes)
4. Radiological studies showed that the customized and cryopreserved groups provided better anatomical detail than the formaldehyde group, although random hyperintense artifacts were identified in the customized specimens
5. The customized embalming formula takes advantage of the best formaldehyde properties – long preservation time and microorganism growth prevention – combined with a retraction profile and physical properties similar to what can be achieved with cryopreservation. Also, a substantial reduction in formaldehyde concentration makes this option safer for researchers
6. The optimal surgical strategy to obtain maximal exposure for an insular glioma requires careful assessment of each patient's tumor location within the insula
7. If the tumor is limited at the Sylvian line in zones 1 and 4 (anterior), it could be sufficiently exposed through a transSylvian approach. However, if the tumor is located in zones 2 and 3 (posterior), the Transcortical approach with mapping is superior.
8. If the tumor is located either in the periphery of the Sylvian line or expands to or beyond the peri-insular sulci, only the transcortical approach will provide a sufficient surgical profile to attempt maximal resection, regardless of the zone.
9. Cutting the bridging veins during a TS approach provided maximal advantage in zone 3, where it provided a significant increase in insular exposure.

10.Whereas cutting the Sylvian bridging veins during TS might seem reasonable, our results suggest that such an option could entail serious venous drainage problems in 30% of cases.

11.We have found that the M2 artery running over the central sulcus of the insula becomes the Rolandic artery in 100% of our specimens

12. Maximal surgical resection of insular gliomas enhances overall survival, progression free survival, and seizure outcome.

13. Zone classification was predictive of EOR with highest mean EOR seen in Zone I and III tumors.

14. Zone classification appears to be predictive of short-term postoperative morbidity with a modestly higher early complication rate seen in Giant and zone I tumors and lowest complication rates seen in zone II and IV tumors ($p=0.03$).

15. We however found no differences in surgical resectability of insular gliomas of any grade or zone based on IDH status

REFERENCES

1. Reil J. Unterfuchungen uber den Bau des grofsen Gehirns im Menfchen: Vierte Fortsetzung VIII. Arch Physiol Halle 1809:136-46.
2. Cunningham DJ. Development of the Gyri and Sulci on the Surface of the Island of Reil of the Human Brain. J Anat Physiol 1891;25:338-48.
3. Guldberg V. Zur Morphologie der Insula Reilii. Anat Anz 1887:659-65.
4. clark T. The comparative anatomy of the insula. J Comp Neurol 1896:59-100.
5. Eberstaller O. Zur Anatomie und Morphologie der Insula Reilii. Anat Anz 1887:739-50.
6. Cushing H. Instruction in operative medicine: With the description of a course in the Hunterian Laboratory of Experimental Medicine. ull Johns Hopkins Hosp 1906;17:123-34.
7. Laws ER, Jr. Neurosurgery's man of the century: Harvey Cushing--the man and his legacy. Neurosurgery 1999;45:977-82.
8. Cushing H. The special field of neurological surgery. Bulletin of the Johns Hopkins Hospital 1905;16:168.
9. curhing H. The special field of neurological surgery: five years later. Bulletin of the Johns Hopkins Hospital 1905;21:325-39.
10. cushing h. The special field of neurological surgery after another interval. Archives of Neurology and Psychiatry 1920;4:603-37.
11. heuer G. Surgical experiences with an intracranial approach to chiasmal lesions. Arch surg 1920;1:368-81.
12. Krayenbühl H YM. Die Zerebral Angiography Thieme; 1965.
13. Lasjaunias P BA. Functional Vascular Anatomy of Brain, Spinal Cord and Spine. Surgical Neuro-Angiography: pringer-Verlag; 1990:233-4.
14. Serrats AA, Vlahovitch B, Parker SA. The arteriographic pattern of the insula: its normal appearance and variations in cases of tumour of the cerebral hemispheres. J Neurol Neurosurg Psychiatry 1968;31:379-90.
15. Wolf BS, Huang YP. The Insula and Deep Middle Cerebral Venous Drainage System: Normal Anatomy and Angiography. Am J Roentgenol Radium Ther Nucl Med 1963;90:472-89.
16. letter E. In memoriam: Sir Peter Mansfield (1933-2017). Magnetic Resonance in Medicine 2017;78:826-7.
17. Glasser MF, Smith SM, Marcus DS, et al. The Human Connectome Project's neuroimaging approach. Nat Neurosci 2016;19:1175-87.
18. Zhang Y, Zhang J, Oishi K, et al. Atlas-guided tract reconstruction for automated and comprehensive examination of the white matter anatomy. Neuroimage 2010;52:1289-301.

19. Tew JM, Jr. M. Gazi Yasargil: Neurosurgery's man of the century. Neurosurgery 1999;45:1010-4.

20. Krayenbühl H YaM. The use of binocular microscopes in neurosurgery. Wien Z Nervenheilkd Grenzgeb 1967;25:268–77.

21. Kriss TC, Kriss VM. History of the operating microscope: from magnifying glass to microneurosurgery. Neurosurgery 1998;42:899-907; discussion -8.

22. Yaşargil G. Microneurosurgery. Microsurgical Anatomy of the Basal Cisterns and Vessels of the Brain, Diagnostic Studies, General Operative Techniques and Pathological Considerations of the Intracranial Aneurysms. Stuttgart: Thieme Verlag; 1984.

23. Yasargil MG, von Ammon K, Cavazos E, Doczi T, Reeves JD, Roth P. Tumours of the limbic and paralimbic systems. Acta Neurochir (Wien) 1992;118:40-52.

24. Yasargil MG, Reeves JD. Tumours of the limbic and paralimbic system. Acta Neurochir (Wien) 1992;116:147-9.

25. Fernandez-Miranda JC, Rhoton AL, Jr., Alvarez-Linera J, Kakizawa Y, Choi C, de Oliveira EP. Three-dimensional microsurgical and tractographic anatomy of the white matter of the human brain. Neurosurgery 2008;62:989-1026; discussion -8.

26. Ture U, Yasargil MG, Friedman AH, Al-Mefty O. Fiber dissection technique: lateral aspect of the brain. Neurosurgery 2000;47:417-26; discussion 26-7.

27. Kucukyuruk B, Richardson RM, Wen HT, Fernandez-Miranda JC, Rhoton AL, Jr. Microsurgical anatomy of the temporal lobe and its implications on temporal lobe epilepsy surgery. Epilepsy Res Treat 2012;2012:769825.

28. Kaneko N, Boling WW, Shonai T, et al. Delineation of the safe zone in surgery of sylvian insular triangle: morphometric analysis and magnetic resonance imaging study. Neurosurgery 2012;70:290-8; discussion 8-9.

29. Sanai N, Mirzadeh Z, Berger MS. Functional outcome after language mapping for glioma resection. N Engl J Med 2008;358:18-27.

30. Foerster O. The cerebral cortex of man. Lancet 1931;2:3019-312.

31. Penfield W. Some observations on the cerebral cortex of man. Proc R Soc Lond B Biol Sci 1947;134:329-47.

32. Penfield W RT. Secondary sensory and motor representation. New York: Macmillan; 1950.

33. Rasmussen T, Penfield W. Further studies of the sensory and motor cerebral cortex of man. Fed Proc 1947;6:452-60.

34. Sanai N, Polley MY, Berger MS. Insular glioma resection: assessment of patient morbidity, survival, and tumor progression. J Neurosurg 2010;112:1-9.

35. Nader Sanai MSB. Recent surgical management of gliomas. In: Yamanaka R, ed. Glioma: Immunotherapeutic Approaches: Landes Bioscience and Springer Science; 2012.

36. Ranck J. Which elements are excited in electrical stimulation of mammalian central nervous system: a

review. Brain Res 1975;98:417-40.

37. Haglund MM, Ojemann GA, Blasdel GG. Optical imaging of bipolar cortical stimulation. J Neurosurg 1993;78:785-93.

38. Duffau H. A personal consecutive series of surgically treated 51 cases of insular WHO Grade II glioma: advances and limitations. J Neurosurg 2009;110:696-708.

39. Moritz-Gasser S, Duffau H. The anatomo-functional connectivity of word repetition: insights provided by awake brain tumor surgery. Front Hum Neurosci 2013;7:405.

40. Duffau H, Capelle L, Lopes M, Faillot T, Sichez JP, Fohanno D. The insular lobe: physiopathological and surgical considerations. Neurosurgery 2000;47:801-10; discussion 10-1.

41. Freyschlag CF, Duffau H. Awake brain mapping of cortex and subcortical pathways in brain tumor surgery. J Neurosurg Sci 2014.

42. Ius T, Pauletto G, Isola M, et al. Surgery for insular low-grade glioma: predictors of postoperative seizure outcome. J Neurosurg 2014;120:12-23.

43. Lang FF, Olansen NE, DeMonte F, et al. Surgical resection of intrinsic insular tumors: complication avoidance. J Neurosurg 2001;95:638-50.

44. Skrap M, Mondani M, Tomasino B, et al. Surgery of insular nonenhancing gliomas: volumetric analysis of tumoral resection, clinical outcome, and survival in a consecutive series of 66 cases. Neurosurgery 2012;70:1081-93; discussion 93-4.

45. Vanaclocha V, Saiz-Sapena N, Garcia-Casasola C. Surgical treatment of insular gliomas. Acta Neurochir (Wien) 1997;139:1126-34; discussion 34-5.

46. Wang P, Wu MC, Chen SJ, Xu XP, Yang Y, Cai J. Microsurgery Resection of Intrinsic Insular Tumors via Transsylvian Surgical Approach in 12 Cases. Cancer biology & medicine 2012;9:44-7.

47. Alimohamadi M, Shirani M, Shariat Moharari R, et al. Application of Awake Craniotomy and Intraoperative Brain Mapping for Surgical Resection of Insular Gliomas of the Dominant Hemisphere. World Neurosurg 2016;92:151-8.

48. Neuloh G, Pechstein U, Schramm J. Motor tract monitoring during insular glioma surgery. J Neurosurg 2007;106:582-92.

49. Potts MB, Chang EF, Young WL, Lawton MT, Project UBAS. Transsylvian-transinsular approaches to the insula and basal ganglia: operative techniques and results with vascular lesions. Neurosurgery 2012;70:824-34; discussion 34.

50. Meybodi AT, Griswold D, Tabani H, et al. Topographic Surgical Anatomy of the Para-Sylvian Anterior Temporal Artery for Intracranial-Intracranial Bypass. World Neurosurg 2016.

51. Tanriover N, Rhoton AL, Jr., Kawashima M, Ulm AJ, Yasuda A. Microsurgical anatomy of the insula and the sylvian fissure. J Neurosurg 2004;100:891-922.

52. Inoue K, Seker A, Osawa S, Alencastro LF, Matsushima T, Rhoton AL, Jr. Microsurgical and endoscopic anatomy of the supratentorial arachnoidal membranes and cisterns. Neurosurgery 2009;65:644-64; discussion 65.

53. Ture U, Yasargil DC, Al-Mefty O, Yasargil MG. Topographic anatomy of the insular region. J Neurosurg 1999;90:720-33.

54. Ture U, Yasargil MG, Al-Mefty O, Yasargil DC. Arteries of the insula. J Neurosurg 2000;92:676-87.

55. Meybodi AT, Griswold D, Tabani H, et al. Topographic Surgical Anatomy of the Parasylvian Anterior Temporal Artery for Intracranial-Intracranial Bypass. World Neurosurg 2016;93:67-72.

56. Gogolla N. The insular cortex. Curr Biol 2017;27:R580-R6.

57. Nieuwenhuys R VJ, van Huijzen C. The Human Central Nervous System. Berlin: Springler-Verlag; 1988.

58. Fernandez-Miranda JC, Rhoton AL, Jr., Kakizawa Y, Choi C, Alvarez-Linera J. The claustrum and its projection system in the human brain: a microsurgical and tractographic anatomical study. J Neurosurg 2008;108:764-74.

59. Ostrowsky K, Isnard J, Ryvlin P, Guenot M, Fischer C, Mauguiere F. Functional mapping of the insular cortex: clinical implication in temporal lobe epilepsy. Epilepsia 2000;41:681-6.

60. Garcia-Larrea L. The posterior insular-opercular region and the search of a primary cortex for pain. Neurophysiol Clin 2012;42:299-313.

61. Dronkers NF. A new brain region for coordinating speech articulation. Nature 1996;384:159-61.

62. Benet A, Hervey-Jumper SL, Sanchez JJ, Lawton MT, Berger MS. Surgical assessment of the insula. Part 1: surgical anatomy and morphometric analysis of the transsylvian and transcortical approaches to the insula. J Neurosurg 2016;124:469-81.

63. Hentschel SJ, Lang FF. Surgical resection of intrinsic insular tumors. Neurosurgery 2005;57:176-83; discussion -83.

64. Ostrom QT, Gittleman H, de Blank PM, et al. American Brain Tumor Association Adolescent and Young Adult Primary Brain and Central Nervous System Tumors Diagnosed in the United States in 2008-2012. Neuro-oncology 2016;18 Suppl 1:i1-i50.

65. Rey-Dios R, Cohen-Gadol AA. Technical nuances for surgery of insular gliomas: lessons learned. Neurosurg Focus 2013;34:E6.

66. Hervey-Jumper SL, Berger MS. Insular glioma surgery: an evolution of thought and practice. J Neurosurg 2019;130:9-16.

67. Chen LF, Yang Y, Ma XD, et al. Optimizing the Extent of Resection and Minimizing the Morbidity in Insular High-Grade Glioma Surgery by High-Field Intraoperative MRI Guidance. Turk Neurosurg 2017;27:696-706.

68. Eyupoglu IY, Buchfelder M, Savaskan NE. Surgical resection of malignant gliomas-role in optimizing patient outcome. Nat Rev Neurol 2013;9:141-51.

69. Eseonu CI, ReFaey K, Garcia O, Raghuraman G, Quinones-Hinojosa A. Volumetric Analysis of Extent of Resection, Survival, and Surgical Outcomes for Insular Gliomas. World Neurosurg 2017;103:265-74.

70. Weller M, van den Bent M, Hopkins K, et al. EANO guideline for the diagnosis and treatment of anaplastic gliomas and glioblastoma. Lancet Oncol 2014;15:e395-403.

71. Rhoton AL, Jr. The lateral and third ventricles. Neurosurgery 2002;51:S207-71.

72. Aboud E, Al-Mefty O, Yasargil MG. New laboratory model for neurosurgical training that simulates live surgery. J Neurosurg 2002;97:1367-72.

73. Bernardo A, Preul MC, Zabramski JM, Spetzler RF. A three-dimensional interactive virtual dissection model to simulate transpetrous surgical avenues. Neurosurgery 2003;52:499-505; discussion 4-5.

74. Menovsky T. A human skull cast model for training of intracranial microneurosurgical skills. Microsurgery 2000;20:311-3.

75. Olabe J, Olabe J, Roda JM, Sancho V. Human cadaver brain infusion skull model for neurosurgical training. Surgical neurology international 2011;2:54.

76. Olabe J, Olabe J, Sancho V. Human cadaver brain infusion model for neurosurgical training. Surg Neurol 2009;72:700-2.

77. Sanan A, Abdel Aziz KM, Janjua RM, van Loveren HR, Keller JT. Colored silicone injection for use in neurosurgical dissections: anatomic technical note. Neurosurgery 1999;45:1267-71; discussion 71-4.

78. Chia SE, Ong CN, Foo SC, Lee HP. Medical students' exposure to formaldehyde in a gross anatomy dissection laboratory. J Am Coll Health 1992;41:115-9.

79. Keil CB, Akbar-Khanzadeh F, Konecny KA. Characterizing formaldehyde emission rates in a gross anatomy laboratory. Appl Occup Environ Hyg 2001;16:967-72.

80. Kerns WD, Pavkov KL, Donofrio DJ, Gralla EJ, Swenberg JA. Carcinogenicity of formaldehyde in rats and mice after long-term inhalation exposure. Cancer Res 1983;43:4382-92.

81. Kriebel D, Sama SR, Cocanour B. Reversible pulmonary responses to formaldehyde. A study of clinical anatomy students. Am Rev Respir Dis 1993;148:1509-15.

82. Nielsen GD, Wolkoff P. Cancer effects of formaldehyde: a proposal for an indoor air guideline value. Arch Toxicol 2010;84:423-46.

83. Organization WH. IARC Monographs on the Evaluation of Carcinogenic Risks to Humans. Volume 71: ReEvaluation of Some Organic Chemicals, Hydrazine and Hydrogen Peroxide. Lyon: IARC Press; 1999:749-67.

84. Agency UEP. Integrated Risk Information System: Formaldehyde. 2014.

85. U.S. Environmental Protection Agency. Integrated Risk Information System (IRIS) on Formaldehyde. In: National Center for Environmental Assessment, Office of Research and Development, eds. Washington, DC1999.

86. Alvernia JE, Pradilla G, Mertens P, Lanzino G, Tamargo RJ. Latex injection of cadaver heads: technical note. Neurosurgery 2010;67:362-7.

87. Benet A, Rincon-Torroella J, Lawton MT, Gonzalez Sanchez JJ. Novel embalming solution for neurosurgical simulation in cadavers. J Neurosurg 2014.

88. Benet A, Rincon-Torroella J, Lawton MT, Gonzalez Sanchez JJ. Novel embalming solution for neurosurgical simulation in cadavers. J Neurosurg 2014;120:1229-37.

89. Hervey-Jumper SL, Li J, Osorio JA, et al. Surgical assessment of the insula. Part 2: validation of the Berger-Sanai zone classification system for predicting extent of glioma resection. J Neurosurg 2016;124:482-8.

90. Martino J, Vergani F, Robles SG, Duffau H. New insights into the anatomic dissection of the temporal stem with special emphasis on the inferior fronto-occipital fasciculus: implications in surgical approach to left mesiotemporal and temporoinsular structures. Neurosurgery 2010;66:4-12.

91. Klingler J, Ludwig E, eds. Atlas cerebri humani: The Inner Structure of the Brain Demonstrated on the Basis of Macroscopical Preparations. basel: s. karger AG; 1956.

92. Olabe J, Sancho V. Human cadaver brain infusion model for neurosurgical training. Surg Neurol 2009;72:700-2.

93. Beane Freeman LE, Blair A, Lubin JH, et al. Mortality from solid tumors among workers in formaldehyde industries: An update of the NCI cohort. American journal of industrial medicine 2013.

94. Burkhart KJ, Nowak TE, Blum J, et al. Influence of formalin fixation on the biomechanical properties of human diaphyseal bone. Biomedizinische Technik Biomedical engineering 2010;55:361-5.

95. International Agency for Research on Cancer. Phenol. Lyon: World Health Organization; 1989:749-67.

96. Whitehead MC, Savoia MC. Evaluation of methods to reduce formaldehyde levels of cadavers in the dissection laboratory. Clin Anat 2008;21:75-81.

97. Seeger W. Microsurgery of Cerebral Veins. 1 ed: Springer Vienna; 2000.

98. Schramm J, Aliashkevich AF. Surgery for temporal mediobasal tumors: experience based on a series of 235 patients. Neurosurgery 2007;60:285-94; discussion 94-5.

99. Schramm J, Aliashkevich AF. Surgery for temporal mediobasal tumors: experience based on a series of 235 patients. Neurosurgery 2008;62:1272-82.

100. John D. Rolston DJE, Arnau Benet, Jing Li, Soonmee Cha, Mitchel S. Berger. Frontal Operculum Gliomas: Language Outcome following Resection. Journal of Neurosurgery 2014.

101. LeRoux PD, Berger MS, Haglund MM, Pilcher WH, Ojemann GA. Resection of intrinsic tumors from nondominant face motor cortex using stimulation mapping: report of two cases. Surg Neurol 1991;36:44-8.

102. Maldonado IL, Moritz-Gasser S, de Champfleur NM, Bertram L, Moulinie G, Duffau H. Surgery for gliomas involving the left inferior parietal lobule: new insights into the functional anatomy provided by stimulation mapping in awake patients. J Neurosurg 2011;115:770-9.

103. Crippa A, Lanting CP, van Dijk P, Roerdink JB. A diffusion tensor imaging study on the auditory system and tinnitus. The open neuroimaging journal 2010;4:16-25.

104. Javad F, Warren JD, Micallef C, et al. Auditory tracts identified with combined fMRI and diffusion tractography. Neuroimage 2014;84:562-74.

105. Wu AS, Witgert ME, Lang FF, et al. Neurocognitive function before and after surgery for insular gliomas. J Neurosurg 2011;115:1115-25.

106. Wu A, Aldape K, Lang FF. High rate of deletion of chromosomes 1p and 19q in insular oligodendroglial tumors. J Neurooncol 2010;99:57-64.

J Neurosurg 120:1229–1237, 2014

Novel embalming solution for neurosurgical simulation in cadavers

Laboratory investigation

Arnau Benet, M.D.,[1] Jordina Rincon-Torroella, M.D.,[2] Michael T. Lawton, M.D.,[1] and J. J. González Sánchez, M.D., Ph.D.[1]

[1]Skull Base and Cerebrovascular Laboratory, Department of Neurosurgery, University of California, San Francisco, California; and [2]Department of Neurosurgery, Johns Hopkins University, Baltimore, Maryland

Object. Surgical simulation using postmortem human heads is one of the most valid strategies for neurosurgical research and training. The authors customized an embalming formula that provides an optimal retraction profile and lifelike physical properties while preventing microorganism growth and brain decay for neurosurgical simulations in cadavers. They studied the properties of the customized formula and compared its use with the standard postmortem processing techniques: cryopreservation and formaldehyde-based embalming.

Methods. Eighteen specimens were prepared for neurosurgical simulation: 6 formaldehyde embalmed, 6 cryopreserved, and 6 custom embalmed. The customized formula is a mixture of ethanol 62.4%, glycerol 17%, phenol 10.2%, formaldehyde 2.3%, and water 8.1%. After a standard pterional craniotomy, retraction profiles and brain stiffness were studied using an intracranial pressure transducer and monitor. Preservation time—that is, time that tissue remained in optimal condition—between specimen groups was also compared through periodical reports during a 48-hour simulation.

Results. The mean (± standard deviation) retraction pressures were highest in the formaldehyde group and lowest in the cryopreserved group. The customized formula provided a mean retraction pressure almost 3 times lower than formaldehyde (36 ± 3 vs 103 ± 14 mm Hg, $p < 0.01$) and very similar to cryopreservation (24 ± 6 mm Hg, $p < 0.01$). For research purposes, preservation time in the cryopreserved group was limited to 4 hours and was unlimited for the customized and formaldehyde groups for the duration of the experiment.

Conclusions. The customized embalming solution described herein is optimal for allowing retraction and surgical maneuverability while preventing decay. The authors were able to significantly lower the formaldehyde content as compared with that in standard formulas. The custom embalming solution has the benefits from both cryopreservation (for example, biological brain tissue properties) and formaldehyde embalming (for example, preservation time and microorganism growth prevention) and minimizes their drawbacks, that is, rapid decay in the former and stiffness in the latter. The presented embalming formula provides an important advance for neurosurgical simulations in research and teaching.

(http://thejns.org/doi/abs/10.3171/2014.1.JNS131857)

Key Words • **embalming** • **neurosurgery** • **simulation** • **anatomy**

Neurosurgery is one of the most challenging surgical specialties because it deals with the most complex and fragile organ in the human body—the brain—and because it requires a combination of precise technical skills, experience in the surgical setting, and superb knowledge of anatomy. Surgical simulation using a cadaveric human head is one of the most valid strategies for neurosurgical research and training because it provides the closest approximation to a live surgical procedure with true human anatomy.

Several models for neurosurgical training have been

Abbreviation used in this paper: IARC = International Agency for Research on Cancer.

This article contains some figures that are displayed in color online but in black-and-white in the print edition.

described in the literature.[1,4,14,16,17] The main goal of anatomical cadaveric processing is to achieve the most realistic model possible. There have been several major breakthroughs in this field.[1,4,16] However, none of these cited studies provides advances in cadaveric embalming methods to maintain the physical properties of a living brain while preserving the brain specimen from decay.

The major physical properties to be considered when addressing embalming research are brain stiffness, preservation time, and biohazard safety. Two common processing techniques used in cadaveric neurosurgical simulations are cryopreservation (unembalmed) and formaldehyde-based preservation. Cryopreserved specimens provide optimal brain stiffness but have a short preservation time and are considered biohazardous. Formaldehyde-based embalming formulas are the standard for long preservation of specimens. However, formaldehyde substantially increases brain stiffness, making retraction and surgical simulation very difficult. Additionally, many studies have reported that long-term exposure to high airborne formaldehyde concentrations in the laboratory is hazardous.[6,9,10,11,15] In 2006, the International Agency for Research on Cancer (IARC)[22] and the US Environmental Protection Agency[19] classified formaldehyde as a probable human carcinogen.

We have customized an embalming formula for neurosurgical simulations that enhances brain compressibility and enables retraction while preventing microorganism growth and brain decomposition. This cadaveric embalming formula also decreases potential chemical biohazards to meet the IARC recommendations for laboratory safety.

In the present work, we studied the properties of our customized formula and compared its use with standard postmortem processing techniques—cryopreservation and formaldehyde embalming—in a sample of cadaveric specimens. We also analyzed the applications of each technique to neurosurgical training and research and provide recommendations on specimen preparation for neurosurgical simulations.

Methods

To study the properties of 3 cadaveric processing techniques (cryopreservation, formaldehyde-based embalming, and customized-formula embalming), 18 human specimens (age range at death 50–95 years) were prepared for surgical simulation. Donors with premorbid conditions of the CNS were excluded from our study. Specimens in the embalmed groups (formaldehyde and custom) were kept immersed in their respective embalming fluids for a mean time of 8 months (range 2 weeks–1 year) before the experiment. Six cryopreserved and 6 formaldehyde-embalmed specimens were prepared according to conventional processing techniques for neurosurgical research.[2] Six additional specimens were prepared using our customized embalming solution. A standard pterional approach was performed in all specimens to compare brain compressibility, retraction profile, and preservation time. One MR image of 2 specimens in each group was obtained. One customized specimen was also prepared to test the feasibility of bleeding simulations.

Head Preparation

All heads were prepared for optimal neurosurgical simulation. The neck was sectioned at vertebrae C5–7 to provide good exposure of cervical vessels and preserve the cervical spinal cord. Common carotid and vertebral arteries along with jugular veins were identified and isolated. Minimal sharp dissection was performed around vessels to prevent undesired rupture of deep arteries and veins, which could cause leakage during silicone injection. Cervical arteries and jugular veins in the embalmed groups were cannulated according to previously described methods.[2,17] Arterial and venous systems were cleaned using saline solution until contralateral outflow was clear. This procedure was repeated bilaterally on each cannulated vessel, alternating arterial and venous irrigation. Once all blood clots were cleared from external and internal vascular systems (carotid and vertebral arteries and jugular veins), the specimens were randomly divided into the customized and formaldehyde groups. Because of their fast decay time, cryopreserved specimens were not cannulated or injected to maximize their experiment time.

Embalming Procedures

Customized and standard formaldehyde embalming solutions were used for comparative analysis. One-half liter of fixative was perfused through common carotid and vertebral arteries (200 ml) and jugular veins (300 ml) in each head. The customized mixture was prepared in the laboratory using the following formula: ethanol 62.4%, glycerol 17%, phenol 10.2%, formaldehyde 2.3%, and water 8.1% (Fig. 1). A conventional 10% formaldehyde solution was used for the formaldehyde group. All embalmed heads were immersed in a 1:10 dilution of the respective embalming fluid and stored at 5°C for at least 2 days before silicone injection. Cryopreserved specimens were frozen at postmortem Day 1–5 at –15°C to –20°C and thawed for approximately 12 hours before proceeding with the surgical simulation.

Vascular Silicone Injection

Arterial systems were injected with red silicone, and venous systems with blue silicone (Fig. 2). The arterial system—common carotid and vertebral arteries—was processed first to secure filling of the distal and small thalamoperforating arteries. Common carotid arteries were bilaterally injected until vertebral artery colored outflow was observed. Bilateral vertebral artery injection was then performed until the arterial system was fully injected. Finally, the arterial system was clamped except for 1 carotid artery, which was used to increase arterial pressure to force small-caliber vessels to fill. Upon completion of arterial silicone injection, jugular veins were processed using the same injection principles.

Comparative Analysis

The durability and retraction (stiffness) properties of specimens treated with our customized formula were compared with the properties of specimens treated with cryopreservation and formaldehyde-based preservation. A standard pterional craniotomy was performed on each

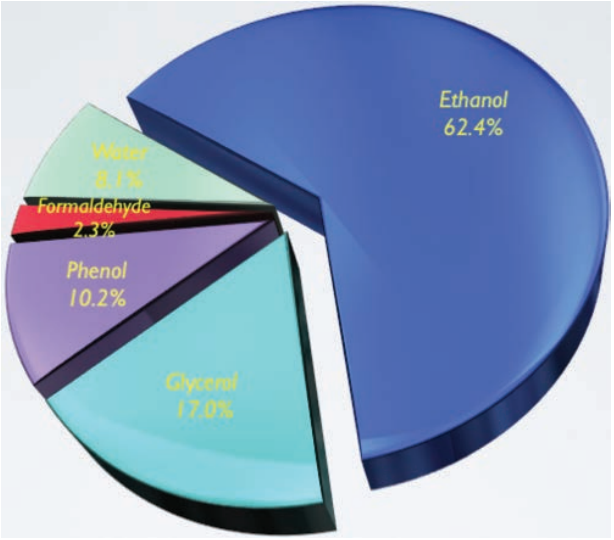

Fig. 1. Pie chart showing the chemicals used in the customized embalming formula containing a base of ethanol and a small amount of formaldehyde, both of which are used to preserve the cellular structure of the cadaveric specimen. Glycerol is used to reduce stiffness produced by the fixative chemicals. Phenol is added for its broad germicidal effect.

specimen. The dura mater and arachnoid membranes were carefully removed, and the temporal lobe was gently retracted dorsally to simulate a subtemporal approach. Retraction profiles were measured using an intracranial pressure transducer and monitor (Integra Camino parenchymal intracranial pressure monitoring kit) inserted 8 mm into the inferior temporal gyrus, 4 cm posterior to the temporal pole (Fig. 3). Pressure measurements were recorded before temporal lobe retraction and at the tissue retraction limit. This limit was set at the highest, most retractile pressure before tissue damage and was dependent on the retraction profile of each specimen. The optic and oculomotor nerves, supraclinoid internal carotid artery, anterior clinoid process, and tentorium were used as surgical landmarks to compare subtemporal surgical exposures among the processing techniques.

The total retraction surface was also measured. Ten pins were inserted along the cortex surface and registered as stereotactic points using a surgical navigation system (Stryker Nav3). The pins remained in the same cortical surface location throughout the experiment. Stereotactic coordinates were obtained from each pin by touching it with the navigation probe at resting state and at the tissue retraction limit (Fig. 3 right). Surface areas were calculated from the stereotactic coordinates using dedicated software (Surface Area Calculator, BitWise Ideas Inc.) and recorded in a spreadsheet for statistical analysis. Retraction surface was obtained by subtracting the area at retraction limit from the area at resting state.

We also sought to study the durability (preservation time) of specimens. Two specimens from each group were prepared and continuously exposed to laboratory working conditions for 2 days. We studied changes in tissue consistency, color, and decay to compare specimen conditions at

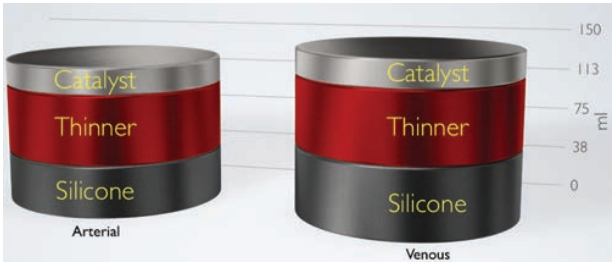

Fig. 2. Composition of the silicone mixture for vascular injection. The vasculature was injected with red- (arteries) and blue- (veins) colored silicone to enhance dissection and vessel identification. The venous system mixture *(right)* contained a 1:1 thinner/silicone ratio, whereas the arterial system *(left)* required more thinner to reach the small-caliber arteries (1.34:1 thinner/silicone ratio). Twenty-three milliliters of catalyst for every 120 ml of mixture was added before injecting the vessels to decrease the curing time.

2-hour intervals for 2 consecutive days. An itemized observational study spreadsheet was completed for the duration of the experiment, and consistency, color, and overall appearance were recorded as dichotomous variables (1 = changes observed, 2 = no changes observed). Subjective appreciations (odor and texture) were also recorded and analyzed after the experiment. To complement the observational study, we administered a blinded survey to a sample of 4 neurosurgery residents and 2 attending neurosurgeons to evaluate the best specimen group after the experiment ended. The volunteers were asked to "please rate hierarchically the images in the attached figure as to their similarity to the real brain in terms of color and texture."

Data were collected and descriptive statistics was performed using SPSS Statistics Desktop, version 21.0 (IBM Corp.). The mean retraction pressures, retraction surfaces, and durability lapsing times were compared using independent Student t-test analysis. A $p < 0.05$ was considered statistically significant.

Imaging and Postprocessing Techniques

Radiological studies are very important in neurosurgical simulation and research; therefore, 3-T T1-weighted FLAIR MRI was performed on 2 heads from each group on the same day as specimen processing. The radiological images were used to compare the quality and preservation of internal nuclei, cortex, white matter, and the whole

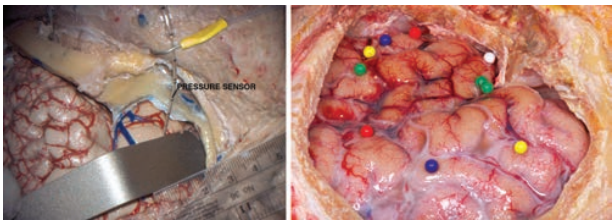

Fig. 3. Photographs of specimen preparation for the morphometric experiments. **Left:** A pterional craniotomy was performed to expose the lateral surface of the brain. The pressure sensor was introduced into the inferior temporal gyrus near the retractor spatula. **Right:** Ten pins were inserted into the lateral surface of each brain to measure the retraction area.

encephalon before starting the surgical simulations. In 1 case, a cryopreserved specimen received on postmortem Day 8 was scanned. Although this specimen provided clear radiological evidence of the decay process in cryopreserved specimens, it was excluded from the morphometric study.

The bleeding model for neurosurgical simulation was prepared and tested in 1 customized specimen as described elsewhere.[1,16]

Results

All formaldehyde and customized specimens were completely embalmed. The cortex surface along the watershed area was uniformly embalmed. Surgical simulation experiments were successfully performed in all specimens included for morphometric study. One cryopreserved specimen with advanced decay on MRI was excluded from the morphometric experiment sample and replaced.

Retraction Profiles

The subtemporal approach was completed in all specimens. Retraction profiles (retraction pressure and surface) of the customized and cryopreserved specimens were very similar to each other and clearly better than that of the formaldehyde specimen. The subtemporal approach provided equivalent exposure of the entire incisural space and cavernous sinus in cryopreserved and customized specimens. However, only the tentorium and superior cerebellar artery in the middle incisural space were exposed in the formaldehyde group. At maximal retraction, deep plane maneuvering and dissection around the parasellar region were identical in the customized and cryopreserved groups and very difficult in the formaldehyde group.

Retraction Pressure. Retraction pressure studies were performed to assess the brain compliance and retraction capabilities of each group (Table 1). Overall mean retraction pressures were highest in the formaldehyde group and lowest in the cryopreserved group. At the maximal retraction point, our customized formula provided a mean retraction pressure almost 3 times lower than formaldehyde (36 ± 3 vs 103 ± 14 mm Hg, $p < 0.01$) but slightly higher than cryopreservation (36 ± 3 vs 24 ± 6 mm Hg, $p < 0.01$; Fig. 4).

Retraction Surface. Retraction surface was calculated to assess brain stiffness during a standardized neurosurgical procedure and to compare the surgical area gained during retraction. There was no statistical difference between the customized and cryopreserved groups ($p = 0.13$), but the retraction area of the customized group was almost 4 times larger than that of the formaldehyde group (1.44 ± 0.4 vs 0.46 ± 0.1 cm^2, $p < 0.01$; Fig. 5). These retraction profiles provided different access to the incisural space and posterior fossa structures.

Specimen Condition

We have observed that flushing the vascular system with isotonic saline solution instead of tap water both prevents brain and tissue edema and provides optimal cleaning of blood clots. In our experience, the low osmolality of the tap water produced massive edema in all cases. It was prevented by the use of an isosmolar saline solution instead of tap water. In addition to using saline solutions, we preferred to repeatedly manually inject at low pressure to cleanse the vessels. This procedure increased the overall quality as relates to color, texture, brightness, and clarity of all specimens, but especially those treated with our customized formula. Silicone injection was completed in all specimens regardless of the embalming method. All thalamoperforating arteries and other distal vessels were fully injected, and no subarachnoid silicone leak was observed. The customized specimens, as compared with the formaldehyde-preserved specimens, exhibited color and texture closer to those in real life.

Using only 2.3% of formaldehyde in the customized formula, we reduced the formaldehyde content by 78%, as compared with standard embalming solutions. Texture and color were similar for the cryopreserved and customized specimens at the time of brain exposure (Fig. 6A and B). However, formaldehyde-fixed specimens were stiffer and slightly darker (Fig. 6C). Degradation of tissue consistency and color was observed in the cryopreserved specimens after continuous exposure to the working environment for 4 hours, whereas customized and formaldehyde-preserved specimens maintained their properties

TABLE 1: Descriptive statistics for the study sample*

Group	Measure	No. of Specimens	Min	Max	Mean ± SD
formaldehyde	control pressure (mm Hg)	6	0	30	10.00 ± 12.198
	pressure at tissue retraction limit (mm Hg)	6	83	125	103.50 ± 14.419
	retraction area (cm^2)	6	0.32	0.69	0.4633 ± 0.14774
customized	control pressure (mm Hg)	6	1	18	6.50 ± 5.992
	pressure at tissue retraction limit (mm Hg)	6	32	40	35.67 ± 3.011
	retraction area (cm^2)	6	0.89	2.14	1.4350 ± 0.43702
cryopreserved	control pressure (mm Hg)	6	0	8	3.33 ± 3.670
	pressure at tissue retraction limit (mm Hg)	6	18	35	24.17 ± 5.981
	retraction area (cm^2)	6	1.23	3.62	2.1100 ± 0.89376

* Control pressure, pressure tissue break, and retraction area were measured in each specimen.

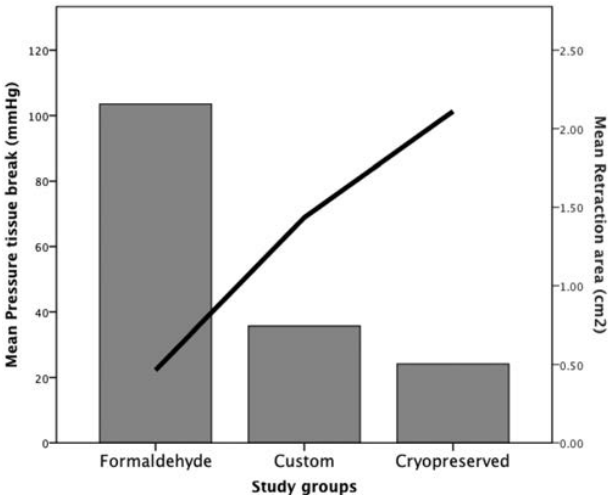

Fig. 4. Retraction profile graph of the study groups. The formaldehyde group had the highest mean pressure at tissue break (over 100 mm Hg, *bar*) and provided the least retraction area (0.5 cm^2, *black line*). The customized and cryopreserved groups had similar retraction profiles. The customized group offered almost 3 times less resistance to retraction than the formaldehyde group. The cryopreserved group provided the largest retraction surface (2.3 cm^2, *black line*) with the lowest retraction pressure (24 mm Hg, *bar*).

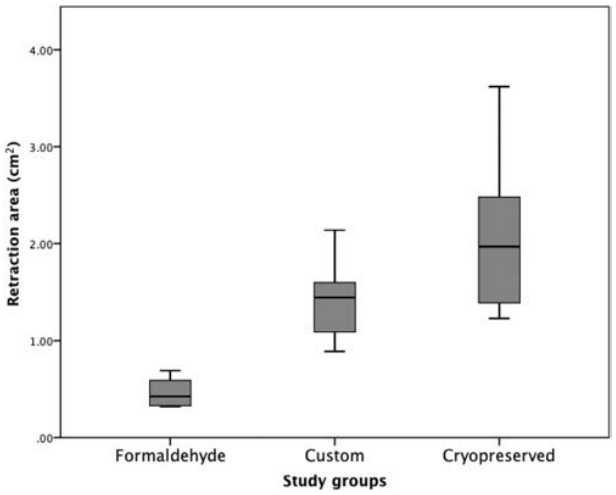

Fig. 5. Box plot of the retraction area for each group. The formaldehyde specimens provided less retraction area than the other groups. There was no statistical difference between the customized and cryopreserved specimens, which had more variability and 1 outlier.

throughout the entire experiment. While evident signs of brain liquefaction were noted in the cryopreserved specimens after working Hour 40 (Fig. 6D), consistency and color were preserved in both customized and formaldehyde-fixed specimens. The customized specimens were consistently rated favorably, as compared with the formaldehyde and cryopreserved specimens at the end of the experiment. Changes in consistency were observed in the cryopreserved group from Hour 2. All the observational variables—color, consistency, and overall appearance—were consistently rated 1 (change observed) from Hour 4 throughout the experiment. Sporadic changes in color and overall appearance were noted in both embalmed groups, which resolved with tissue hydration.

Formaldehyde vapors emanating from the formaldehyde-fixed specimens were noticeable in the working environment immediately after positioning the head for dissection. Placing the specimens under running water for 15 minutes before dissection diluted the vapors. Unpleasant, aggressive odor from decay and microorganism growth prevented researchers from continuing dissection of cryopreserved specimens at working Hour 7. In contrast, no microorganism growth or brain decay was obvious in the embalmed specimens during the study.

Imaging and Postprocessing Techniques

Overall, radiological studies of the customized specimens were similar to and better than those of the cryopreserved group, whereas the formaldehyde group imaging was notably worse in terms of the level of anatomical detail and MRI signal contrast. Although T1-weighted MRI of the customized group showed optimal definition of the cortex, sulci, and white matter, some artifacts and hyperintensities were observed randomly along the internal nuclei (Fig. 7B and E). The best images of the internal nuclei were obtained from the cryopreserved group (Fig. 7C and F). The embalmed specimens had better tissue preservation than the cryopreserved specimens, which showed signs of brain shrinking and frontal pneumocephalus. At postmortem Day 8, the cryopreserved specimens showed signs of advanced decay compared with the embalmed specimens (Fig. 8).

The bleeding model for neurosurgical simulation de-

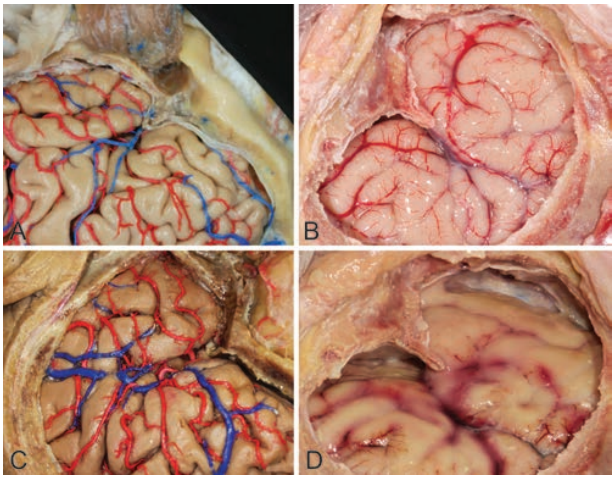

Fig. 6. Photographs showing specimen conditions. The customized **(A)**, cryopreserved **(B and D)**, and formaldehyde **(C)** groups were exposed to continuous dissection for 48 hours. The color and texture of the customized and cryopreserved specimens were similar. Specimens in the formaldehyde group were darker in color and stiffer in texture than those in the other groups. All specimens were kept wet during the experiment. The customized and formaldehyde specimens maintained initial conditions, and no changes were noticed. In contrast, the cryopreserved specimens showed advanced signs of decay at Hour 40 **(D)**.

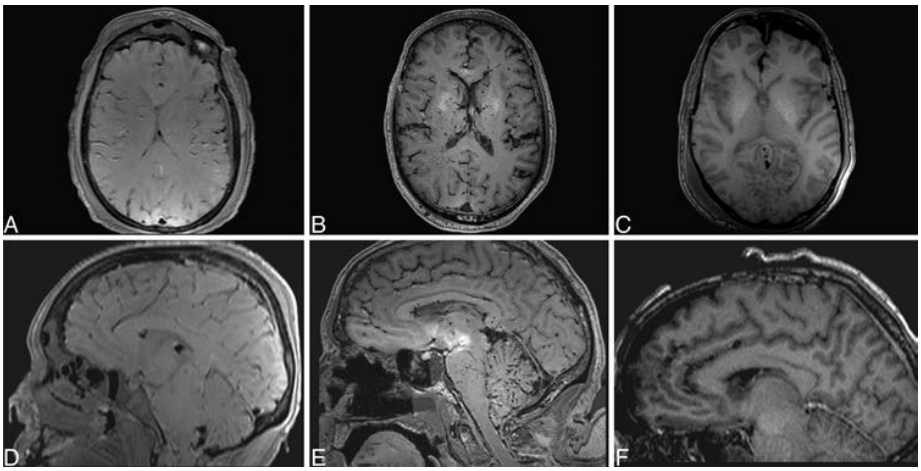

Fig. 7. Radiological studies of specimens. Axial and sagittal 3D T1-weighted MR images of the formaldehyde **(A and D)**, customized **(B and E),** and cryopreserved **(C and F)** specimens revealed better overall results in the customized group. The cortex and subcortical nuclei were best identified in the cryopreserved group and were not identified in the formaldehyde group. The cryopreserved specimen showed signs of decay and pneumocephalus.

scribed by Aboud et al.[1] was also tested in 1 customized specimen. Brain movements encompassing arterial beating were observed at a normal arterial pressure resembling live surgery. Hemorrhage from deliberate arterial rupture permitted deep surgical field hemostasis simulation. Gentle retraction of the sylvian fissure together with careful sharp dissection and hemostasis allowed exposition of the middle cerebral artery in a highly simulative surgical scenario.

Discussion

Results of this study show that the customized embalming formula provides an optimal brain retraction profile, long use time, and low biohazard risk for neurosurgical simulation in cadavers. Overall, the customized group provided the best feature combination for cadaveric neurosurgical research. We found that specimens embalmed with our customized formula offered 3 times less retraction pressure and 4 times larger surgical retraction area than the specimens in the formaldehyde group. When surgical simulation was performed, we obtained best access to surgical landmarks and maneuverability in the customized and cryopreserved groups. Nevertheless, cryopreserved specimens had a very limited working time because of fast decay (4 hours for research purposes). Moreover, radiological studies showed that the customized and cryopreserved groups provided better anatomical detail than the formaldehyde group, although random hyperintense artifacts were identified in the customized specimens. Furthermore, we demonstrated that surgical bleeding simulation is feasible in our custom-embalmed specimens.

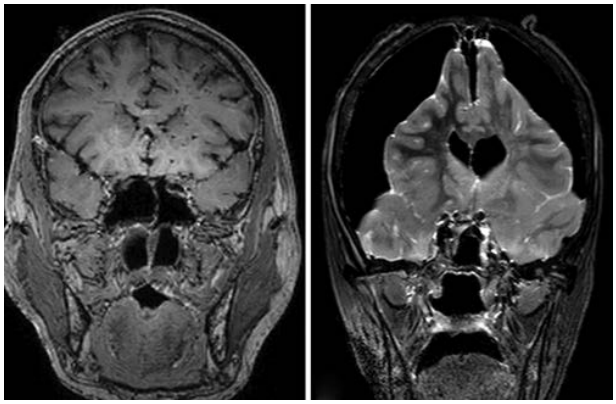

Fig. 8. Coronal 3D T1-weighted MR images of the customized **(left)** and cryopreserved **(right)** specimens at postmortem Day 8. The cryopreserved specimen showed evident signs of decay—Mount Fuji sign of pneumocephalus with its superior surface tethered to the superior sagittal sinus.

The key concept when choosing a processing technique is to know exactly the dissection objectives and requirements of the proposed work and to have a thorough understanding of the different properties of the available preservation methods. Many specimen-processing techniques are available for laboratory use, and each has specific advantages and disadvantages.

Solutions containing large formaldehyde concentrations have been used as the standard in specimen preservation because they offer long-term preservation and prevent microorganism growth. Despite these desired properties, however, formaldehyde remains a suboptimal fixation method for neurosurgical simulation because the brain stiffness it produces makes retraction very challenging. Nonetheless, formaldehyde embalming has provided researchers with an excellent processing method for gross anatomy teaching and white matter dissection. Formaldehyde-related brain hardening combined with sequential freezing causes axons to separate from each other, thus facilitating the dissection of fine fiber bundles.[8,12,13,18] In contrast, color distortion is a well-known drawback that has an important impact on the overall quality of the illustrative work in terms of more lifelike and better contrast. White, pallid cortical and subcortical structures are far

from natural brain color and can sometimes be difficult to contrast with cranial nerves during surgical simulations.

It has been widely accepted that cryopreservation (not embalmed) is the cadaveric processing technique that least modifies the biological properties of brain tissue. Nonetheless, the natural appearance of the brain only lasts for a very limited time. At working Hour 4 (around postmortem Day 2–5), specimens are no longer useful for neurosurgical simulation research, as liquefaction prevents reliable morphometric analysis and tissue distortion becomes evident. This fast degradation is a major drawback during hands-on courses or other teaching activities where an extended period of time but reliable anatomy and surgical maneuverability are needed to understand and practice the different surgical approaches. Another significant drawback of cryopreserved specimens is biohazard safety. Because unembalmed specimens lack germicidal agents, uncontrolled microorganism growth can occur early in the dissection process. However, unembalmed specimens continue to be used in procedure demonstrations and educational workshops because they used to be the only means of obtaining features most similar to those of a living brain in the operating room (that is, the possibility of brain retraction). In our opinion, our customized embalming technique opens a new possibility for brain retraction and provides brain features similar to those of cryopreserved specimens while also offering a more cost-effective and safer option.

The customized embalming formula takes advantage of the best formaldehyde properties—long preservation time and microorganism growth prevention—combined with a retraction profile and physical properties similar to those attained with cryopreservation. Moreover, a substantial reduction in the formaldehyde concentration makes this option safer for researchers according to IARC recommendations.

Surgical Simulation Profiles

Despite important advances in surgical simulation,[1,2,14,16,17] an embalming formula customized to allow brain retraction while preserving living brain properties is necessary to recreate neurosurgical scenarios in cadavers. In 2002, Aboud et al. introduced a revolutionary laboratory model for neurosurgical training that enabled blood hemorrhage simulations in cadaveric specimens.[1] This advance represented a breakthrough in the recreation of neurosurgical approaches because it allowed training in bleeding avoidance, management, and control in a cadaveric human surgical scenario. However, one of the major limitations of that study was not directly related to the model but to brain embalming. Formaldehyde-related brain stiffness constrained surgical exposure and cerebral retraction. To overcome these limitations, the authors used cryopreserved, partially embalmed cadavers. Although brain relaxation allowed retraction and wide surgical exposure, specimen working time was restricted.[1] In the present study, we observed the same limitations in cryopreserved (unembalmed) and formaldehyde-embalmed specimens. However, our custom-embalmed specimens overcame these limitations. In addition, prolonged and multisession work was possible because embalming fixatives preserved the brain for at least 2 days of continued exposure to the working environment. The customized and formaldehyde specimens remained immersed in embalming fluid for 8 months (mean 8 months, range 2 weeks–1 year), which in our experience represents the approximate embalming time when using specimens in the laboratory. Immersion in embalming fluid during storage and the prevention of specimen desiccation during dissection is critical in preserving the original qualities in both the formaldehyde and customized specimens and determines prolonged use. In our experience using this embalming fluid in our studies over the last 5 years, the specimens maintain their properties for months, even years, if maintained in optimal conditions (nonfrozen and submerged in embalming fluid).

Imaging and Postprocessing Techniques

Radiological studies of cadaveric specimens represent an excellent option to complement training and research in neurosurgical laboratories. Computerized tomography and MRI of the specimens provide useful spatial orientation and become essential in assisting new landmark and approach research during surgical simulations. In our study, radiological images of the customized specimens offered more detail of the anatomical structures than those of the formaldehyde specimens and showed less decay distortion (for example, pneumocephalus) than the cryopreserved specimens. Artifacts on T1-weighted MR images of the customized specimens are likely to be caused by the high glycerol content of the embalming mixture rather than a fixation failure. Postdissection cross-sectional examination confirmed distal and uniform embalming perfusion.

The customized specimens provided an unparalleled surgical scenario when using the bleeding model. Our formula provided good brain retraction capabilities, allowing surgical exposure, vascular dissection, and bleeding control in a very realistic scenario.

Biohazard Risk and Health Standards

Health protection is a primary concern and must be seriously considered in a surgical simulation laboratory. Although general protection standards (physical barriers) must always be used, special measures tailored to embalming chemicals are necessary to provide a safe workplace.

Neurosurgical simulation, especially for research and illustrative purposes, takes time, and a continuous dissection process demands a high level of concentration to perform meticulous and precise anatomical exposures. In our study, microorganism growth together with unpleasant aggressive odor and evident signs of tissue decomposition forced researchers using cryopreserved specimens to finish dissection prematurely. This situation can be frustrating because dissection targets and research objectives are most often achieved in the last steps of dissection work. Moreover, intense continuous work in a crowded workplace (for example, hands-on workshops) lowers the ventilation rate and increases room temperature, thus increasing the decay rate in cryopreserved specimens and airborne formaldehyde particles when using formalde-

hyde-preserved specimens. Maintaining these circumstances over a prolonged time could result in a harmful biohazard situation. Therefore, the federal government and the state of California have established permissible exposure limits for chemical exposures in the workplace.[7]

Airborne formaldehyde is the most harmful volatile chemical among those included in the present study and has the strictest biohazard security control codes.[3,7,19,22] Many institutions and government regulations have considered it to be a carcinogenic agent.[3,5,7,10,11,15,19,22] Although formaldehyde is still needed to prevent microorganism growth (especially fungi), formaldehyde content in the customized embalming fluid described here was almost 80% less than in a conventional formaldehyde mixture. Furthermore, customized specimens provided a less aggressive and contaminated environment than the formaldehyde and cryopreserved specimens. Researchers noticed no airway or mucosal irritations when working with either the customized or cryopreserved group. However, slight to mild oropharynx and eye mucosal irritation was present when using formaldehyde specimens.

Fixative and germicidal properties of the customized embalming formula are provided mainly by phenol and ethanol. Although phenol is considered to be more hazardous than ethanol, its toxic effects are limited to skin contact.[7] Furthermore, IARC evaluation of phenol concludes that it is "not classifiable as to its carcinogenicity to humans."[21] Thus, airborne biohazard particles in the laboratory are drastically reduced when using a specimen preserved with our customized embalming formula. However, pertinent physical barriers as well as a high ventilation rate in the workplace are strongly recommended while manipulating specimens or the embalming mixture.

Study Limitations

Although most laboratories do not disclose their embalming formulas, we chose to share our customized formula for neurosurgical simulations and evaluated its properties through a comparative analysis. Embalming options other than those included in this study are also available on the market.[20] Moreover, there are tissue softeners that presumably reduce brain stiffness by removing formaldehyde (fixative) from the specimen. Although it is beyond the scope of this study to compare all of the available processing techniques, the proposed customized embalming formula is easier to produce than other special chemicals and easier to use than the successive embalming and softening steps or complex measurements in other techniques.

Conclusions

Evidence in the present study supports the use of specimens embalmed with a customized formula for cadaveric neurosurgical simulations, especially for work times lasting more than 4 hours. Moreover, this embalming technique provides a better balance of the major physical properties to be considered in embalming research—brain stiffness, preservation time, and biohazard safety—than cryopreserved or classic formaldehyde-based processing methods.

Acknowledgments

We acknowledge Drs. Jason Davies, Nathan Roland, Rajiv Saigal, and Dario Englot for volunteering for the survey as part of the observational study.

Disclosure

The authors report no conflict of interest concerning the materials or methods used in this study or the findings specified in this paper.

Author contributions to the study and manuscript preparation include the following. Conception and design: Benet, Rincon-Torroella. Acquisition of data: Benet, Rincon-Torroella, González Sánchez. Analysis and interpretation of data: all authors. Drafting the article: Benet, Rincon-Torroella, González Sánchez. Critically revising the article: all authors. Reviewed submitted version of manuscript: all authors. Approved the final version of the manuscript on behalf of all authors: Benet. Statistical analysis: Benet, Rincon-Torroella. Administrative/technical/material support: Benet, Lawton. Study supervision: all authors. Figure preparation: Benet.

References

1. Aboud E, Al-Mefty O, Yaşargil MG: New laboratory model for neurosurgical training that simulates live surgery. **J Neurosurg 97:**1367–1372, 2002
2. Alvernia JE, Pradilla G, Mertens P, Lanzino G, Tamargo RJ: Latex injection of cadaver heads: technical note. **Neurosurgery 67 (2 Suppl Operative):**362–367, 2010
3. Beane Freeman LE, Blair A, Lubin JH, Stewart PA, Hayes RB, Hoover RN, et al: Mortality from solid tumors among workers in formaldehyde industries: an update of the NCI cohort. **Am J Ind Med 56:**1015–1026, 2013
4. Bernardo A, Preul MC, Zabramski JM, Spetzler RF: A three-dimensional interactive virtual dissection model to simulate transpetrous surgical avenues. **Neurosurgery 52:**499–505, 2003
5. Burkhart KJ, Nowak TE, Blum J, Kuhn S, Welker M, Sternstein W, et al: Influence of formalin fixation on the biomechanical properties of human diaphyseal bone. **Biomed Tech (Berl) 55:**361–365, 2010
6. Chia SE, Ong CN, Foo SC, Lee HP: Medical students' exposure to formaldehyde in a gross anatomy dissection laboratory. **J Am Coll Health 41:**115–119, 1992
7. Division of Industrial Safety: Control of Hazardous Substances, Article 107. Dusts, Fumes, Mists, Vapors and Gases, §5155 Airborne Contaminants. San Francisco: Department of Industrial Relations, 2011 (http://www.dir.ca.gov/title8/sub7.html) [Accessed January 14, 2014]
8. Fernández-Miranda JC, Rhoton AL Jr, Alvarez-Linera J, Kakizawa Y, Choi C, de Oliveira EP: Three-dimensional microsurgical and tractographic anatomy of the white matter of the human brain. **Neurosurgery 62 (6 Suppl 3):**989–1028, 2008
9. Keil CB, Akbar-Khanzadeh F, Konecny KA: Characterizing formaldehyde emission rates in a gross anatomy laboratory. **Appl Occup Environ Hyg 16:**967–972, 2001
10. Kerns WD, Pavkov KL, Donofrio DJ, Gralla EJ, Swenberg JA: Carcinogenicity of formaldehyde in rats and mice after long-term inhalation exposure. **Cancer Res 43:**4382–4392, 1983
11. Kriebel D, Sama SR, Cocanour B: Reversible pulmonary responses to formaldehyde. A study of clinical anatomy students. **Am Rev Respir Dis 148:**1509–1515, 1993
12. Ludwig E, Klingler J: **Atlas Cerebri Humani: The Inner Structure of the Brain Demonstrated on the Basis of Macroscopical Preparations.** Boston: Little, Brown, & Co., 1956
13. Martino J, Vergani F, Robles SG, Duffau H: New insights into the anatomic dissection of the temporal stem with special emphasis on the inferior fronto-occipital fasciculus: implications

in surgical approach to left mesiotemporal and temporoinsular structures. **Neurosurgery 66 (3 Suppl Operative):**4–12, 2010
14. Menovsky T: A human skull cast model for training of intracranial microneurosurgical skills. **Microsurgery 20:**311–313, 2000
15. Nielsen GD, Wolkoff P: Cancer effects of formaldehyde: a proposal for an indoor air guideline value. **Arch Toxicol 84:**423–446, 2010
16. Olabe J, Olabe J, Sancho V: Human cadaver brain infusion model for neurosurgical training. **Surg Neurol 72:**700–702, 2009
17. Sanan A, Abdel Aziz KM, Janjua RM, van Loveren HR, Keller JT: Colored silicone injection for use in neurosurgical dissections: anatomic technical note. **Neurosurgery 45:**1267–1274, 1999
18. Türe U, Yaşargil MG, Friedman AH, Al-Mefty O: Fiber dissection technique: lateral aspect of the brain. **Neurosurgery 47:**417–427, 2000
19. US Environmental Protection Agency: **Integrated Risk Information System: Formaldehyde (CASRN 50-00-0).** (http://www.epa.gov/iris/subst/0419.htm) [Accessed January 13, 2014]
20. Whitehead MC, Savoia MC: Evaluation of methods to reduce formaldehyde levels of cadavers in the dissection laboratory. **Clin Anat 21:**75–81, 2008
21. World Health Organization: **IARC Monographs on the Evaluation of Carcinogenic Risks to Humans. Volume 71: Re-Evaluation of Some Organic Chemicals, Hydrazine and Hydrogen Peroxide.** Lyon: IARC Press, 1999, pp 749–767
22. World Health Organization: **IARC Monographs on the Evaluation of Carcinogenic Risks to Humans. Volume 88: Formaldehyde, 2-Butoxyethanol and 1-*tert*-Butoxypropanol-2-ol.** Lyon: IARC Press, 2006

Manuscript submitted August 27, 2013.
Accepted January 10, 2014.
Please include this information when citing this paper: published online February 14, 2014; DOI: 10.3171/2014.1.JNS131857.

Address correspondence to: Arnau Benet, M.D., Department of Neurosurgery, UCSF, Rm. M779, 505 Parnassus Ave., San Francisco, CA 94143. email: arnaubenet@gmail.com.

JNS

LABORATORY INVESTIGATION

J Neurosurg 124:469–481, 2016

Surgical assessment of the insula. Part 1: surgical anatomy and morphometric analysis of the transsylvian and transcortical approaches to the insula

Arnau Benet, MD, Shawn L. Hervey-Jumper, MD, Jose Juan González Sánchez, MD, PhD, Michael T. Lawton, MD, and Mitchel S. Berger, MD

Department of Neurosurgery, University of California, San Francisco, California

OBJECTIVE Transcortical and transsylvian corridors have been previously described as the main surgical approaches to the insula, but there is insufficient evidence to support one approach versus the other. The authors performed a cadaveric comparative study regarding insular exposure, surgical window and freedom, between the transcortical and transsylvian approaches (with and without cutting superficial sylvian bridging veins). Surgical anatomy and skull surface reference points to the different insular regions are also described.

METHODS Sixteen cadaveric specimens were embalmed with a customized formula to enhance neurosurgical simulation. Two different blocks were defined in the study: first, transsylvian without (TS) and with the superficial sylvian bridging veins cut (TSVC) and transcortical (TC) approaches to the insula were simulated in all (16) specimens. Insular surface exposure, surgical window and surgical freedom were calculated for each procedure and related to the Berger-Sanai insular glioma classification (Zones I–IV) in 10 specimens. Second, the venous drainage pattern and anatomical landmarks considered critical for surgical planning were studied in all specimens.

RESULTS In the insular Zone I (anterior-superior), the TC approach provided the best insular exposure compared with both TS and TSVC. The surgical window obtained with the TC approach was also larger than that obtained with the TS. The TC approach provided 137% more surgical freedom than the TS approach. Only the TC corridor provided complete insular exposure. In Zone II (posterior-superior), results depended on the degree of opercular resection. Without resection of the precentral gyrus in the operculum, insula exposure, surgical windows and surgical freedom were equivalent. If the opercular cortex was resected, the insula exposure and surgical freedom obtained through the TC approach was greater to that of the other groups. In Zone III (posterior-inferior), the TC approach provided better surgical exposure than the TS, yet similar to the TSVC. The TC approach provided the best insular exposure, surgical window, and surgical freedom if components of Heschl's gyrus were resected. In Zone IV (anterior-inferior), the TC corridor provided better exposure than both the TS and the TSVC. The surgical window was equivalent. Surgical freedom provided by the TC was greater than the TS approach. This zone was completely exposed only with the TC approach. A dominant anterior venous drainage was found in 87% of the specimens. In this group, 50% of the specimens had good alternative venous drainage. The sylvian fissure corresponded to the superior segment of the squamosal suture in 14 of 16 specimens. The foramen of Monro was 1.9 cm anterior and 4.42 cm superior to the external acoustic meatus. The M_2 branch over the central sulcus of the insula became the precentral M_4 (rolandic) artery in all specimens.

CONCLUSIONS Overall, the TC approach to the insula provided better insula exposure and surgical freedom compared with the TS and the TSVC. Cortical and subcortical mapping is critical during the TC approach to the posterior zones (II and III), as the facial motor and somatosensory functions (Zone II) and language areas (Zone III) may be involved. The evidence provided in this study may help the neurosurgeon when approaching insular gliomas to achieve a greater extent of tumor resection via an optimal exposure.

http://thejns.org/doi/abs/10.3171/2014.12.JNS142182

KEY WORDS insula; glioma; transsylvian approach; transcortical approach; brain tumor; sylvian fissure; oncology; anatomy

ABBREVIATIONS TC = transcortical; TS = transsylvian; TSVC = transsylvian with bridging veins cut.

SUBMITTED September 17, 2014. **ACCEPTED** December 31, 2014.

INCLUDE WHEN CITING Published online September 4, 2015; DOI: 10.3171/2014.12.JNS142182.

Insular gliomas are among the most challenging lesions to manage in neurosurgery. In contrast to other regions of the cerebral cortex, the insular lobe is located beyond the cerebral surface, in the depth of the sylvian fissure and covered by the opercula and many critical vascular structures. Additionally, a fair amount of cortical areas covering the insula are functional. Also, the venous complex covering the sylvian fissure often contains important drainage that must be preserved, further narrowing surgical options for tumor removal. Despite this challenging situation, there is evidence that the extent of tumor resection greatly impacts survival in patients with insular gliomas.[3,6,13,17] Therefore, although surgically complex, neurosurgeons should be able to aggressively, yet safely, resect these tumors.

Insular gliomas were initially accessed through the sylvian fissure via the transsylvian approach, as previously described by Yaşargil and further developed in the last 2 decades.[5,9,20,21] The transsylvian fissure approach requires wide opening of the superficial and deep sylvian cisterns and careful protection of the opercular arteries and their perforators, as well as preservation of the dominant superficial sylvian veins. The transsylvian approach to the insula requires opercular retraction, which is often limited by the superficial sylvian veins bridging the sylvian fissure. Thus, for larger insular lesions, this approach will not yield optimal surgical access to achieve the desired surgical results.

With the use of cortical and subcortical electrical stimulation, the lateral surface of the opercula may be mapped during an awake procedure, allowing identification and preservation of functional areas. Removing silent cortical areas such as the operculum and superior temporal gyrus is an emerging strategy to maximize the extent of tumor resection while preserving the superficial vascular structures.[4] We have previously reported our transcortical "window" technique and developed an anatomical division of the insula that enabled a preoperative prediction for extent of resection.[13] Nevertheless, it is often the experience of the surgeon, rather than the rationale to enhance exposure of the insula, that determines which approach (i.e., transsylvian or transcortical) is optimal.

At present, there are no supportive data based on cadaveric surgical simulation to determine the differences in surgical access to the insula between the transsylvian (TS) and transcortical (TC) approach. Furthermore, there is a lack of evidence as to which technique or a combination of the two would yield the optimal surgical window to maximize the extent of resection safely.

In this study, we assessed the surgical profile (i.e., insula exposure, surgical window, and surgical freedom) of the TS and TC approaches to the insula using a cadaveric surgical simulation model. Using a sequential experimental design, we asked whether there is a significant difference in insular exposure, surgical window, and surgical freedom (Fig. 1) between the following approaches: the TS approach, the TS after cutting the superficial sylvian veins bridging over the sylvian fissure (TSVC), and the TC approach. Also, we sought to evaluate the venous drainage of the perisylvian region to provide evidence on the likelihood of venous dominancy as a limitation for venous sacrifice during a TS approach. Additionally, we studied the surgical anatomy related to each procedure along with the final surface exposure of the insula. Finally, we describe 2 skull surface reference points to infer the position of the insular zones.

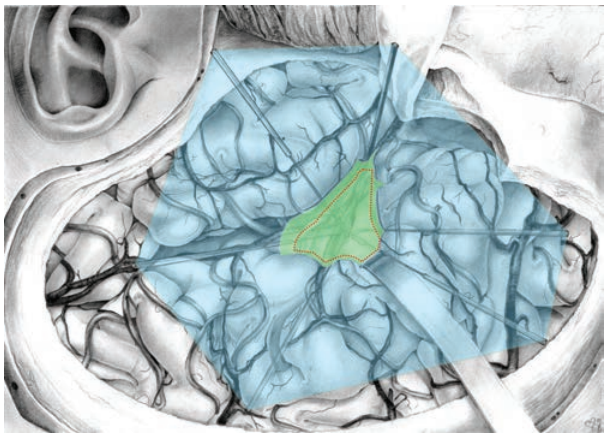

FIG. 1. Illustration of the concepts of insular exposure and surgical window and freedom. The left transsylvian approach to insular Zone I was conceptualized by the medical illustrator. The insular exposure *(dotted shape)* is the area over the insular cortex available through a surgical approach. The insular exposure is the amount of access to the insular cortex provided by each approach. The surgical window (*green* [shaded area in center of figure]) is the area existing between the neurovascular structures limiting the space to access the insula, i.e., the corridor. The surgical window provides information on the space available to pass instruments to a particular insular zone by each approach. The surgical freedom (*blue* [outer shape]) is the area formed by the top of a dissector that, while pivoting on a surgical landmark, contacts the perimeter of the surgical opening. The surgical freedom provides a measure of the degree of maneuverability or ease of manipulating instruments to a particular point in the insula. Copyright Arnau Benet. Published with permission. Figure is available in color online only.

Methods

Study Design

To study and compare the surgical corridors of the transsylvian (TS), transsylvian with bridging veins cut (TSVC), and transcortical (TC) approaches (independent variables) to the insula, an experimental laboratory investigation was designed. Measurements included insular exposure, surgical window, and surgical freedom (dependent variables) resulting from each approach in 10 specimens (all continuous ratio variables). Additionally, we carried out a descriptive study in 16 specimens, providing critical information for the surgical planning and approach selection process. The descriptive study included categorical dichotomous variables, such as the presence of bridging veins over the sylvian fissure, dominance of the superficial sylvian vein complex, presence of vein clustering, continuity from the artery of the central sulcus of the insula to the rolandic artery, and the relationship between the superior segment of the squamosal suture and the sylvian fissure. Additionally, the number of M_2, M_3, and M_4 (continuous interval variables), the distance from the external acoustic meatus to the foramen of Monro (anterior-posterior and cranial-caudal), and the distance from the temporal pole

to the cortical resection margin (continuous ratio variables) were recorded.

Insula Surgical Classification

To facilitate data interpretation and enhance the surgical relevance of this study, the Berger-Sanai surgical classification scheme of the insula was used to subdivide the insula into 4 zones.[13] Therefore, the insula was divided into anterior and posterior from the axial projection of the foramen of Monro; and superior to inferior by the sylvian fissure line projected over the insular cortex (Fig. 2).

Description of the Variables

Independent Variables

The TS approach utilizes only the sylvian fissure split and retraction over the opercula to expose the insula. In this approach, the superficial and deep sylvian cisterns are opened widely throughout the fissure. The TSVC allows additional retraction to the TS by cutting the bridging veins crossing the sylvian fissure. The TC approach uses different degrees of cortical resection to expose the insula. In the TC, the bridging veins are preserved and the space to access the insula results from multiple windows between the middle cerebral arteries and the superficial sylvian veins. In Zones 2 and 3, the TC was further divided into two subcategories. In Zone II, the first set of dependent variables was taken before and after the operculum portion of the precentral gyrus was resected. In Zone III, the first set of dependent variables was taken before and after removing Heschl's gyrus. This subcategorization was set in the experimental design to include the option for a less invasive cortical resection and to investigate the significance that resecting these areas may have during a TC approach.

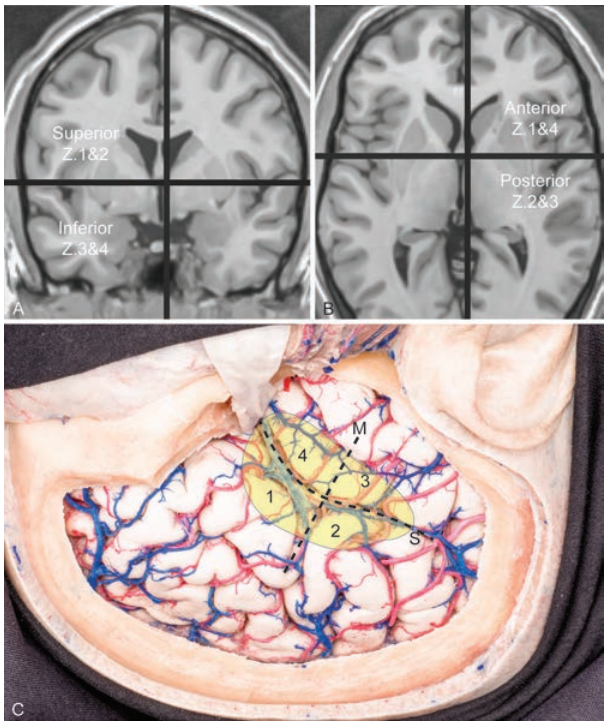

FIG. 2. Anatomical classification of the insula. A T1-weighted MR image was obtained from each specimen, and the foramen of Monro was identified in each volume. A linked radiological display was used to identify the projected point of the foramen of Monro in the insula cortex **(A–C)**. In the coronal view (A), the insula is divided into superior and inferior halves by the sylvian line—the sylvian fissure projected to the insular cortex. In the axial view (B), the projection of the foramen of Monro was used to divide the insula into anterior and posterior halves. A photograph of the intradural phase of a right pterional approach was taken to superimpose the insula *(yellow label)* on the cortical surface (C). The line passing through the foramen of Monro and the line projected from the sylvian fissure divide the insula in 4 zones. M = projected line of the foramen of Monro; S = projected line of the sylvian fissure.

Dependent Variables

The insula exposure is the area (in cm^2) of insular cortex exposed and surgically reachable for bimanual dissection. This area was obtained by touching the insular cortex with the navigation probe to obtain the stereotactic coordinates as previously described.[1] The surgical window is a polygonal area formed by the structures that, in more superficial planes, limit the corridor to the insula exposure. Typical structures limiting the surgical window were arteries, veins and cerebral cortex. The surgical window area was obtained by touching the limiting structures of the corridor with the navigation. The surgical freedom provides an objective indication on how freely an instrument can be moved in relation to a particular target. In our study, the surgical freedom (cm^2) was targeted to a point in the center of each insular zone. A Rhoton No. 5 dissector was pivoted to a target selected at the center of each insular zone and its handle moved in the perimeter of the surgical window to capture the contour of the corridor. The navigation probe touched the tip of the dissector handle in each major change in trajectory and recorded a set of stereotactic coordinates.[1] Additionally, we measured the extent of cortical resection after a transcortical approach to each insular zone. Three stereotactic points were obtained in each zone by touching the lips of the sylvian fissure with the navigation probe. After the resection was complete for each zone, the same points were touched with the navigation probe over the resection rim. Three linear measurements were obtained by calculating the distance between each point obtained over the lip of the sylvian fissure (preresection) and its equivalent at the resection margin (postresection).

Specimen Preparation

We included 16 embalmed human cadaveric specimens from donors without previous history of head and neck pathology and with a postmortem window of 72 hours. The specimens were embalmed with our customized formula for neurosurgical simulation and prepared for surgical research as described by our group.[1] A 3-T T1-weighted MR images were acquired from all specimens before the study. Radiological data were uploaded to the navigation system (Stryker NAV3) and registered to the specimen before each experiment.

Experiment Design

The specimen was positioned for a pterional approach

to the insula and rigidly attached to a surgical table. After exposure of the skull, the foramen of Monro was identified with the aid of navigation and measurements referenced to the external acoustic meatus were taken. The squamosal suture was touched with the navigation probe to identify the relationship to the sylvian fissure, which in turn was marked on the skull. A wide pterional craniotomy was designed based on the foramen of Monro, the sylvian fissure (already marked in the skull) and the opercula including at least 3 cm of extra cortical surface to allow retraction. The dura mater was incised and reflected anteriorly over the sphenoid ridge.

The sylvian fissure was completely split as previously described.[12] All venous channels were carefully dissected and preserved. Dynamic retraction was applied to each zone's operculum following the navigation probe as the stereotactic measurements were taken. The amount of retraction, which was measured in length, was the maximum allowed by the bridging veins or before cortical damage. The arterial and venous cortical systems were manually drawn separately in a printed hemispheric template map. The number, size, and trajectory of the veins were recorded as well.

Next, the veins crossing the sylvian fissure were marked and cut. All dependent variables were measured again in the zones previously limited by bridging veins. Following this, the veins previously cut were anastomosed using 8-0 sutures and a Lawton bypass set (Mizuho America).

After restoring the venous system completely, the TC approach was started. The corticotomy was performed using microsurgical instruments and magnified dissection under the surgical microscope (Carl Zeiss Pentero), with caution taken to preserve M_3 and M_4 arteries transitioning to the cortical surface. Multiple arterial-venous windows were generated by the end of each corticotomy. All dependent variables were measured at this point, including the TC subdivision into Zone II with and without the precentral motor cortex and Zone III with and without Heschl's gyrus. Reference pins were set along the margins of the corticotomy to guide the transition to the next zone. The cortical limits after the corticotomy were drawn into the hemispheric template map to track the extent of cortical resection. The distances between the cortical resection margin and both the operculum and the temporal pole were also taken at this point. Finally, the insular vasculature was also drawn.

Statistical Analysis

All data collected in this study were entered in a spreadsheet that was uploaded into statistical software (JMP v. 11.0, SAS institute) for statistical processing. Unpaired Student t-tests were calculated on the dependent continuous variables to determine significance between the compared variables and groups. A p value of 0.05 was considered significant. The mean and standard deviation for continuous variables and percentages for continuous and categorical variables were also calculated from the spreadsheet.

Results

Data collected in the present study include quantitative analysis of surgical variables (i.e., insular exposure, surgical window, and surgical freedom) for each approach as well as a descriptive analysis of the surgical anatomy of the transsylvian and transcortical approaches to the insula.

Morphometric Assessment

To ease data interpretation, insular exposure and surgical freedom for each approach were grouped and provided for each insular zone (Figs. 3 and 4).

Zone I

The TC corridor provided the best insular exposure in Zone I compared with both TS (4.62 ± 0.6 [SD] vs 7.21 ± 0.8 cm^2, $p < 0.05$) and TSVC (5.21 ± 0.98 vs 7.21 ± 0.8 cm^2, $p < 0.05$). Even with the veins cut, the TC approach provided 140% more insula exposure than the TS. Also, cutting the bridging veins in Zone I did not provide a significant increase in either the final insula exposure or the

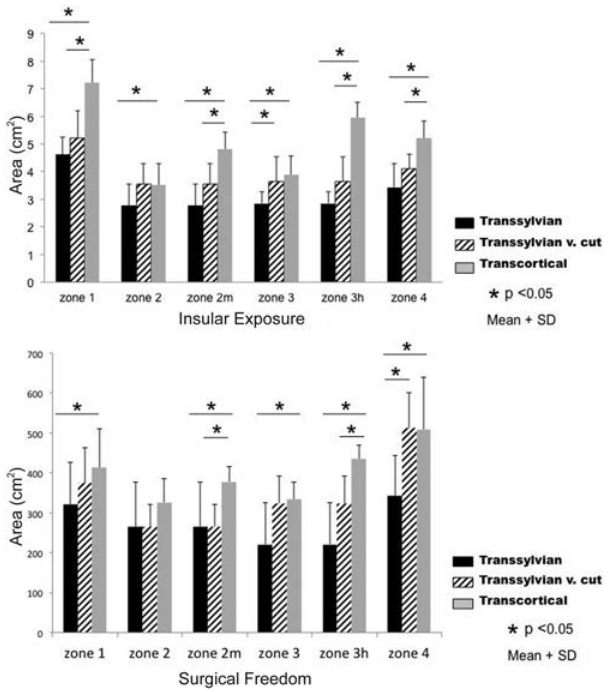

FIG. 3. Graph of the statistical analysis of the insular exposure **(upper)** and surgical freedom **(lower)** obtained during the transsylvian approach (TS), transsylvian approach with bridging veins cut (TSVC) and transcortical approach (TC). The mean, standard deviation *(error bars)*, and statistical significance of the difference in insular exposure (upper) or surgical freedom (lower) for the TS, TSVC, and TC approaches to the insula are shown for each zone. The TC approach provides more insular exposure than the TS and TSVC except in Zone II. Only when the opercular rim of the precentral gyrus was resected did the TC approach provide more exposure than the TSVC. The maximum difference in insular exposure was found in Zone I and IIIh. Overall, surgical freedom is smallest in the TS group and largest in the TC group, except in Zone IV. Surgical freedom obtained during a complete TC approach was significantly greater than in the TSCV. Cutting the bridging veins provided greater surgical freedom in Zone IV only. v. = bridging veins; Zone IIm = Zone II where the opercular rim of the precentral gyrus was resected during the transcortical approach; Zone IIIh = Zone III where Heschl's gyrus was partially resected during the transcortical approach.

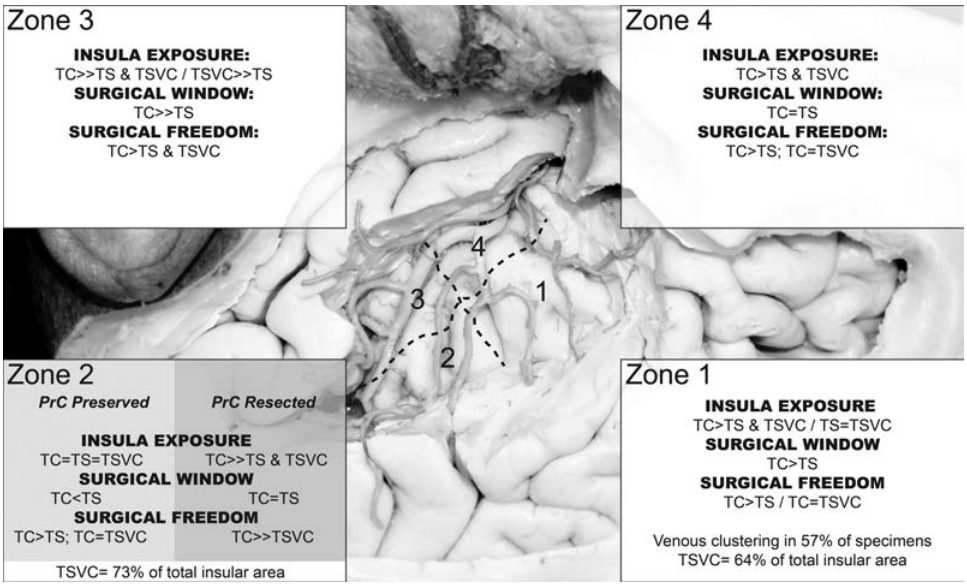

FIG. 4. Summary of the comparative analysis between the TS, TSVC, and TC approaches to each zone of the left insula. A photograph of the surgical simulation after a left TC approach was taken and used to illustrate the division of the insular cortex into 4 zones according to the Berger-Sanai classification of the insula. The sylvian line *(anterior-posterior dashed line)* divides the insula into ventral and dorsal parts. The Monro foramen and its lateral projection *(superior-inferior dashed line)* divide the insula into rostral and caudal parts. Zone II is further divided into 2 groups depending on the degree of frontoparietal opercula corticotomy during the TC approach. In Zone III, the TC group includes partial resection of Heschl's gyrus. All results included in the vignettes are statistically significant. PrC = precentral gyrus.

surgical freedom when the TS was used. The mean surgical window obtained in the TC was larger than in the TS (6.18 ± 0.6 vs 9.65 ± 1.7 cm^2, $p < 0.05$). The maximal retraction length at Zone I was 1 ± 3 cm. Cortical resection for total exposure of Zone I was 1.5 ± 0.5 cm at the inferior frontal gyrus. Although the TC provided a significant increase in surgical freedom compared with the TS (137%, $p < 0.05$), there was no statistically significant difference in comparison with the TSVC.

Zone II

Results obtained in Zone II were dependent on the degree of the corticotomy. When the precentral gyrus was preserved during the TC dissection, the insular exposure, surgical window, and surgical freedom were equivalent to that of the TSVC. The mean insular exposure in the TC group was greater than the TS (2.76 ± 0.8 vs 3.51 ± 0.8 cm^2, $p < 0.05$) but similar to that of the TSVC (3.56 ± 0.7 vs 3.51 ± 0.8 cm^2, $p = 0.9$). There was no statistically significant difference in insular exposure between the TS and the TSVC, thus cutting the bridging veins was not advantageous in Zone II. The mean surgical window obtained in the TS (obtained by applying maximal retraction along the opercular lip at the inferior parietal lobule) was greater than that of the TC (with the precentral gyrus preserved) (4.43 ± 1.1 vs 3.42 ± 0.7 cm^2, $p < 0.05$). The maximal retraction length at Zone I was 1.2 ± 2 cm. There were no differences in surgical freedom between the TS, TSVC, and TC.

On the other hand, when the opercular rim of the precentral gyrus was removed during the TC dissection, there was a clear advantage on the TC over all other groups. Specifically, the insula exposure obtained in the TC was 146% that of the TSVC ($p < 0.05$). Also, the surgical windows obtained during the TC and TS were similar (5.08 ± 0.8 vs 4.43 ± 1.1 cm^2, $p = 0.16$). Moreover, the mean surgical freedom obtained in the TC was 171% that of the TSVC ($p < 0.05$). Complete TC exposure of the insular cortex at Zone II required excision of the inferior 1.2 ± 0.2 cm of the precentral and postcentral gyri, which completely exposed the superior peri-insular sulcus, the anterior and posterior long gyri and Heschl's gyrus in the temporal operculum.

Zone III

In Zone III, The TC approach provided better surgical exposure than the TS (3.89 ± 0.6 vs 2.85 ± 0.4 cm^2, $p < 0.05$). However, if Heschl's gyrus was removed, the insula exposure of the TC was superior to that of the TSVC. In this zone, cutting the bridging veins during the TS increased insular exposure substantially (3.64 ± 0.8 vs 2.85 ± 0.4 cm^2, $p < 0.05$). Resecting Heschl's gyrus provided 156% of the insula exposure obtained during a TC approach. Also, when the TC included resection of Heschl's gyrus, the insular exposure obtained was 164% that of TSVC, which was a statistically significant increase ($p < 0.05$). When Heschl's gyrus was resected during TC, the surgical window was 176% that of the TS ($p < 0.05$). The surgical freedom obtained in the TC group was greater than that of the TS group (334.16 ± 43 vs 221.14 ± 105 cm^2, $p < 0.05$) but similar to that of the TSVC ($p = 0.75$). However, after resection of Heschl's gyrus, the surgical freedom obtained in the TC was greater than in either of the other groups ($p < 0.05$). Cutting the bridging veins during

the TS approach did not increase the surgical freedom ($p = 0.09$). The maximal retraction length at Zone III was 1 ± 2 cm. Cortical resection for complete exposure of Zone III was 1.3 ± 0.3 cm of the superior temporal gyrus.

Zone IV

The TC corridor provided greater insular exposure than both the TS (5.2 ± 0.6 vs 3.44 ± 0.8 cm^2, $p < 0.05$) and the TSVC (5.2 ± 0.6 vs 4.11 ± 0.5 cm^2, $p < 0.05$). Cutting the veins during the TS approach did not increase insula exposure (TSVC 4.11 ± 0.5 vs TS 3.44 ± 0.8 cm^2, $p = 0.08$). There was no difference between the TC and the TS with respect to surgical window (5.96 ± 1.1 vs 5.38 ± 1.2 cm^2, $p = 0.28$). The TC provided greater surgical freedom than the TS (508.8 ± 131 vs 341.7 ± 101 cm^2, $p < 0.05$), but equivalent to that of the TSVC (508.8 ± 131 vs 513.14 ± 87 cm^2, $p < 0.05$). The TSVC provided greater surgical freedom than the TS (513.14 ± 87 vs 341.76 ± 101 cm^2, $p < 0.05$). The maximal retraction length at Zone IV was 1 ± 3 cm. Complete exposure of the inferior peri-insular sulcus required resection of the entire width of the superior temporal gyrus from the foramen of Monro anteriorly to 1.5 ± 0.6 cm posterior to the temporal pole.

Surgical Anatomy

In Zone I, the TS corridor provided exposure of the insular apex and the sylvian line, and only the TC provided exposure of the superior peri-insular sulci (Fig. 5). The TSVC provided exposure to 64% of Zone I, which included the proximal portion of the anterior, middle and posterior short gyri as well as the apical portion of the accessory gyrus. In 57% of cases, a vein cluster arising from the prefrontal cortex severely limited exposure to the middle short gyrus and the posterior half of the anterior short gyrus. When the TSVC was used, the middle short gyrus of the insula was better accessed, as the main bridging veins cross the sylvian fissure at this region. However, it did not provide a significant increase in surgical exposure. Only the TC corridor allowed complete exposure of the superior peri-insular sulcus and the entire area of the anterior, middle, posterior and accessory insular gyri in Zone I. Moreover, if the surgical table was tilted to the ipsilateral side and the head turned down 15° (by either increasing Trendelenburg or tilting the back rest down), the Eberstaller gyrus and the lateral lenticulostriate arteries were also exposed. The corticotomy necessary to reach Zone I completely required excision of 60% of the pars orbicularis and opercularis, and 20% of the pars triangularis.

In Zone II, the TS corridor provided insular exposure limited to the sylvian line whereas the TC corridor allowed greater exposure of the posterior long gyrus and the anterior long gyrus. The TS corridor was severely limited by the narrow shape of the posterior half of the sylvian fissure (Fig. 6). Even when the bridging veins were cut dur-

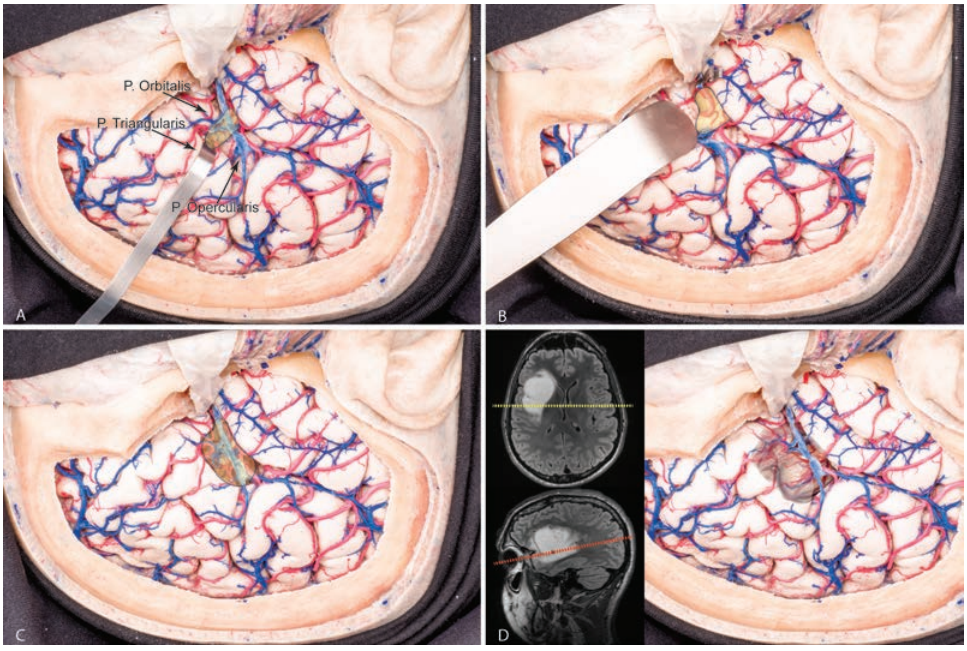

FIG. 5. Surgical simulation of the TS **(A)**, TSVC **(B)**, and TC **(C)** approaches for the Zone I of the right insula **(D)**. A right-side pterional approach was carried out, and the dura was incised and reflected toward the sphenoid bone. The superficial and deep sylvian cisterns were dissected completely with great care to protect all the vessels. The frontal operculum over Zone I of the insula was retracted to simulate a TS approach (A). Next (B), the superficial sylvian vein was cut and the self-retaining retractors were relocated to simulate the TSVC. The veins were then re-anastomosed, and the frontal operculum was allowed to return to its natural position. The transcortical approach was performed respecting the venous complex and the large veins to the dorsal and orbital aspect of the frontal lobe (C). A typical Zone I insular tumor was photographically fused to the surgical simulation to illustrate the relationship to the cortex before any surgical maneuver was started (D). Axial-superior and sagittal-inferior views of a typical Zone I insular tumor are included to show the relation of the tumor to the Monro line *(yellow)* and the sylvian line *(red)*. The *yellow semitransparent labels* in each photograph represent the surgical corridor provided by each approach to the insula. P. = pars.

ing the TSVC approach and maximal retraction pressure was applied, only 73% of the total area of the anterior and posterior long gyri could be exposed. The superior peri-insular sulcus was not exposed through the TSVC. The precentral gyrus covers the majority of the anterior long gyrus of the insula. Only when the opercular portion of the precentral gyrus was removed, the TC provided more insular exposure than the TSVC.

In Zone III, the TSVC provided greater exposure of the inferior part of the anterior and posterior long gyri, yet the planum temporalis and inferior peri-insular sulcus were only completely exposed through the TC approach (Fig. 7). Heschl's gyrus is a large portion of the posterior aspect of the temporal operculum that blocks the surgical trajectory to the planum temporalis and the posterior long gyrus of the insula. Thus, if Heschl's gyrus is preserved during the TC corridor, the final insular exposure is similar to that of a TSVC with maximal retraction applied uniformly to the superior temporal gyrus. Zone III of the insula, including the inferior peri-insular sulcus, could only be completely exposed when 90% of the Heschl's gyrus was removed during a TC. Also, if the head was tilted down

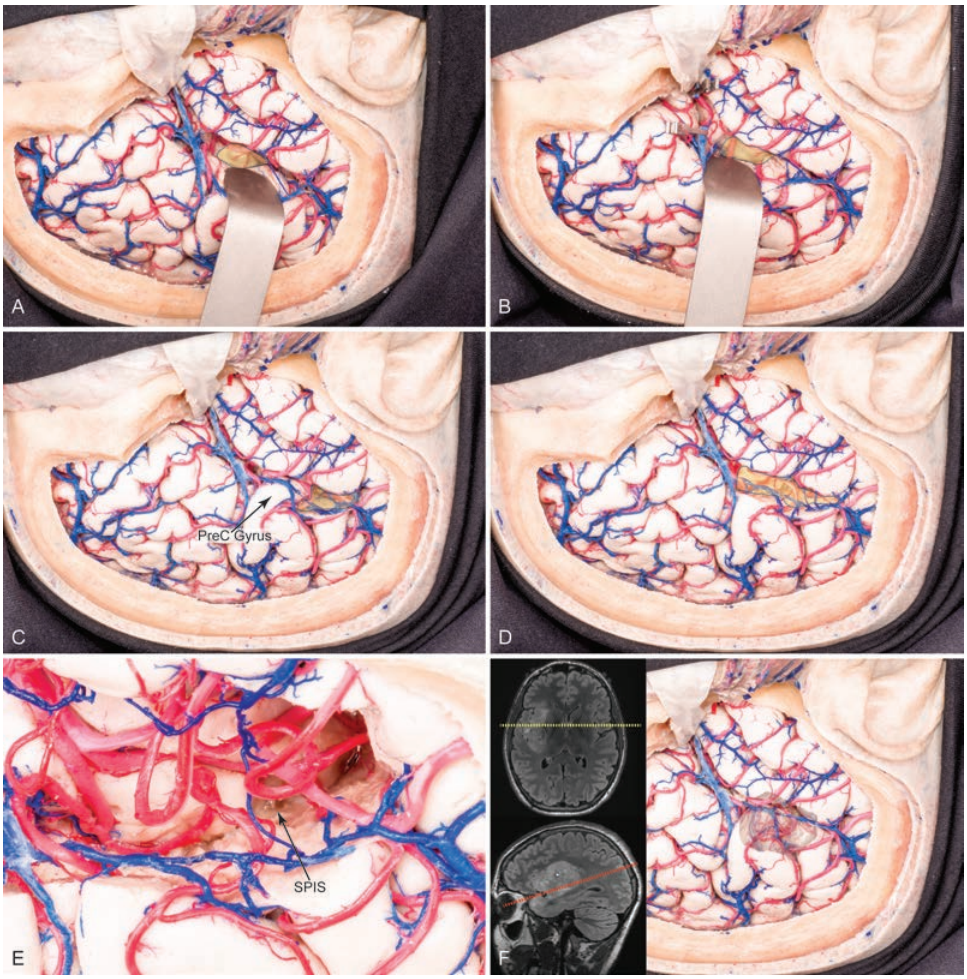

FIG. 6. Surgical simulation of the TS **(A)**, TSVC **(B)**, TC **(C)**, and TC with the precentral gyrus resected **(D and E)** approaches for Zone II of the insula **(F)** on the right side. The superficial and deep sylvian cisterns were widely dissected posteriorly with great care to protect all the vessels. The posterior aspect of the frontal operculum and the parietal operculum over Zone II of the insula were retracted to simulate a TS approach (A). Next (B), the main trunk of the superficial sylvian vein was cut and the self-retaining retractors were relocated to simulate the surgical approach with the bridging veins cut. The veins were then re-anastomosed, and the opercula were allowed owed to return to their natural position. The transcortical approach was performed respecting the cortex of the precentral gyrus as well as the venous complex and the large veins to the dorsal aspect of the parietal lobe (C). Next (D and E), the opercular rim of the precentral gyrus was resected to simulate a complete TC approach. A close-up picture of the TC approach to Zone II reveals that the insular cortex of this zone was completely exposed and the superior peri-insular sulcus was also accessible (E). Multiple windows were created between the M_3 arteries and the superior sylvian veins, forming multiple flexible corridors to the insular surface. A typical Zone II insular tumor was photographically fused to the surgical simulation to illustrate the relationship to the cortex (F). Axial-superior and sagittal-inferior views of a typical Zone II insular tumor are included in Panel F to show the relation of the tumor to the Monro line *(yellow)* and the sylvian line *(red)*. The *yellow semitransparent labels* represent the surgical corridor provided by each approach to the insula. PreC = precentral gyrus; SPIS = superior peri-insular sulcus.

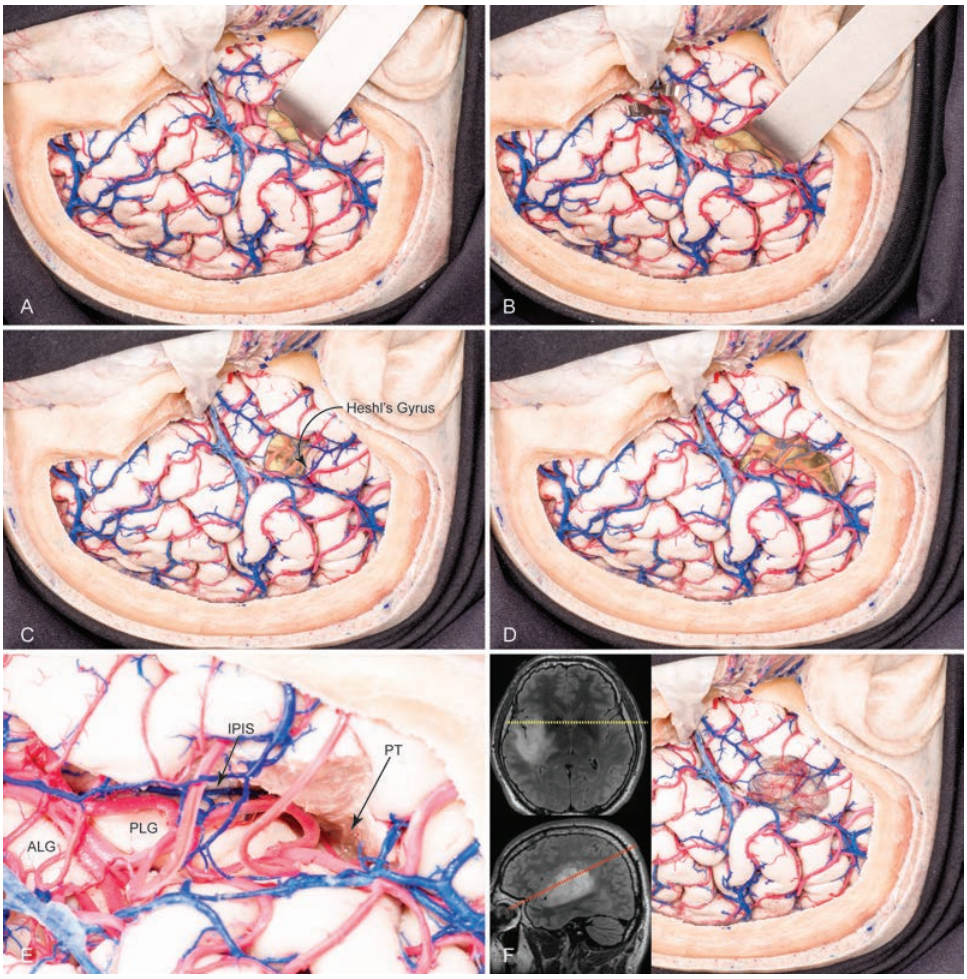

FIG. 7. Surgical simulation of the TS **(A)**, TSVC **(B)**, TC **(C)**, and TC with the Heschl's gyrus resected **(D and E)** approaches for Zone III of the right insula **(F)**. The superficial and deep sylvian cisterns were completely exposed with great care to protect all the vessels transitioning to the cortex. The posterior segment of the temporal operculum over Zone III of the insula was retracted to simulate a TS approach (A). Following this, the superficial sylvian vein was cut and the self-retaining retractors were reoriented to simulate the surgical approach with the bridging veins cut (B). The veins were then re-anastomosed, and the temporal operculum was allowed to return to its original position. The TC approach was performed next, preserving both Heschl's gyrus and the sylvian venous complex (C). Following this, Heschl's gyrus was resected for a complete TC approach to Zone III of the insula (D and E). A close-up photograph of the TC exposure of the insula revealed complete exposure of the Zone III cortex as well as the planum temporale and inferior peri-insular sulcus (E). The large veins to the dorsal aspect of the temporal and occipital lobes and the Labbé complex as well as the transitioning M_4 branches were preserved during all the transcortical dissection. These vessels formed multiple corridors to access the surface of the insula. A typical Zone III insular tumor was photographically fused to the surgical simulation to illustrate the relationship to the cortex before starting the surgical simulation (F). Axial-superior and sagittal-inferior views of a typical Zone III insular tumor were included to illustrate the relation of the tumor to the Monro line *(yellow)* and the sylvian line *(red)*. The *yellow semitransparent labels* represent the surgical corridor provided by each approach to the insula. ALG = anterior long gyrus; IPIS = inferior peri-insular sulcus; PLG = posterior long gyrus; PT = planum temporale.

10°–20° (Trendelenburg or turning down the back rest of the surgical table), the long gyri could be further dissected toward Zone II.

In Zone IV, cutting the bridging veins (TSVC) did not significantly increase insular exposure during a TS corridor, which was completely exposed only through the TC corridor (Fig. 8). The TS corridor exposed the anterior portion of the anterior long gyrus and the insular apex. A large bridging vein limited insular exposure in more than 50% of specimens. Exposure of the inferior peri-insular sulcus was achieved by cutting this vein (TSVC), applying maximal retraction to the superior temporal gyrus, and tilting the head upward 20°. However, the TC provided more insular exposure than the TSVC. The inferior peri-insular sulcus in Zone IV and the insular portion of the planum polaris were completely exposed through the TC corridor.

Venous Drainage

The venous drainage patterns were carefully studied to

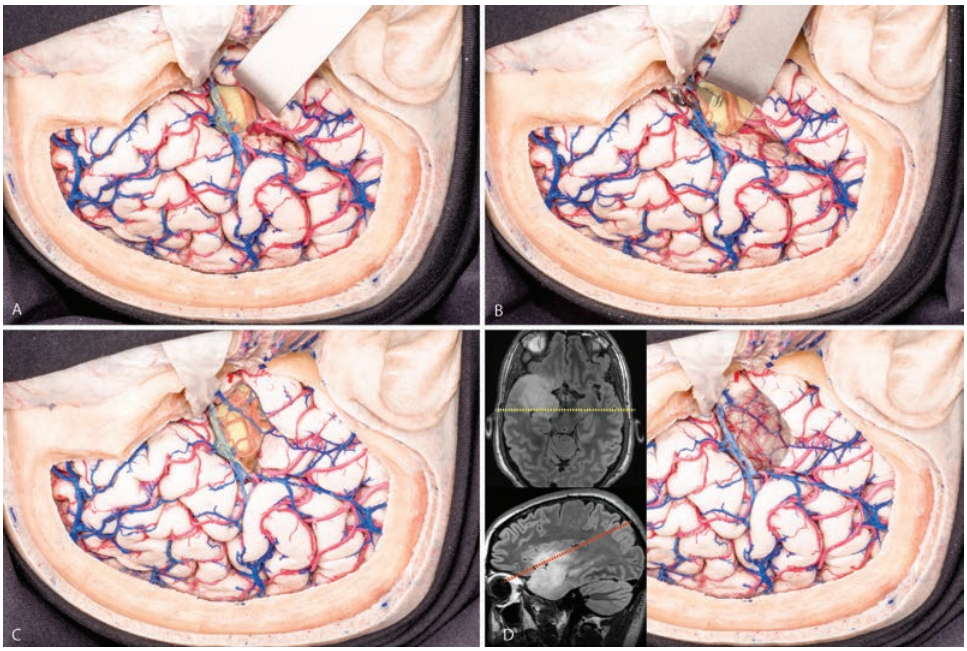

FIG. 8. Surgical simulation of the TS **(A)**, TSVC **(B)**, and TC **(C)** approaches for Zone IV of the right insula **(D)**. The superficial and deep sylvian cisterns were completely dissected with great care to preserve all the transiting vessels. The temporal operculum over Zone IV was retracted to simulate a TS approach (A). Following this (B), the superficial sylvian vein was cut and the self-retaining retractors were reoriented to simulate the surgical approach with the bridging veins cut. Next, the veins were re-anastomosed, and the temporal operculum was allowed to return to its natural position. The TC approach was performed respecting the venous complex and the large veins to the dorsal aspect of the temporal lobe and the temporal pole (C). Numerous arteriovenous windows were created after the cortical resection and used to access the insular surface. A typical Zone IV insular tumor was photographically fused to the surgical simulation exposure to show the relationship to the cortex before any surgical maneuver was started (D). Axial-superior and sagittal-inferior views of a typical Zone I insular tumor are included to show the relation of the tumor to the Monro line *(yellow)* and the sylvian line *(red)*. The *yellow semitransparent labels* represent the surgical corridor provided by each approach to the insula.

determine their dominance in the venous outflow of the lateral surface of the brain, the number of bridging veins and their relationship to the different zones, and the clustering patterns.

We found bridging veins crossing the sylvian fissure in 70% (11/16) of the studied specimens. A dominant drainage pattern was found in 87% (14/16) of cases, where the number and size of veins draining anteriorly was greater than the number and size draining to both the Labbé complex and the superior sagittal sinus. Good alternative outflow was identified in 50% (8/16) of the dominant venous patterns. In 30% of specimens, there were dominant bridging veins with poor collateral drainage. Moreover, venous clustering around the premotor and prefrontal cortex draining the lower part of the lateral surface of the frontal lobe was found in 56% (9/16) of the specimens.

Surgical Landmarks

The observational and descriptive analysis of the surgical anatomy of the pterional transsylvian approach provided 3 key relationships that were consistent: the relationship between the middle cerebral artery running in the central sulcus of the insula (M_2) and the rolandic artery (M_4); the relationship between the superior segment of the squamosal suture and the sylvian fissure; and the localization of the foramen of Monro in relation to the external acoustic meatus at the surface of the skull.

There were 2–4 trunks of the M_2 that branched into 12 ± 2 M_3 branches on the insular surface. In all our specimens, the M_2 branches running through the central sulcus of the insula became the precentral (rolandic) artery, feeding the precentral and postcentral gyri. In 81% of cases (13/16), this artery remained at the surface of the operculum. However, in 18% (3/16) of cases, the M_3 component of the artery running in the central sulcus of the insula ran in the depth of the precentral sulcus of the brain and became superficial at 0.8 ± 0.2 cm from the opercular rim.

The external acoustic meatus was easily identified in all surgical simulations and used as a landmark to infer the position of the foramen of Monro and, therefore, the division of the insula into anterior (I+IV) and posterior (II+III) zones before the craniotomy was done. The foramen of Monro was 1.9 ± 0.26 cm anterior and 4.42 ± 0.6 cm cranial to the external acoustic meatus.

The squamosal suture was a reliable landmark to infer the position of the sylvian fissure, which defined the surgical division of the insula into superior (I+II) and inferior (III+IV) zones. The superior portion of the squamosal suture, from the pterion anteriorly to its major inferior bend posteriorly corresponded to the sylvian fissure in the ma-

jority of specimens (14/16) and was inferior to the sylvian fissure in only 1 specimen (8%).

Discussion

This study shows that the TC corridor provides the greatest access to lesions, such as gliomas, within the insular region. The evidence is that even when the comparison between TC, TS, and TSVC is limited to the confines of the insula, the TC still provides the best overall surgical exposure, window, and freedom. In our dissections, the degree of corticotomy in Zones II and III provided significantly different surgical profiles. We found that the value of cutting the bridging veins during a TS approach was maximal in Zone III, where it provided a significant increase in insular exposure. From our observations of the venous drainage of the lateral surface of the brain, we identified a venous pattern that would make the TSVC unsafe in 30% of cases due to the existence of large dominant sylvian bridging veins with poor alternative outflow to the Labbé or superior sagittal sinus complex. Also, venous clustering at the pars triangularis, opercularis and motor cortex was observed in 56% of specimens (9/16), further limiting the transsylvian corridor to Zones I and II.

The present study suggests that the optimal surgical strategy to obtain maximal exposure for an insular glioma requires careful assessment of each patient's tumor location within the insula. Determining the tumor location in relation to the different zones of the insula allows for preoperative estimation of the extent of tumor resection[13] and anticipation of the surgical approach that will be required once the cortex is exposed. If the tumor is limited at the sylvian line in Zones I and IV (anterior), our data suggest that the tumor could be sufficiently exposed through a transsylvian approach. However, if the tumor is located in Zones II and III (posterior), using a transsylvian approach may require splitting the sylvian fissure completely and using both extensive retraction and venous sacrifice. This is especially important if the tumor invades into Zone III. However, if the tumor is located either in the periphery of the sylvian line or expands to or beyond the peri-insular sulci, only the transcortical approach will provide a sufficient surgical profile to attempt maximal resection, regardless of the zone. In such cases, direct cortical and subcortical mapping will determine the trajectory and degree of resection in each particular patient.

Whereas cutting the sylvian bridging veins during TS might seem reasonable, our results suggest that such an option could entail serious venous drainage problems in 30% of cases. Also, we identified clustering of veins in the opercula in more than half of our specimens. Regardless of the overall venous pattern, we consider that a cluster of bridging veins drainingmost of the blood from the inferior frontal gyrus and inferior parietal lobule is, in itself, a limitation to the TSVC. In his study on the cerebral veins, Seeger identified that the direction of the venous blood flow at the lateral surface of the brain was toward the sylvian fissure in 56% of cases, followed by the Labbé complex and the bridging veins to the superior sagittal sinus.[16] This finding adds to the important role of the sylvian venous system in the venous outflow of the lateral surface of the brain. In the subgroup of patients who have critical bridging veins that must be preserved, our findings suggest that the TS approach might be insufficient even to expose tumors sitting within the sylvian line, especially in the posterior zones (II+III).

There are several reports on the surgical technique and outcomes of the transsylvian approach to insular tumors.[5,9,14,19–21] There is common consensus between all groups that large amounts of retraction are required to expose the insula when using the transsylvian corridor, which we have confirmed in our study. However, none of these reports mention the rate in which the sylvian bridging veins were cut. In their series, Lang et al.[9] and Hentschel and Lang[5] stated that 2–2.5 cm of retraction was required to expose the insular tumor. However, the authors did not mention the standard deviation of their measurements, whether they found significant differences in the different parts of the opercula or if the measure referred to the retraction length to one operculum or the distance between opercula after splitting the sylvian fissure. We addressed this uncertainty in our study by measuring the maximal retraction length that could be applied to each operculum without damaging the venous system. In all our specimens, we could not apply 2 cm of retraction length without cutting the bridging veins. Also, when preserving the venous system (TS approach) the insular exposure was limited and significantly inferior to that of the TSVC and TC. On the basis of these findings, we suspect that in the majority cases in which large insular tumors were described as being successfully removed through a TS approach, the approach was actually TSVC. Although a TSVC corridor would be an acceptable option for those cases in which the venous bridging veins can be sacrificed (70%) and the insular tumor is within the confines of the peri-insular sulci, we find a major limitation of this strategy in the remaining 30% of cases, in which a TC approach would potentially overcome this limitation.

Previous studies have shown that TC approaches to subcortical lesions are safe.[3,5,13,14] Furthermore, our group has reported the first large surgical experience for insular tumors using the TC approach.[13] Our data suggest that the TC approach provides a better surgical profile than the other options. In fact, the maximum difference in insular exposure between the TC and the TSVC was observed in the posterior insular zones, where the TS corridor is severely limited by the narrow sylvian cistern. However, the surgical profile of the TC approach to the posterior zones is highly dependent on brain mapping and therefore impossible to predict before surgery. Although cortical sacrifice is inherent to the TC corridor, direct cortical and subcortical stimulation during awake surgery allows the neurosurgeon to identify function and work around eloquent areas. In contrast, when dissecting the sylvian cistern, especially the posterior portion, the neurosurgeon has to perform meticulous dissection of critical neurovascular structures in a very narrow corridor. In a study of surgical approaches to temporal tumors in 235 patients, Schramm et al.[14,15] reported that the TS approach was associated with the highest combined rate of complications, which could be caused by inadvertent subpial dissection or transection of an insular artery. Using a transsylvian approach to in-

sular tumors, Hentschel and Lang reported a postoperative speech complication rate of 30%, which they attributed to transient ischemia related to both retraction and arterial dissection. These results are congruent with the evidence of our morphometric analysis, where large amounts of retraction over the opercula, including the pars opercularis and the precentral gyrus, are required for maximal insular exposure.

The transcortical approach to the insula uses direct cortical and subcortical stimulation to assess and preserve cortical function. While the anatomical location of cortical function is variable, there are general patterns of functional anatomy that may guide surgical planning. In Zone I, the transcortical approach transgressed 60% of pars orbicularis and opercularis, and 20% of pars triangularis. In the dominant hemisphere, language function is classically described in Brodmann Areas 44 and 45 (also known as Broca's area). In our experience, only the posterior aspect of pars opercularis of the dominant hemisphere is highly involved in speech production.[8] However, in those patients with tumors affecting pars opercularis, transcortical resection under constant cortical mapping may be safe.[8] In Zone II, the opercular segment of the precentral gyrus, which may account for the contralateral motor control of the face, sits on top of the anterior long gyrus of the insula. Our data show that if the opercular portion of the precentral gyrus is removed, the insular exposure is 146%, and the surgical freedom is 171% that of TSVC. There is evidence of recovery after resection of the facial motor cortex in the nondominant hemisphere,[10] which has been congruent with the surgical results published by our group[13] and that of Duffau et al.[4] If resection of the facial motor cortex in the dominant hemisphere is attempted, it should be limited to pure facial expression, which will cause transient central facial paralysis. After studying a series of 14 patients who underwent an awake transcortical approach for tumors affecting Zone II of the insula and the inferior parietal lobule, Maldonado et al. identified speech function in the majority of cases. Interestingly, they found high interindividual variability in the anatomical location of language. Therefore, awake cortical and subcortical stimulation must be performed in each case to assess the location of functional cortex and white matter tracts for language, which will further characterize the final transcortical corridor in each patient.[11] The posterior margin of the transcortical approach in Zone II involved 1 cm of the postcentral gyrus, which may account for the somatosensory function of the contralateral half of the face. In Zone III, exposure of the posterior long gyrus and planum temporalis requires excision, to some degree, of Heschl's gyrus. When Heschl's gyrus is resected along with the anterior segment of the superior temporal gyrus, the insular exposure becomes 164% that of the TSVC. The primary auditory cortex, located at the Heschl's gyrus in both hemispheres, receives bilateral afferent sensory signaling from the cochlear and superior olivary nucleus via the inferior colliculus and medial geniculate body of the thalamus.[2] In a recent study, Javad et al. provided evidence of interhemispheric transcallosal linkage between the auditory areas using diffusion tensor imaging in humans.[7] Hence, complete resection of Heschl's gyrus in 1 hemisphere (e.g., TC to Zone III of the insula) should not cause a perceivable loss in audition. Nonetheless, our experience is congruent with other authors in that resection of the superior temporal gyrus under direct cortical stimulation is safe.[4,13] Cortical resection to expose Zone III does not involve the angular gyrus, or regions posterior to Heschl's gyri, which, in the dominant hemisphere, may account for Wernicke's area (Brodmann Area 22). When resecting tumors in Zone II and III of the insula, constant direct cortical and subcortical stimulation of the superior temporal gyrus and parietal operculum are performed before any corticectomy to assess for language function, especially in the dominant hemisphere.[4] The arcuate and middle longitudinal fascicles, and Wernicke's area, which are in the vicinity of Heschl's gyrus, are presumed to be a core part of the language pathway, therefore potentially limiting the transcortical corridor around the primary auditory cortex in the dominant hemisphere. However, the location and composition of such areas and tracts varies considerably in the population. Therefore intraoperative functional mapping becomes essential to guide the resection in each patient.

Although the use of intraoperative navigation is very important in modern neurosurgery, it should not replace anatomical knowledge. In this study, we identified two anatomical landmarks that may be used to infer the location of the insular zones before opening the skull. We found a strong correlation between the division of the insular lobe into anterior and posterior parts and the external acoustic meatus over the skull surface. Also, we found that the superior segment of the squamosal suture could be used to infer the location of the sylvian fissure, which divides the insular lobe into dorsal and ventral segments. Knowledge of these anatomical relations may aid in tailoring the craniotomy to the insular lesion.

Thorough knowledge of the arterial blood supply beyond M_2 is critical to preserve function while dissecting an insular tumor. When using microsurgical dissection around the insula, the high power magnification reduces peripheral view. It is crucial to recognize the cortical distribution related to each M_2 artery transiting within the middle cerebral artery's candelabra, as it is being dissected. We have found that the M_2 artery running over the central sulcus of the insula becomes the rolandic artery in 100% of our specimens, which is in agreement to the findings reported by Türe et al. in their study on the insular arteries.[18] Interestingly, we observed that the M_3 segment of the rolandic artery runs in the depth of the operculum in 18% of (3/16) cases, which requires careful dissection when using the TC corridor to approach Zone I or II.

Study Limitations

Human postmortem surgical simulation provides the best alternative to surgical experimentation because it is safe, provides a very realistic scenario of the human anatomy, and allows for prolonged research time. In our recent publication,[1] we described our customized surgical simulation method for neurosurgical research. One of the most interesting findings of the study was that there were no differences on the retraction profile between the specimens prepared with our customized embalming formula

and that of unembalmed (i.e., fresh) cadavers.[1] This new method overcomes the major limitations for surgical simulation when using classical cadaver processing techniques (brain stiffness and inability to retract), allowing a very realistic surgical simulation with life-like manipulation of the brain. Therefore, the present study uses the most advanced cadaveric neurosurgical research methods to provide information on the surgical profile of the transsylvian and transcortical approaches to the insula. However, several limitations, intrinsic to postmortem research, may limit direct application of our findings to clinical practice. These limitations include the lack of effective brain relaxation; absence of anatomical distortion due to mass-effect; and the impossibility to study cortical function. In this study, thorough dissection of arachnoid adhesions, evacuation of cerebrospinal fluid, and opercular retraction allowed splitting the sylvian fissure widely. However, brain relaxation techniques such hyperventilation and the use of brain osmotic agents could not be applied therefore limiting the surgical results of the study. The mass effect related to insular lesions may cause substantial anatomical distortion and should be considered in the preoperative planning. However mass effect is highly variable and case-specific. We used specimens without known brain pathology to maximize statistical power and internal validity when comparing surgical approaches. Direct assessment of cortical function is an inherent limitation of postmortem research and may limit the clinical application of this study. However, the anatomical location of brain function is specific to each patient and situation (e.g., neural plasticity) and therefore the impact of cortical function location to the transcortical approach should be assessed in every case using intraoperative stimulation mapping of the language function.

Conclusions

There are 3 surgical options to approach insular gliomas: the transsylvian approach, the transsylvian approach with the bridging veins cut, and the transcortical approach (referred to in this paper as TS, TSVC, and TC, respectively). Overall, the TC approach provided better insula access than the TS approach. Although in some circumstances the TC provides similar surgical exposure and surgical freedom to that of the TSVC, cutting bridging veins may be unsafe in 30% of patients. Cortical and subcortical mapping is critical before and during the transcortical approach to the posterior zones (Zones II and III), as the facial motor and somatosensory functions (Zone II) and the language pathways (Zone III) are involved. The greatest insular exposure in Zones II and III requires resection of the precentral gyrus and superior temporal gyrus. While the TC and TSVC provide equivalent access to the insula in Zones I and II, a TC approach may be needed to maximize access Zones III and IV (inferior). Thus, preoperative assessment using radiological imaging and our insula classification scheme is useful in guiding the surgical planning. This study demonstrates that the TC approach may be superior to the TSVC approach in accessing gliomas that, while primarily within the insula, extend to and beyond the peri-insular sulcus. However, neurosurgeons may also consider the TS and TSVC approaches for small to moderate size lesions located within the confines of the insula. Selecting the surgical option providing the greatest insular exposure should also help reduce surgical morbidity.

Acknowledgments

We wish to thank all individuals and their families who, without any other interest than that of research, willed their bodies to achieve these results. This study would not have been possible without their contribution and therefore to them we dedicate the present report. The authors would like to also thank Annette Molinaro for her contribution to the statistical analysis and Simar Singh for the medical illustration included in the present study.

References

1. Benet A, Rincon-Torroella J, Lawton MT, González Sánchez JJ: Novel embalming solution for neurosurgical simulation in cadavers. **J Neurosurg 120:**1229–1237, 2014
2. Crippa A, Lanting CP, van Dijk P, Roerdink JB: A diffusion tensor imaging study on the auditory system and tinnitus. **Open Neuroimaging J 4:**16–25, 2010
3. Duffau H: A personal consecutive series of surgically treated 51 cases of insular WHO Grade II glioma: advances and limitations. **J Neurosurg 110:**696–708, 2009
4. Duffau H, Capelle L, Lopes M, Faillot T, Sichez JP, Fohanno D: The insular lobe: physiopathological and surgical considerations. **Neurosurgery 47:**801–811, 2000
5. Hentschel SJ, Lang FF: Surgical resection of intrinsic insular tumors. **Neurosurgery 57 (1 Suppl):**176–183, 2005
6. Ius T, Pauletto G, Isola M, Gregoraci G, Budai R, Lettieri C, et al: Surgery for insular low-grade glioma: predictors of postoperative seizure outcome. **J Neurosurg 120:**12–23, 2014
7. Javad F, Warren JD, Micallef C, Thornton JS, Golay X, Yousry T, et al: Auditory tracts identified with combined fMRI and diffusion tractography. **Neuroimage 84:**562–574, 2014
8. Rolston JD, Englot DJ, Benet A, Li J, Cha S, Berger MS: Frontal operculum gliomas: language outcome following resection. **J Neurosurg 122:**725–734, 2015
9. Lang FF, Olansen NE, DeMonte F, Gokaslan ZL, Holland EC, Kalhorn C, et al: Surgical resection of intrinsic insular tumors: complication avoidance. **J Neurosurg 95:**638–650, 2001
10. LeRoux PD, Berger MS, Haglund MM, Pilcher WH, Ojemann GA: Resection of intrinsic tumors from nondominant face motor cortex using stimulation mapping: report of two cases. **Surg Neurol 36:**44–48, 1991
11. Maldonado IL, Moritz-Gasser S, de Champfleur NM, Bertram L, Moulinié G, Duffau H: Surgery for gliomas involving the left inferior parietal lobule: new insights into the functional anatomy provided by stimulation mapping in awake patients. **J Neurosurg 115:**770–779, 2011
12. Potts MB, Chang EF, Young WL, Lawton MT: Transsylvian-transinsular approaches to the insula and basal ganglia: operative techniques and results with vascular lesions. **Neurosurgery 70:**824–834, 2012
13. Sanai N, Polley MY, Berger MS: Insular glioma resection: assessment of patient morbidity, survival, and tumor progression. **J Neurosurg 112:**1–9, 2010
14. Schramm J, Aliashkevich AF: Surgery for temporal mediobasal tumors: experience based on a series of 235 patients. **Neurosurgery 60:**285–295, 2007
15. Schramm J, Aliashkevich AF: Surgery for temporal mediobasal tumors: experience based on a series of 235 patients. **Neurosurgery 62 (6 Suppl 3):**1272–1282, 2008
16. Seeger W: **Microsurgery of Cerebral Veins.** Vienna: Springer, 2000

17. Skrap M, Mondani M, Tomasino B, Weis L, Budai R, Pauletto G, et al: Surgery of insular nonenhancing gliomas: volumetric analysis of tumoral resection, clinical outcome, and survival in a consecutive series of 66 cases. **Neurosurgery 70:**1081–1094, 2012
18. Türe U, Yaşargil MG, Al-Mefty O, Yaşargil DC: Arteries of the insula. **J Neurosurg 92:**676–687, 2000
19. Vanaclocha V, Sáiz-Sapena N, García-Casasola C: Surgical treatment of insular gliomas. **Acta Neurochir (Wien) 139:**1126–1135, 1997
20. Wang P, Wu MC, Chen SJ, Xu XP, Yang Y, Cai J: Microsurgery resection of intrinsic insular tumors via transsylvian surgical approach in 12 cases. **Cancer Biol Med 9:**44–47, 2012
21. Yaşargil MG, von Ammon K, Cavazos E, Doczi T, Reeves JD, Roth P: Tumours of the limbic and paralimbic systems. **Acta Neurochir (Wien) 118:**40–52, 1992

Disclosure

Dr. Lawton receives royalties related to the "Lawton Bypass set" from Mizuho instruments.

Author Contributions

Conception and design: Benet, Hervey-Jumper, Lawton, Berger. Acquisition of data: Benet. Analysis and interpretation of data: all authors. Drafting the article: Benet. Critically revising the article: all authors. Reviewed submitted version of manuscript: all authors. Approved the final version of the manuscript on behalf of all authors: Benet. Statistical analysis: Benet, Hervey-Jumper, González Sánchez. Administrative/technical/material support: Benet, González Sánchez, Lawton, Berger. Study supervision: Benet, Lawton, Berger. Surgical simulations/experiments: Benet.

Supplemental Information

Companion Paper

Hervey-Jumper SL, Li J, Osorio JA, Lau D, Molinaro AM, Benet A, et al: Surgical assessment of the insula. Part 2: validation of the Berger-Sanai zone classification system for predicting extent of glioma resection. DOI: 10.3171/2015.4.JNS1521.

Correspondence

Arnau Benet, Department of Neurosurgery, University of California San Francisco, 505 Parnassus Ave., Rm. M779, San Francisco, CA 94143. email: arnaubenet@gmail.com.

JNS

CLINICAL ARTICLE

J Neurosurg 124:482–488, 2016

Surgical assessment of the insula. Part 2: validation of the Berger-Sanai zone classification system for predicting extent of glioma resection

Shawn L. Hervey-Jumper, MD, Jing Li, MD, Joseph A. Osorio, MD, PhD, Darryl Lau, MD, Annette M. Molinaro, PhD, Arnau Benet, MD, and Mitchel S. Berger, MD

Department of Neurological Surgery, University of California, San Francisco, California

OBJECTIVE Though challenging, maximal safe resection of insular gliomas enhances overall and progression-free survival and deters malignant transformation. Previously published reports have shown that surgery can be performed with low morbidity. The authors previously described a Berger-Sanai zone classification system for insular gliomas. Using a subsequent dataset, they undertook this study to validate this zone classification system for predictability of extent of resection (EOR) in patients with insular gliomas.

METHODS The study population included adults who had undergone resection of WHO Grade II, III, or IV insular gliomas. In accordance with our prior published report, tumor location was classified according to the Berger-Sanai quadrant-style classification system into Zones I through IV. Interobserver variability was analyzed using a cohort of newly diagnosed insular gliomas and independent classification scores given by 3 neurosurgeons at various career stages. Glioma volumes were analyzed using FLAIR and T1-weighted contrast-enhanced MR images.

RESULTS One hundred twenty-nine procedures involving 114 consecutive patients were identified. The study population from the authors' previously published experience included 115 procedures involving 104 patients. Thus, the total experience included 244 procedures involving 218 patients with insular gliomas treated at the authors' institution. The most common presenting symptoms were seizure (68.2%) and asymptomatic recurrence (17.8%). WHO Grade II glioma histology was the most common (54.3%), followed by Grades III (34.1%) and IV (11.6%). The median tumor volume was 48.5 cm^3. The majority of insular gliomas were located in the anterior portion of the insula with 31.0% in Zone I, 10.9% in Zone IV, and 16.3% in Zones I+IV. The Berger-Sanai zone classification system was highly reliable, with a kappa coefficient of 0.857. The median EOR for all zones was 85%. Comparison of EOR between the current and prior series showed no change and Zone I gliomas continue to have the highest median EOR. Short- and long-term neurological complications remain low, and zone classification correlated with short-term complications, which were highest in Zone I and in Giant insular gliomas.

CONCLUSIONS The previously proposed Berger-Sanai classification system is highly reliable and predictive of insular glioma EOR and morbidity.

http://thejns.org/doi/abs/10.3171/2015.4.JNS1521

KEY WORDS anaplastic astrocytoma; glioma; glioblastoma; low-grade glioma; insular glioma; oncology

Insular gliomas remain a challenge to manage. Given the complexity of the insular lobe, its proximity to functionally significant areas, and its intimate relationship with middle cerebral and lenticulostriate artery branches, these tumors were often deemed too dangerous for surgical treatment. However, improvements in neuroanesthesia, microsurgical technique, and functional mapping have allowed greater access to these tumors with a low complication rate. Prior published reports suggest that aggressive resection of both low- and high-grade insular gliomas may be accomplished with an acceptable morbidity profile.[2,3,7–10,13,14,17] Maximal extent of resection (EOR) predicts superior overall and progression-free survival as well as improved seizure control.[6,11,13] The majority of insular gliomas not only involve the insular lobe but can also infiltrate into portions of the frontal operculum and temporal lobe. Given their proximity to functional language and motor networks, the surgical approach may vary depending on the predominant component of the tumor within the insula. Recent publications have focused on the role of

ABBREVIATIONS EOR = extent of resection; FLAIR = fluid-attenuated inversion recovery; IDH = isocitrate dehydrogenase; WHO = World Health Organization.

SUBMITTED January 5, 2015. **ACCEPTED** April 9, 2015.

INCLUDE WHEN CITING Published online September 4, 2015; DOI: 10.3171/2015.4.JNS1521.

surgery to improve survival for patients with insular gliomas.[6,8,13–15] In our prior retrospective series, we analyzed perioperative outcomes after surgery for 115 consecutive insular gliomas focusing on morbidity and the effect of EOR on patient outcome and proposed an anatomical classification system for insular gliomas to help preoperatively predict the likely extent of tumor resection.[13] In this current study, we assign the previously described "Berger-Sanai" classification system to a new cohort of insular gliomas to determine the interobserver reliability among clinicians at different levels of clinical experience and expertise in order to validate our previous EOR predictions.

Methods

Patient Selection

Using a prospectively collected database of insular gliomas assigned to one of 4 previously described zones,[13] we studied 114 consecutive patients undergoing a total 129 resections between September 2007 and April 2014. All procedures were performed by the study's senior author (M.S.B). Patients were all adults older than 18 years of age who had undergone surgery at the University of California, San Francisco. Perioperative patient parameters including zone classification based on preoperative fluid-attenuated inversion recovery (FLAIR) and T1-weighted postcontrast MR images, clinical presentation, handedness, age at diagnosis, immediate postoperative MRI (within 48 hours of surgery), and histopathology review (in accordance with World Health Organization [WHO] guidelines) were prospectively collected. Given substantial differences in their natural history, patients with WHO Grade I histology, those with multifocal glioma, and gliomatosis cerebri were excluded from analysis. All aspects of microsurgical tumor removal, including a description of the functional mapping, have been previously described in our prior publication on insular gliomas.[13] Approval for this study was granted by the University of California, San Francisco Committee on Human Research.

Interobserver Reliability of Berger-Sanai Insular Glioma Classification System

According to our prior published protocol, the insula was divided into 4 zones (Fig. 1). Along the horizontal plane in a sagittal view, the insula was seen to straddle the overlying sylvian fissure. This plane was intersected by a perpendicular line at the foramen of Monro. Tumor location was assigned to one or more of these zones.[13] For tumors occupying more than 1 zone, this condition was denoted as such (e.g., Zones I+II). For cases in which the tumor occupied all 4 zones, these insular gliomas were defined as "Giant." Using this method, a total of 9 possible options existed for classification: Zones I, II, III, IV, I+II, I+IV, II+III, and III+IV and Giant.

To test agreement of insular zone assignment between clinicians, a subset of 80 cases of newly diagnosed insular glioma were independently scored by 3 examiners. With the goal of testing clinicians across a varied distribution of clinical experiences, 1 junior level neurosurgery resident (J.O.), 1 junior level neurosurgery faculty member (S.H.J.), and 1 senior neurosurgeon (M.S.B.) were chosen to participate. Participants were blinded to each other's score. The kappa coefficient was used to determine the significance of this agreement. Interpretation of the kappa coefficient was performed in accordance to prior published reports in which 0 indicated agreement equivalent to chance, 0.01–0.20 slight agreement, 0.21–0.40 fair agreement, 0.41–0.60 moderate agreement, 0.61–0.80 substantial agreement, 0.81–0.99 almost perfect agreement, and a kappa coefficient of 1 indicated perfect agreement.[5]

Patient Outcome Measurements

Patients underwent sequential neurological examinations performed by 4 clinicians during the perioperative period: the senior attending neurosurgeon, a neurosurgical resident, a speech and language neurophysiologist, and the attending neuro-oncologist. Clinical examinations were performed preoperatively, every day during the postoperative period, and at each follow-up appointment by at least 1 of the above-mentioned clinicians (4–6 weeks and 3–6 months following surgery). Short-term neurological morbidity was defined as new-onset language or sensorimotor deficits within the first 3–5 postoperative days. Long-term neurological morbidity was defined as persistent dysfunction 90 days after surgical intervention. Our protocol for language function testing has been previously described.[12] Differences between findings of the 4 examiners were adjudicated by accepting the results showing the greatest impairment if more than 1 examiner was involved at a given time point. MRI results were reviewed to confirm that the patient's symptoms were not a function of tumor progression at each time point. Malignant progression was defined as a change in histopathology of WHO Grade II or III tumors to higher-grade lesions on a subsequent procedure.

Volumetric Analyses

One author (J.L.) conducted volumetric measurement of pre- and postoperative imaging. Each measurement and calculation was examined for accuracy by another author (S.H.J.) and the primary surgeon (M.S.B.). Low- and high-grade tumors were volumetrically analyzed by measuring hyperintense regions on axial T2-weighted FLAIR MR images (low-grade gliomas) and T1-weighted contrast-enhanced MR images (high-grade gliomas). For each case, the tumor was segmented manually across all slices with region-of-interest analysis to compute pre- and postoperative volumes in cubic centimeters. The EOR was calculated as follows: [100 – (postoperative tumor volume/preoperative tumor volume)*100], with 100% indicating gross total resection and < 100% representing subtotal resection. Determination of tumor volume and EOR was made without consideration of the clinical outcome.

Statistical Analyses

Descriptive statistics were calculated for all variables and stated as median (unless otherwise specified) for continuous variables and frequency of distribution for categorical variables. Cross-tabulations were generated, and the Wilcoxon signed-rank test (for continuous variables) and chi-square (for categorical variables) tests were used to compare distributions. The Fisher exact test was used if more than 80% of values were less than 5. The kappa coefficient was used to determine strength of agreement be-

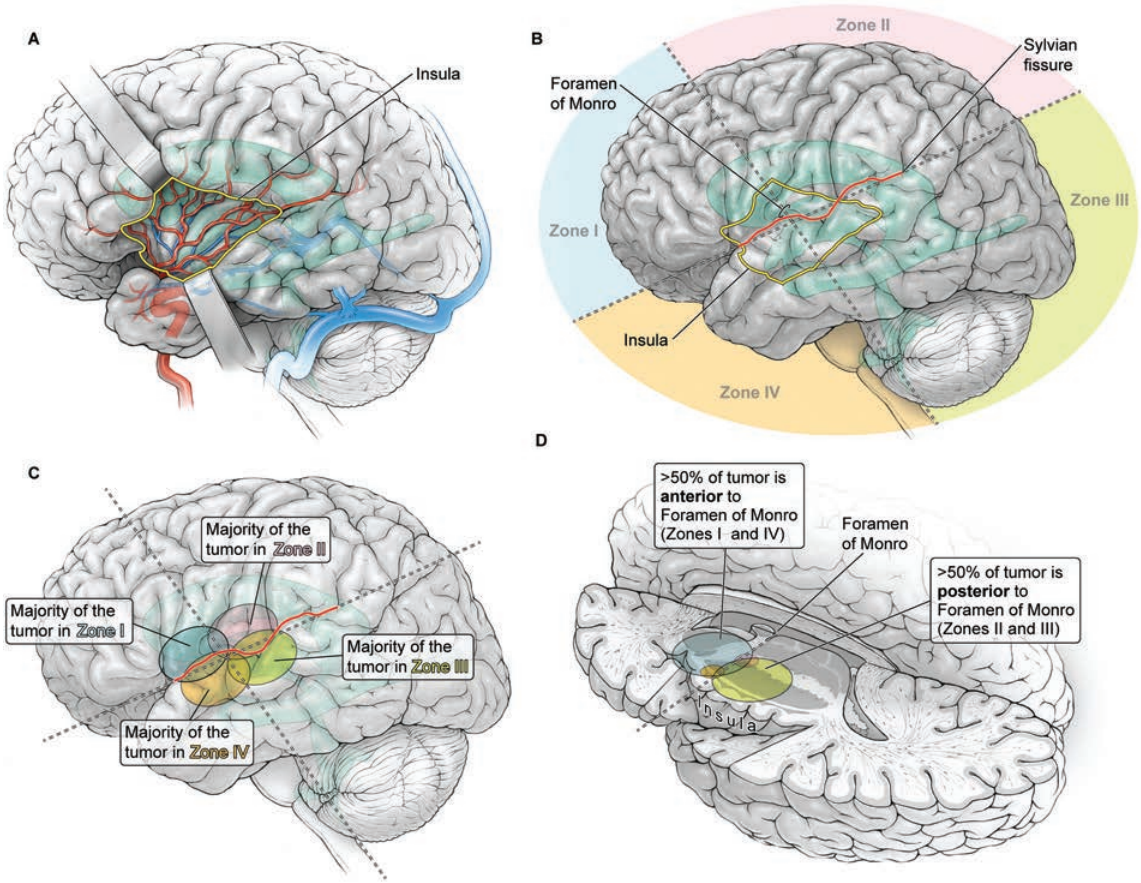

FIG. 1. Illustration showing insular surface with Berger-Sanai insular glioma classification system. **A:** The insula is covered by the frontoparietal and temporal opercula. **B:** Zones I to IV are divided along the sylvian fissure and a perpendicular plane crossing the foramen of Monro. **C:** Insular tumor location is determined by the position of the majority of the tumor mass. **D:** Axial illustration of Zones I and II located anterior to the foramen of Monro and Zones II and III located behind the foramen of Monro. Copyright Kenneth X. Probst. Published with permission.

tween clinicians. All p values were obtained from 2-sided tests, with statistical significance defined as $p < 0.05$. A biostatistician (A.M.) assisted with statistical analyses in this study, using JMP statistical software, version 10.0.2 (SAS Institute, Inc.).

Results

Patient Demographics

The study population included 114 consecutive patients for a total of 129 procedures representing 74 men and 55 women with a median age of 41 years (range 18–72 years) (Table 1). The study population from our previously published experience included 115 procedures involving 104 patients. As such, our total experience included 244 procedures involving 218 patients with insular glioma treated at our institution. Eighty (62.0%) of the 129 procedures in the current experience represented primary craniotomies, whereas 49 (38.0%) of the operations involved patients who had undergone at least 1 prior surgical procedure for the treatment of insular glioma. Sixty-eight (52.7%) of the procedures were for the treatment of left-sided tumors, and there were 58 awake craniotomy procedures (45.0%). Patients most commonly presented with new-onset seizures (88 cases, 68.2%), or asymptomatic tumor progression (23 cases, 17.8%); other presentations included headaches (9 cases, 7.0%), cognitive decline (3 cases, 2.3%), motor deficits (3 cases, 2.3%), and language deficits (1 case, 0.8%). Insular gliomas were rarely discovered incidentally, representing 1.6% of cases (2 patients). In the 129 operations, the most common histological grade was WHO Grade II (70 tumors, 54.3%), followed by WHO Grade III (44 tumors, 34.1%), and WHO Grade IV (15 tumors, 11.6%). The median tumor volume was 48.5 cm^3 (range 0.11–245.7 cm^3). Fifteen percent of insular tumors (19) were confined entirely within the insula, while 85% of tumors were primarily based in the insula (i.e., > 75%) with tumor extending beyond the insula to involve portions of the frontal, temporal, or parietal lobes. The median duration of clinical follow-up was 3.5 years (range 0.26–25.8 years) and, as part of planned adjuvant therapy, 107 patients (82.9%) were treated with chemotherapy and 82 (63.6%) underwent radiation therapy after surgery (decisions about use of adjuvant chemo-radiation were made on a case-by-case basis dependent on tumor recurrence, WHO grade, and histol-

TABLE 1. Demographic and clinical characteristics of study patients who underwent surgery for treatment of insular glioma (129 procedures)*

Parameter	Value
Age at diagnosis (yrs)	
Median	41
Range	18–72
Sex	
Male	74 (57.4%)
Female	55 (42.6%)
Side of tumor	
Left	68 (52.7%)
Right	61 (47.3%)
WHO tumor grade	
II	70 (54.3%)
III	44 (34.1%)
IV	15 (11.6%)
Tumor volume (cm^3)	
Median	48.5
Range	0.11–245.7
Insular glioma location by zone	
I	40 (31.0%)
II	2 (1.6%)
III	17 (13.2%)
IV	14 (10.9%)
I+II	4 (3.1%)
I+IV	21 (16.3%)
II+III	7 (5.4%)
III+IV	12 (9.3%)
Giant	12 (9.3%)
Median insular glioma volume by zone (cm^3)	
I	49.1
II	11.4
III	22
IV	20.1
I+II	72
I+IV	52.3
II+III	63.8
III+IV	41.4
Giant	91.2
Handedness	
Right	126 (97.7%)
Left	3 (2.3%)
Symptoms at presentation	
Seizure	88 (68.2%)
Cognitive decline	3 (2.3%)
Headache	9 (7.0%)
Incidental	2 (1.6%)
Language deficit	1 (0.8%)
Motor deficit	3 (2.3%)
Asymptomatic recurrence	23 (17.8%)
Type of surgery	
Motor mapping	122 (94.6%)
Language mapping	58 (45.0%)
Awake surgery	58 (45.0%)
New	80 (62.0%)
Reoperation	49 (38.0%)
Adjuvant oncologic treatment	
Patients with postoperative chemotherapy	107 (82.9%)
Patients with postoperative radiation	82 (63.6%)
Malignant transformation	49 (38.0%)
Clinical follow-up (yrs)	
Median	3.5
Range	0.26–25.8
EOR	
0–40%	1 (0.8%)
41–69%	19 (14.7%)
70–89%	58 (45.0%)
>90%	51 (39.5%)
Median	85%
Range	40–100%

* Values indicate numbers of cases (by procedure) unless otherwise indicated.

ogy). Histologically confirmed malignant transformation from WHO Grade II to WHO Grade III or from WHO Grade III to WHO Grade IV occurred in 49 cases (38.0%). Tumor laterality was evenly distributed (Table 1).

Distribution of Insular Glioma Location

Based on our prior published report,[13] insular gliomas were assigned to 1 of 4 zones (Table 1). The majority of insular gliomas were located in the anterior portion of the insula (anterior to the foramen of Monro), with 31.0% (40 cases) within the anterior-superior quadrant (Zone I), 10.9% (14 cases) within the anterior inferior quadrant (Zone IV), and 16.3% (21 cases) within Zones I+IV (total of 58.2% of cases within the anterior insula). Twelve insular gliomas (9.3%) were classified as Giant, occupying all 4 zones.

Interobserver Reliability of Berger-Sanai Insular Glioma Classification System

Interobserver reliability was tested using preoperative FLAIR or T1-weighted gadolinium-enhanced MR images obtained in 80 patients with new WHO Grade II, III, or IV insular gliomas. Three neurosurgeons with varying amounts of clinical experience scored each tumor's location according to our previously published zone classification criteria.[13] Interobserver agreement was 89.1% (41 of 46 cases) for WHO Grade II gliomas, 84.0% (21 of 25 cases) for WHO Grade III anaplastic gliomas, and 100% (9 of 9 cases) for WHO Grade IV gliomas. Overall observer agreement was 89%. Interobserver reliability testing showed strong agreement with a kappa coefficient of

0.857 (95% CI 0.77–0.94; p < 0.001). There was no correlation between observer agreement and WHO grade (p = 0.42).

Extent of Resection

EOR was determined as follows: in 1 case (0.8%), the EOR was less than or equal to 40%; in 19 (14.7%), it was between 41% and 69%; in 58 (45.0%), it was between 70% an 89%; and in 51 (39.5%), it was greater than 90%. The median EOR was 85% (range 40%–100%) across all zones (Table 1). Among cases of WHO Grade II glioma (70 cases), the median EOR was 81%; in 55 cases (78.6%), the EOR was greater than or equal to 70% (this included 32 cases [45.7%] with 70%–89% resection and 23 [32.9%] with > 90% resection). A total of 44 operations were for treatment of anaplastic astrocytoma (WHO Grade III), with a median EOR of 88%. In 41 cases (93.2%), the EOR was 70% or greater (this included 23 cases [52.3%] with a 70%–89% resection and 18 [40.9%] with a > 90% resection). Among cases of WHO Grade IV glioma (15 cases), the median EOR was 97%, and 13 cases (86.7%) had an EOR greater than or equal to 70% (this included 3 cases [20.0%] with 70%–89% resection and 10 [66.7%] with > 90% resection). Zone II insular gliomas were the smallest, with a median tumor volume of 11.4 cm^3, while Giant insular gliomas had a median volume of 91.2 cm^3 (Table 1). The greatest EOR was accomplished in tumors located in Zones I (median EOR 90.1%) and IV (median EOR 89.5%), compared with Zones I+IV (median EOR 75%) and Giant tumors (median EOR 80%) (p = 0.008) (Table 2). In our initial series, the smallest EOR was associated with Zone II tumors; however, with a greater willingness to maximize resections using either a transcortical surgical corridor through silent portions of the face motor cortex or splitting the posterior sylvian fissure, the median EOR increased to 83.5%. There were no significant differences in median EOR between tumors across all zones in our 2 insular glioma series (Table 2).

In addition to zones predictive of EOR, there was also a positive correlation between tumor size and EOR. The median glioma volume was highest in Giant (91.2 cm^3), Zone I+II (72.0 cm^3), and Zone II+III (63.8 cm^3) tumors. The smallest median tumor volumes were observed in Zone II (11.4 cm^3), Zone III (22.0 cm^3), and Zone IV (20.1 cm^3) tumors (median volumes for Zone I, Zone I+IV, and Zone III+IV tumors were 49.1 cm^3, 52.3 cm^3, and 41.4 cm^3, respectively) (p = 0.002). In cases with EOR < 40%, the median tumor volume was 38 cm^3 (mean 38 cm^3); in those with EOR of 41%–69%, the median tumor volume was 46 cm^3 (mean 61 cm^3); in those with EOR of 70%–89%, the median volume was 62 cm^3 (mean 62 cm^3); and in those with an EOR > 90%, the median glioma volume was 25 cm^3 (mean 46 cm^3) (p = 0.0183). This suggests a more complete resection for smaller insular tumors.

Insular Glioma Molecular Characteristics and Impact on EOR

There is inconsistency in the literature regarding the rate of 1p and 19q chromosomal co-deletions in insular gliomas.[4,16] In 60 (46.5%) of the cases in our new series, the tumors were either WHO Grade II oligodendroglioma (n = 24), WHO Grade II oligoastrocytoma (n = 24), or WHO Grade III anaplastic oligodendroglioma or oligoastrocytoma (n = 12). Forty-three percent (n = 23) of WHO Grade II and III insular oligodendroglioma and oligoastrocytomas had 1p19q co-deletions (p = 0.04). Other previously published reports have suggested that isocitrate dehydrogenase (IDH) status confers a higher degree of resectability on WHO Grade III and IV gliomas.[1] We therefore analyzed EOR focusing on insular gliomas that were positive for the IDH mutation (IDH+). There was no significant difference in the volume of IDH+ and nonmutated (IDH–) insular gliomas (IDH+ gliomas had a median tumor volume of 47.1 cm^3, while IDH– insular gliomas had a median tumor volume of 28.9 cm^3; p = 0.18). Furthermore, IDH+ insular gliomas were evenly distributed across zones, with no statistically significant differences noted (Zone I, 36%; Zone II, 2%; Zone III, 13%; Zone IV, 2%; Zones I+II, 4%; Zones I+IV, 19%; Zones II+III, 6%; Zones III+IV, 9%; Giant, 4%; p = 0.13). Among WHO Grade II insular gliomas, IDH+ tumors had a median EOR of 81%, while IDH– WHO Grade II insular gliomas had a median EOR of 86% (p = 0.62). WHO Grade III IDH+ insular gliomas had a median EOR of 79%, while IDH– WHO Grade III insular gliomas had a median EOR of 88% (p = 0.06). The median EOR for WHO Grade IV

TABLE 2. Summary of resected insular gliomas by zone (n = 244)

Zone	WHO Grade II	WHO Grade III	WHO Grade IV	Median EOR, % (new series, n = 129)	Median EOR, % (combined series, n= 244)*	p Value†
I (n = 80)	50 (62.5)	21 (26.3)	9 (11.3)	90.1	**92**	0.47
II (n = 8)	4 (50.0)	3 (37.5)	1 (12.5)	83.5	**75.5**	0.41
III (n = 23)	11 (47.8)	8 (34.8)	4 (17.4)	88	**89**	0.75
IV (n = 20)	9 (45.0)	8 (40.0)	3 (15.0)	89.5	**89.2**	0.79
I+II (n = 8)	5 (62.5)	2 (25.0)	1 (12.5)	86.5	**78.9**	0.35
I+IV (n = 47)	25 (53.2)	20 (42.6)	2 (4.3)	75	**78**	0.06
II+III (n = 16)	13 (81.3)	2 (12.5)	1 (6.3)	85	**84**	0.77
III+IV (n = 16)	8 (50.0)	6 (37.5)	2 (12.5)	82	**83**	0.61
Giant (n = 26)	15 (57.7)	9 (34.6)	2 (7.7)	80	**76.4**	0.60
Totals	140 (57.4)	79 (32.4)	25 (10.2)			

* Bold type is used to highlight the values for the combined series.

† For comparison of EOR between Sanai et al.[13] and the current series.

IDH+ insular gliomas was 83%, while IDH– WHO Grade IV insular gliomas had a median EOR of 95% (p = 0.31).

Morbidity Profile

There were no deaths related to surgery in this series. The overall short-term complication rate was 26.4% (34 complications in 129 procedures) (Table 3). Short-term (within 3–5 days after surgery) neurological complications occurred most frequently after procedures involving Zone 1 and Giant insular gliomas. New motor neurological deficits excluding face motor weakness (within 3–5 days after surgery) occurred after 7.8% of the procedures (10 of 129). New face motor deficits occurred after 9.3% (12 of 129). Early postoperative language deficits occurred after 16.3% (21 of 129). At the 3-month follow-up visit, 99.2% of face motor deficits resolved. The overall long-term (90-day) neurological deficit rate was 3.2%. All but 1 language deficit resolved (0.8%), while the long-term rate of motor disability also remained low at 1.6% (n = 2). These rates compared favorably with results from our prior retrospective series.

TABLE 3. Postoperative morbidity and complication rates in 129 procedures

Variable	Short Term*	Long Term†	Prior Series Long-Term Disability	p Value‡
Morbidity				
Language deficit	21 (16.3%)	1 (0.8%)	1 (1.0%)	
Motor deficit	10 (7.8%)	2 (1.6%)	2 (1.7%)	
Face motor deficit	12 (9.3%)	1 (0.8%)	2 (1.7%)	
Complication rates				**0.03**
Zone I	9 (26%)			
Zone II	0 (0%)			
Zone III	3 (8.8%)			
Zone IV	1 (3%)			
Zones I+II	2 (5.9%)			
Zones I+IV	4 (12%)			
Zones II+III	5 (15%)			
Zones III+IV	4 (12%)			
Giant	6 (18%)			

* Occurring postoperative Days 3–5.
† Remaining at 90-day-postoperative examination.
‡ Boldface indicates statistical significance.

Discussion

The insula's proximity to middle cerebral artery vessels, primary motor and sensory areas, and the perisylvian language network makes accessing and resecting gliomas in this area challenging. Prior studies demonstrated that maximal resection of insular gliomas enhances overall and progression-free survival and improves seizure outcome.[6,11,13] Furthermore, surgery can be accomplished with a median EOR of 80%–82% and minimal morbidity of long-term language (0.8%) and motor function (1.6%).[2,3,8,13,14] The significance of volumetric EOR on overall survival for patients with both low- and high-grade insular gliomas has been demonstrated in multiple previously published reports.[6,13,14] Sanai et al. analyzed 115 procedures involving 104 patients with insular glioma and demonstrated a 5-year overall survival of 100% when the EOR was 90% and 84% for an EOR less than 90% in cases of low-grade glioma. In cases of high-grade glioma, the 2-year overall survival was 91% with an EOR of 90% and 75% when the EOR was less than 90%.[13] This observation was later confirmed by Skrap et al., who found an overall survival of 92% for patients with an EOR greater than 90% and overall survival of 57% for those with an EOR less than 70%.[14] With respect to WHO Grade III gliomas, greater than 90% EOR has been shown to be associated with a 2-year overall survival of 78%, in contrast with less than 90% EOR, which was associated with a 2-year overall survival of 19.6%.[14] Recently it has been further demonstrated that EOR greater than 90% for insular gliomas is predictive of a favorable postoperative seizure outcome.[6]

In our previously published retrospective series of patients with insular gliomas, we assessed postoperative morbidity and patient survival while describing an anatomical characterization system to help predict extent of tumor resection. In this study, we use the previously described classification scheme to 1) determine if it is robust when used by other surgeons and 2) determine if it continues to be predictive of extent of tumor resection. We found this system to be highly reliable with minimal variability between clinicians and highly predictive of the expected EOR across all zones.

Few insula-based gliomas are confined entirely within the insula (15% in this series). Furthermore, depending on where within the insula a glioma is based, the surgical approach and anatomical considerations vary. For this reason, a common terminology is helpful when discussing individual lesions. Yaşargil et al. proposed a classification system based on whether the lesion is restricted to the insula (Type 3), part of the insula (Type 3A), or included in the adjacent operculum (Type 3B).[18,19] In that classification system, insular lesions involving one or both of the paralimbic orbitofrontal and temporopolar areas are classified, respectively, as Type 5A or Type 5B.[18,19] We found that this classification system failed to address many of the anatomical features relevant to surgery for insular gliomas, such as proximity to potentially functional areas. Additionally, it is difficult to use this classification to preoperatively predict EOR. We therefore proposed a classification system based on an anatomical split of the insula along the sylvian fissure and foramen of Monro, thereby dividing it into 4 parts (Zones I–IV) using preoperative high-resolution MR images.[13] This approach allowed us to consider and describe each insular tumor in relation to 1) the perisylvian language network (above and below the sylvian fissure in the dominant hemisphere), 2) primary sensory and motor areas (commonly for Zone I or II gliomas), 3) Heschl's gyrus (Zone III gliomas), and 4) middle cerebral artery branches (particularly lateral lenticulostriate branches found within the suprasylvian region of Zone I). It is critically important that a classification system have little variability between examiners. We tested this by asking 3 clinicians at varying stages in their careers to rate a cohort of insular gliomas, and found a strong correlation among examiners (kappa coefficient 0.857).

We set out to determine if the zone classification was predictive of EOR based on the previously described EOR in our original series. We found no differences in EOR for any zone between these 2 series. In this current patient series, we therefore reconfirmed our prior observation that zone classification was predictive of EOR, with the highest EOR seen in Zone I and Zone IV tumors. We also showed that the zone classification appears to be predictive of short-term postoperative morbidity, with a modestly higher early complication rate seen in Giant and Zone I tumors, and lowest complication rates seen in Zone II and Zone IV tumors ($p = 0.03$). In this current series of patients, we identified a slightly higher rate of short-term face motor deficits, which likely corresponds to using a transcortical window of entry through silent portions of the face motor area for purposes of enhancing exposure. The rate of long-term morbidity continued to be minimal at 3.5% and virtually unchanged from our initial series (3.8%).[13]

To our knowledge, the combined experience of this and our previously published report represents the largest series of insular glioma resections. The Berger-Sanai classification system is robust with little interobserver variability, and appears to validate our original description using this classification to predict EOR. Even so, there are study limitations that must be considered. Although there was little interobserver variability between clinicians with varying degrees of clinical experience and expertise, the investigation remained a single-institution study. The adoption of this classification system with external clinical validation is a topic of future study.

Conclusions

Maximal safe resection of insular gliomas continues to be associated with improved patient outcome and acceptable morbidity. Our previously proposed classification system is highly reliable and predictive of insular glioma EOR and perioperative morbidity.

References

1. Beiko J, Suki D, Hess KR, Fox BD, Cheung V, Cabral M, et al: IDH1 mutant malignant astrocytomas are more amenable to surgical resection and have a survival benefit associated with maximal surgical resection. **Neuro Oncol 16:**81–91, 2014
2. Duffau H: Surgery of low-grade gliomas: towards a 'functional neurooncology.' **Curr Opin Oncol 21:**543–549, 2009
3. Duffau H, Moritz-Gasser S, Gatignol P: Functional outcome after language mapping for insular World Health Organization Grade II gliomas in the dominant hemisphere: experience with 24 patients. **Neurosurg Focus 27(2):**E7, 2009
4. Gozé C, Rigau V, Gibert L, Maudelonde T, Duffau H: Lack of complete 1p19q deletion in a consecutive series of 12 WHO grade II gliomas involving the insula: a marker of worse prognosis? **J Neurooncol 91:**1–5, 2009
5. Griessenauer CJ, Miller JH, Agee BS, Fisher WS III, Curé JK, Chapman PR, et al: Observer reliability of arteriovenous malformations grading scales using current imaging modalities. **J Neurosurg 120:**1179–1187, 2014
6. Ius T, Pauletto G, Isola M, Gregoraci G, Budai R, Lettieri C, et al: Surgery for insular low-grade glioma: predictors of postoperative seizure outcome. **J Neurosurg 120:**12–23, 2014
7. Kim YH, Kim CY: Current surgical management of insular gliomas. **Neurosurg Clin N Am 23:**199–206, vii, 2012
8. Lang FF, Olansen NE, DeMonte F, Gokaslan ZL, Holland EC, Kalhorn C, et al: Surgical resection of intrinsic insular tumors: complication avoidance. **J Neurosurg 95:**638–650, 2001
9. Mehrkens JH, Kreth FW, Muacevic A, Ostertag CB: Long term course of WHO grade II astrocytomas of the Insula of Reil after I-125 interstitial irradiation. **J Neurol 251:**1455–1464, 2004
10. Moshel YA, Marcus JD, Parker EC, Kelly PJ: Resection of insular gliomas: the importance of lenticulostriate artery position. **J Neurosurg 109:**825–834, 2008
11. Pallud J, Audureau E, Blonski M, Sanai N, Bauchet L, Fontaine D, et al: Epileptic seizures in diffuse low-grade gliomas in adults. **Brain 137:**449–462, 2014
12. Sanai N, Mirzadeh Z, Berger MS: Functional outcome after language mapping for glioma resection. **N Engl J Med 358:**18–27, 2008
13. Sanai N, Polley MY, Berger MS: Insular glioma resection: assessment of patient morbidity, survival, and tumor progression. **J Neurosurg 112:**1–9, 2010
14. Skrap M, Mondani M, Tomasino B, Weis L, Budai R, Pauletto G, et al: Surgery of insular nonenhancing gliomas: volumetric analysis of tumoral resection, clinical outcome, and survival in a consecutive series of 66 cases. **Neurosurgery 70:**1081–1094, 2012
15. Vanaclocha V, Sáiz-Sapena N, García-Casasola C: Surgical treatment of insular gliomas. **Acta Neurochir (Wien) 139:**1126–1135, 1997
16. Wu A, Aldape K, Lang FF: High rate of deletion of chromosomes 1p and 19q in insular oligodendroglial tumors. **J Neurooncol 99:**57–64, 2010
17. Wu AS, Witgert ME, Lang FF, Xiao L, Bekele BN, Meyers CA, et al: Neurocognitive function before and after surgery for insular gliomas. **J Neurosurg 115:**1115–1125, 2011
18. Yaşargil MG, von Ammon K, Cavazos E, Doczi T, Reeves JD, Roth P: Tumours of the limbic and paralimbic systems. **Acta Neurochir (Wien) 118:**40–52, 1992
19. Zentner J, Meyer B, Stangl A, Schramm J: Intrinsic tumors of the insula: a prospective surgical study of 30 patients. **J Neurosurg 85:**263–271, 1996

Disclosure

The authors report no conflict of interest concerning the materials or methods used in this study or the findings specified in this paper.

Author Contributions

Conception and design: Hervey-Jumper, Li, Berger. Acquisition of data: all authors. Analysis and interpretation of data: all authors. Drafting the article: Hervey-Jumper. Critically revising the article: Hervey-Jumper, Berger. Reviewed submitted version of manuscript: all authors. Approved the final version of the manuscript on behalf of all authors: Hervey-Jumper. Study supervision: Berger.

Supplemental Information

Companion Paper

Benet A, Hervey-Jumper SL, González Sánchez JJ, Lawton MT, Berger MS: Surgical assessment of the insula. Part 1: surgical anatomy and morphometric analysis of the transsylvian and transcortical approaches to the insula. DOI: 10.3171/2014.12.JNS142182.

Correspondence

Shawn L. Hervey-Jumper, Department of Neurological Surgery, University of California, San Francisco, 505 Parnassus Ave., M779, San Francisco, CA 94143. email: herveyju@umich.edu.

"Success is not final; failure is not fatal:
It is the courage to continue that counts"

Winston S. Churchill

Que l'amor a la terra que m'ha vist crèixer, a la llengua que ha esculpit la meva ànima, i a la cultura que ha fet fort el meu cor inspiri el meu servei al pacient, sereni el bisturí i hem faci fort davant l'adversitat quirúrgica.